



Departamento de Ciências e Engenharia do Ambiente

The influence of sludge characteristics from full-scale MBR in membrane filterability

Francisco Miguel Martins Correia da Piedade

Dissertação apresentada na Faculdade de Ciências e Tecnologia da Universidade Nova de Lisboa para a obtenção do grau de Mestre em Engenharia do Ambiente, perfil Sanitária

Orientador científico: Professora Doutora Leonor Amaral

Lisboa, 2009

I dedicate this thesis to my parents

ACKNOWLEDGEMENTS

The research project took place at the Sanitary Department in the Civil Engineering Faculty at TU Delft University from September 2008 till February 2009. Through this University it was possible to visit and apply practical work in MBR systems in The Netherlands and Germany.

This thesis was mostly written in Portugal at the Faculty of Science and Technology of the New University of Lisbon.

I would like to thank my supervisor Leonor Amaral for all her support throughout this entire project, for her trust in me and for being fully available to answer any of my doubts.

Maria Lousada Ferreira, I'm deeply thankful for your encouragement during the research period, and for sharing your knowledge which enriched the core of this thesis. I would also like to express my appreciation for making me feel welcomed at TU Delft since the day I arrived and for your daily support. Not only are you a friend, you are also my mentor.

I would like to express my appreciation to everyone in the Sanitary Department of TU Delft for their friendship and support.

I would also like to thank Tony Schuit for his help and good advices during practical work in the laboratory. Patrick Andeweg, it was great to meet you. Not only were you always there for me but you also made the laboratory a fun place to work. Thanks for the wonderful conversations and I believe someday we'll be talking in Portuguese.

Patrícia Palma helped me improve the english of this thesis. Thank you so much for your effort and advice, which resulted in a better thesis.

I am very grateful to my parents for giving me this opportunity and for their support during this period. Special thanks to my brother and sister for their support.

I would also like to thank Inês and all my friends in The Netherlands and in Portugal.

RESUMO

No tratamento de águas residuais, o uso de bioreactores de membranas (MBR), oferece várias vantagens quando comparado com sistemas de tratamento convencionais. A possibilidade de necessitar apenas de uma reduzida área em planta, a produção de um efluente final de elevada qualidade e uma baixa produção de lamas são algumas dessas vantagens. No entanto, o fenómeno *fouling* ao nível da membrana constitui a principal limitação desta nova tecnologia, aumentando os custos operacionais associados ao arejamento intensivo e à limpeza física e química.

Esta tese tem como objectivo o estudo de características presentes nas lamas e a forma como estas contribuem para a filterabilidade da mesma.

No âmbito, mais alargado, deste projecto de investigação, entre Setembro de 2008 a Fevereiro de 2009, foram visitados cinco sistemas de MBR à escala real. Foram efectuadas três tipos de experiências: a *Caracterização de Amostras* de diferentes sistemas MBR; uma experiência com base em *Diluições* para obter diferentes concentrações de sólidos; e ainda a experiência *Concentração de Sólidos* também para estudar o impacto de diferentes concentrações de sólidos através da alteração do tempo de retenção hidráulico (TRH) num sistema MBR.

Em todas as experiências a filterabilidade das amostras de lamas foi medida através do método de caracterização de filtração (DFC_m) desenvolvido pela Universidade de Tecnologia de Delft (Evenblij *et.al.*, 2005). Este método permite medir a resistência adicional na membrana, ΔR_{20} , durante um ensaio de filtração. Para além da filterabilidade das amostras, foi medido, sempre que possível, a concentração de sólidos, as partículas nos intervalos 2-100 μm e 0.4-5.0 μm , produtos microbianos solúveis e viscosidade. Para cada amostra correlacionou-se filterabilidade com os restantes parâmetros medidos, com vista à explicação para o desempenho observado no processo de filtração.

Nos resultados obtidos não foi encontrada nenhuma relação entre a filterabilidade e a concentração de sólidos. Na experiência *Caracterização de Amostras* foi encontrada uma relação tripla entre filterabilidade, produtos microbianos solúveis e temperatura. Nas

temperaturas mais baixas foram registadas elevadas concentrações destas substâncias, que coincidiram com as piores filterabilidades observadas. Esta relação também foi observada na experiência das *Diluições*, embora a nível inferior.

As partículas no intervalo 0.4-1.0 μm revelaram uma relação significativa com os produtos microbianos solúveis. Embora se considere que as partículas destes produtos se encontrem em intervalos de menores dimensões, a contagem de partículas no intervalo 0.4-1.0 μm parece ser uma boa ferramenta indicativa das concentrações de produtos microbianos solúveis existentes em lamas activadas.

Na experiência de Concentração de Sólidos uma melhoria na filterabilidade foi observada quando o TRH variou de 17 para 30.8-40.8 horas, período durante o qual a concentração de sólidos se alterou de 14.3 para 18.2 g/L. No entanto, não é possível assegurar se a concentração de sólidos teve um papel fundamental na filterabilidade.

ABSTRACT

In wastewater treatment, membrane bioreactor systems (MBR) offer several advantages when compared with conventional treatment processes. A small footprint, the production of a high quality effluent, and low sludge production are some of the advantages of this “recent” technology. However, membrane fouling is still a major drawback, increasing the operational costs since intensive aeration and physical/chemical cleaning are required.

This thesis aims to study which characteristics/components present in the sludge constitute an influence in the filterability of activated sludge, which is a measure of fouling propensity.

A research was conducted between September 2008 and February 2009, in which five full-scale MBR were visited. Three different experiments occurred during this period: the *Blank Characterization* experiment to study the characteristics of sludge from MBR; the *Dilutions* experiment to see the effect of different MLSS in membrane filterability, using sludge dilutions with permeate; and the *Solids Concentration* experiment to study the impact of MLSS in filterability through manipulating hydraulic retention time (HRT) in a full-scale MBR. In all experiments the filterability of the sludge was measured through the Delft Filtration Characterization method developed by TUDelft (Evenblij *et. al.*, 2005). This method allows measuring the additional resistance in the membrane during membrane filtration. Also, when possible, other parameters were measured in the sludge such as MLSS, particles in the ranges 2-100 μm and 0.4-5.0 μm , soluble microbial products (SMP), and viscosity. A relationship between filterability and each one of the other parameters was tried to explain the membrane performance.

The results showed that no single or direct correlation between filterability and MLSS existed. From the analysis of sludge from a full-scale MBR, a three-way relationship was observed between filterability, SMP and temperature. Higher concentrations of SMP were observed at lower temperatures, while at the same time filterability showed worst results. This was also confirmed by the analysis of the diluted samples, though at a lower level. The particles in the range 0.4-1.0 μm demonstrated a significant relationship with SMP. Although SMP particles are considered to be smaller than the observed range, particle

counting in the range 0.4-1.0 μm seems to be a good indicative of SMP levels in the activated sludge. The *Solids Concentration* experiment showed that an improvement in membrane filtration occurred when hydraulic retention time (HRT) was changed from 17 hours to 30.8-40.8 hours at the same time that MLSS varied between approximately 14.3 and 18.2 g/L. However, it cannot be assured that MLSS by itself played a major role in filterability.

ABBREVIATIONS

ASP – Activated Sludge Process

BOD - Biological oxygen demand

COD – Chemical oxygen demand

D10p – dilution with 10L of permeate + 20L of sludge

D20p - dilution with 20L of permeate + 10L of sludge

ΔR_{20} - Added resistance when 20 L/m² of permeate have been extracted

DFCi - Delft filtration characterization installation

DFCm - Delft filtration characterization method

DWF – Dry weather flow

EPS - Extracellular polymeric substances

F/M - Food to microorganism ratio

MBR – Membrane Bioreactor

MF - Microfiltration

MLSS - Mixed liquor suspended solids

MLVSS - Mixed liquor volatile suspended solids

MT – Membrane Tank

MWCO – Molecular weight cut-off

NF - Nanofiltration

RO - Reverse osmosis

SMP - Soluble microbial products

SRT - Solids retention time

SVI – Sludge volume index

TMP – Trans membrane pressure

TSS – Total suspended solids

UF - Ultrafiltration

WWTP – Wastewater treatment plant

CONTENTS

1	INTRODUCTION	1
1.1	Membrane Bioreactors, technology of the future?	1
1.2	Goals of this Thesis.....	2
1.3	Structure of the Thesis	2
2	FUNDAMENTALS	3
2.1	Introduction.....	3
2.2	Activated Sludge Process.....	3
2.3	Membrane filtration	6
2.3.1	Membrane filtration process.....	6
2.3.2	Membrane materials	7
2.3.3	Membrane configurations.....	8
2.3.4	Membrane process operation.....	9
2.3.5	Membrane fouling	11
2.4	Membrane bioreactor technology	14
2.4.1	MBR configurations	14
2.4.2	MBR history	15
2.4.3	MBR operating conditions	16
2.4.4	Fouling control and mitigation	19
2.4.5	Comparison between MBR and Conventional Activated Sludge (CAS).....	22
3	LITERATURE REVIEW ON MEMBRANE FOULING	25
3.1	Mixed liquor suspended solids (MLSS)	25
3.2	Particle size	26
3.2.1	Characterization of the wastewater	26
3.2.2	Particle size distribution (PSD) in MBR	27
3.3	Extracellular Polymeric Substances (EPS).....	29
3.3.1	EPS background	29
3.3.2	EPS and membrane fouling	31
3.4	Viscosity	32
3.4.1	Rheology theory	32

3.4.2	Viscosity and membrane fouling.....	35
4	METHODOLOGY	37
4.1	Three different experiments.....	37
4.1.1	Blanks Characterization experiment.....	38
4.1.2	Dilutions experiment	38
4.1.3	Solids Concentration Experiment.....	38
4.2	General measuring protocol.....	39
4.3	Delft Filtration Characterization installation (DFCi).....	41
4.3.1	Membrane	43
4.3.2	Pumps	43
4.3.3	Online measuring instruments	44
4.3.4	Mass balance.....	45
4.3.5	Pressure transmitters.....	46
4.3.6	Programmable Logic Controller (PLC).....	46
4.3.7	Measuring Protocol - DFCm	46
4.3.8	Data acquisition and output	47
4.4	Particle counting in range 2-100 μm	49
4.4.1	Materials	49
4.4.2	Measuring protocol.....	51
4.4.3	Data acquisition	53
4.5	Particle counting in range 0.4 - 5 μm	55
4.5.1	Materials	55
4.5.2	Measuring protocol.....	56
4.5.3	Data acquisition	57
4.6	Soluble Microbial Products (SMP).....	58
4.6.1	Materials	58
4.6.2	Measuring protocol for Proteins	58
4.6.3	Measuring protocol for Polysaccharides	59
4.7	Viscosity	60
4.7.1	Materials	60
4.7.2	Measuring protocol.....	61
4.8	Mixed Liquor Suspend Solids (MLSS)	62

5	BLANKS CHARACTERIZATION EXPERIMENT	63
5.1	Characterization of five MBR systems	63
5.2	Filtration characteristics - ΔR_{20} , MLSS and Temperature	65
5.2.1	Results	65
5.2.2	Correlating filterability with MLSS and Temperature	68
5.3	Particle counting in the range size of 2-100 μm	70
5.3.1	Characterization of the particle size and volume distributions.....	70
5.3.2	Correlation between filterability with particle counting in range 2-87 μm	75
5.4	Particle counting in the range size of 0.4-5 μm	78
5.4.1	Characterization of the particle size and volume distributions.....	78
5.4.2	Correlation between filterability and particle counting in range 0.4-1.0 μm	81
5.5	Soluble Microbial Products	83
5.5.1	SMP results.....	83
5.5.2	Correlating filterability with SMP	85
5.6	Viscosity	87
5.6.1	Results	88
5.6.2	Correlating viscosity.....	89
5.7	Conclusions.....	91
6	DILUTIONS EXPERIMENT.....	95
6.1	Filtration characteristics - MLSS and ΔR_{20}	95
6.1.1	Results and Discussion	95
6.2	Particle counting in the range size 2-100 μm	98
6.2.1	Particle counting characterization	98
6.2.2	Correlation between filterability with particle counting in range 2-87 μm	100
6.3	Particle counting in the range size of 0.4-5.0 μm	101
6.3.1	Characterization of the particle size and volume distributions.....	101
6.3.2	Correlation between filterability and particle counting in range 0.4-1.0 μm ...	102
6.4	Soluble Microbial Products	105
6.4.1	Results	105
6.4.2	Correlating filterability with SMP	107
6.5	Viscosity	109
6.5.1	Results	109

6.5.2	Correlating viscosity.....	111
6.6	Conclusions.....	113
7	SOLIDS CONCENTRATION EXPERIMENT.....	117
7.1	Filterability.....	118
7.1.1	Results	118
7.1.2	Correlating filterability.....	120
7.2	Particle counting in the range size of 2-100 μm	121
7.2.1	Results and Discussion.....	121
7.3	Viscosity	123
7.3.1	Results and discussion.....	123
7.4	Conclusions.....	126
8	GENERAL CONCLUSIONS AND RECOMMENDATIONS FOR FURTHER RESEARCH.....	129
8.1	General conclusions	129
8.2	Recommendations for further research.....	131
9	REFERENCES	132
	APPENDIX I - MBR market in Europe	143
	APPENDIX II – Product details ultrafiltration membrane.....	145
	APPENDIX III – Product details particle counter in range 2-100 μm	147
	APPENDIX IV – Product details particle counter in range 0.4-5.0 μm	149
	APPENDIX V – Product details Anton Paar rheometer	151
	APPENDIX VI – Standard Methods for MLSS.....	153
	APPENDIX VII – Blanks Characterization experiment results.....	157
	APPENDIX VIII – MBR systems configurations.....	163
	APPENDIX IX – Dilutions experiment results.....	165
	APPENDIX X – Solids Concentration experiment results.	175

LIST OF FIGURES

Figure 2-1 - Schematic representation of membrane filtration process.....	7
Figure 2-3 – Membrane types	8
Figure 2-4 –Dead-end and cross-flow filtration	11
Figure 2-5 – Fouling mechanisms in cross-flow filtration	13
Figure 2-7 – Evolution of municipal and industrial MBR applications in Europe along the period 1990-2005	16
Figure 3-1 –Relative contributions (%) of the different biomass fractions to MBR fouling	27
Figure 3-2 –Schematic of EPS and SMP.....	30
Figure 3-3 – Schematic flow curves for model time-independent materials	33
Figure 4-1 – Schematic overview of the DFCm	42
Figure 4-2 – DFCi during filtration campaign at Monheim	43
Figure 4-3 - Additional resistance and TMP alongside permeate volume extraction	47
Figure 4-4 – Overview of resistance, flux, and TMP while extracting permeate.....	48
Figure 4-5 – Overview of CFV, pH, oxygen content, and temperature, during a filtration test.....	49
Figure 4-7 – Particle counting installation at TUDelft laboratory.....	51
Figure 4-8 – Schematic overview of the particle counting installation in range 0.4-5.0 μm	56
Figure 4-9 – Particle counting installation at TUDelft laboratory.....	56
Figure 4-10 – Viscosity installation at TUDelft laboratory.....	61
Figure 5-1 –Filterability plotted against MLSS according to each WWTP	67
Figure 5-2 – Temperature and ΔR_{20} by experiment date.....	68
Figure 5-3 –Filterability plotted against MLSS according to sludge quality	69
Figure 5-4 – Temperature “in situ” vs. ΔR_{20}	69
Figure 5-5 – Particle number distribution representative of different full-scale MBR	71
Figure 5-6 –Cumulative particle number of different WWTP	72
Figure 5-7 - Mean particle size of maximum particle number per WWTP.....	73
Figure 5-8 – Particle volume distribution representative of different full-scale MBR.....	74
Figure 5-9 – Cumulative particle volume per WWTP.....	74

Figure 5-10 – Mean particle size of maximum particle volume.....	75
Figure 5-11 – Cumulative particle number and ΔR_{20} by group quality.....	76
Figure 5-12 – Mean particle size of maximum particle volume per group quality	77
Figure 5-13 – Mean particle size of maximum particle volume vs. filterability	77
Figure 5-14 – Particle number distribution in the range 0.4-5 μm	79
Figure 5-15 – Cumulative particle number in the range 0.4-1.0 μm	80
Figure 5-16 - Particle volume distribution in the range 0.45-1.0 μm	80
Figure 5-17 Cumulative particle number and ΔR_{20} by group quality.....	81
Figure 5-18 - Proteins and polysaccharides by WWTP with respective temperature	84
Figure 5-19 – Protein concentrations plotted against ΔR_{20}	85
Figure 5-20 – Polysaccharide concentrations plotted against ΔR_{20}	85
Figure 5-21 – Proteins and polysaccharides plotted against temperature.....	86
Figure 5-22 – Rheogram for all blanks with the respective MLSS concentration	88
Figure 5-23 – Apparent viscosity per blank samples.....	89
Figure 5-24 – Apparent viscosity from the rheometer measurements and Rosenberger’s and Laera’s formulas	90
Figure 5-25 – Apparent viscosity (100 s^{-1}) and filterability	91
Figure 6-1 – MLSS plotted against ΔR_{20} by set	96
Figure 6-2 MLSS plotted against ΔR_{20} – Group A and Group B	97
Figure 6-4 – Mean particle size of maximum particle number (all sets).....	100
Figure 6-5 – Particle volume distribution (Set 8)	100
Figure 6-6 – Particle number distribution (Set 1).....	102
Figure 6-7 – Cumulative particle number in the range 0.4-1.0 μm vs. ΔR_{20} , by set and group.....	103
Figure 6-8 – Cumulative particle number in the range 0.4-1.0 μm vs. ΔR_{20}	104
Figure 6-9 – Variation of protein and polysaccharide concentrations compared to blank initial concentration (%)	106
Figure 6-11 – Protein concentration and ΔR_{20} by set	108
Figure 6-12 – Shear rate vs. apparent viscosity for Set 3 ($T=20 \pm 1^\circ\text{C}$).....	110
Figure 6-13 – Shear rate vs. apparent viscosity for D10p ($T=20 \pm 1^\circ\text{C}$).....	110
Figure 6-14 – Shear rate vs. apparent viscosity for D20p ($T=20 \pm 1^\circ\text{C}$).....	111
Figure 6-15 - Apparent viscosity (100 s^{-1}) and filterability – D10p and D20p	113
Figure 7-1 – ΔR_{20} and MLSS in January 20 th	119

Figure 7-2 – MLSS and ΔR_{20} in January 22 nd	119
Figure 7-3 – Correlation between ΔR_{20} and MLSS in January 20 th and 22 nd	120
Figure 7-4 – Cumulative particle number and ΔR_{20} on January 20 th and 22 nd	122
Figure 7-5 – Shear rate vs. apparent viscosity for day 20 th	123
Figure 7-6 – Shear rate vs. apparent viscosity for day 22 nd	124
Figure 7-7 – Filterability and apparent viscosity (100 s^{-1}) – January 20 th	125

LIST OF TABLES

Table 2-1 – Membrane processes overview.....	7
Table 2-3 – Cost comparison study between MBR and CAS	23
Table 2-4 – Main advantages and disadvantages of MBR	24
Table 4-1 – Overview of all experiments between September 08 and February 09.....	41
Table 4-2 – Sludge quality according to ΔR_{20} values.....	48
Table 5-1 – Overview of the main differences in the five WWTP.....	65
Table 5-2 - Experiments carried out in the period of September 08 – February 09	66
Table 5-3 – Results from particle counting analysis in the range 2-100 μm	70
Table 5-4 – Results from particle counting analysis in the range 0.4-5 μm	78
Table 5-6 – SMP results: protein and polysaccharide concentrations	83
Table 5-7 – Correlation factors between SMP and particle counting parameters in range 0.4-1.0 μm	87
Table 6-1 – Filtration characteristics from Dilutions experiment.....	95
Table 6-2 – Correlations between filterability and particle counting parameters.....	104
Table 6-3 – Protein and polysaccharide concentrations in mg/L by set	105
Table 6-4 – Proteins and polysaccharides retained in the membrane	107
Table 6-6 – Correlation factors between MLSS and apparent viscosity, according to dilution type.....	112
Table 7-1 – Main results from the filterability tests performed (January 20 th and 22 nd)..	118

1 INTRODUCTION

1.1 Membrane Bioreactors, technology for the future?

The Membrane Bioreactor (MBR) process is a combination of the activated sludge process with a membrane separation step. This recent technology is currently experiencing accelerated growth, and this growth is expected to be sustained over the next decade (Judd, 2006).

One of the major advantages of this technology is the replacement of the secondary sedimentation tank by a membrane, allowing a smaller footprint. Besides reducing the size of the treatment plant, other advantages are inherent to an MBR: a high quality effluent, which can be reused, is achieved as a result of the selectivity of the membrane; higher rates can be reached for removal of biological oxygen demand (BOD) and chemical oxygen demand (COD); a lower excess sludge production takes place.

However, the MBR technology is not yet optimized with membrane fouling being the main drawback. Fouling leads to a decrease of the filtration flux and subsequently of the effluent production. In order to minimize fouling, several procedures are applied such as physical and chemical cleaning, intensive aeration, and pre-treatment of the biomass suspension. These reasons, and also the membrane prices, make MBR an expensive technology.

Membrane fouling can be mainly influenced by three factors: operating conditions, nature of the membrane, and the biomass which is mainly influenced by the nature of the feed solution (Lojkine *et.al.*, 1992).

This thesis focuses on the influence of biomass in membrane fouling.

1.2 Goals of this Thesis

This thesis aims to study which characteristics/components present in the sludge constitute an influence to the filterability of activated sludge, which is a measure of fouling propensity.

In order to obtain results for the proposed objective a careful protocol was defined. Five key parameters for the sludge analysis were chosen: filterability, mixed liquor suspended solids (MLSS), particles in ranges 2-100 μm and 0.4-5.0 μm , soluble microbial products (SMP), and viscosity. Three different experiments were applied with different objectives.

The experiments carried out were always performed with sludge from a full-scale MBR so that the conclusions drawn were closer to “reality”. For this reason, sludge samples were collected from five different MBR located both in The Netherlands and Germany.

1.3 Structure of the Thesis

In *Chapter 2 Fundamentals* the general terms and concepts associated to wastewater treatment, membrane filtration and membrane technology are addressed.

Next, a literature review is given in *Chapter 3* concerning four main topics related to membrane fouling: mixed liquor suspended solids (MLSS), particle size, extracellular polymeric substances (EPS), and viscosity.

The methodology followed on this thesis is presented in *Chapter 4*, where the general measuring protocol is described as well as the materials and methods for each test applied in this research.

The results and discussion from the three experiments realized are presented in *Chapters 5, 6 and 7*. At the end of each chapter the conclusions drawn are shown.

In *Chapter 8*, the general conclusions obtained are demonstrated, and recommendations for further research are given.

2 FUNDAMENTALS

2.1 Introduction

In this chapter, background information is given for this thesis. The Chapter is divided in three parts, firstly focusing on the main characteristics and parameters inherent to the activated sludge process; secondly, membrane filtration is addressed regarding the filtration process, membrane materials and configurations, and also a short overview of membrane fouling; thirdly, membrane bioreactor technology is discussed considering background history, materials and operation process.

In the first part of this chapter, the 4th edition of the handbook on *Wastewater engineering: treatment and reuse* (Metcalf & Eddy, 2003) is used. The second and third parts are a combination of several sources and, especially in the third part, the publications *The MBR book: Principles and Applications of Membrane Bioreactors in Water and Wastewater Treatment* (Judd, 2006) and *Filtration Characteristics in Membrane Bioreactors* (Evenblij, 2006) are used.

2.2 Activated Sludge Process

The activated sludge process (ASP) dates back to 1914 when Arden and Lockett discovered that sludge could be “active” when intensively aerated. Then, the biomass would be able to achieve an aerobic stabilization of organic material which would have an important role in the treatment of wastewater.

The process was developed all over the world and many configurations have been applied since then. Nevertheless, there are three main basic components inherent to this process:

- Bioreactor, where the biomass is kept in suspension and aerated
- Liquid-solids separation, commonly in a sedimentation tank
- Recycle system, to bring back to the bioreactor part of the solids removed in the sedimentation tank

A major feature in the ASP is the formation of floc particles (flocculent settleable solids), between the range size of 50 μm and 200 μm , that can be removed by gravity in sedimentation tanks. The resulting clarified liquid can be discharged and part of the settled sludge can now return to the bioreactor.

In the wastewater treatment two important processes precede the ASP. The first is a preliminary treatment consisting in the removal of coarse solids, grit and grease that may cause maintenance or operational problems in the following processes. Next, a primary treatment is frequently applied to remove part of the suspended solids and organic matter from the wastewater.

Generally, activated sludge aims to remove biodegradable organics, nutrients (nitrogen and phosphorous), and pathogens. The biodegradable organics are principally composed of proteins, carbohydrates and fats, most commonly measured in terms of biochemical oxygen demand (BOD) and chemical oxygen demand (COD). The wide range of microorganisms in activated sludge, principally bacteria, has an essential role in the removal of dissolved and particulate carbonaceous BOD and in the stabilization of organic matter in wastewater.

Nitrogen and phosphorous are also removed by microorganisms. Nitrogen removal consists first in a nitrification reaction where ammonia is oxidized to nitrite and nitrate by specific bacteria, and subsequently in a denitrification process in which oxidized nitrogen is converted into gaseous nitrogen by other bacteria. For phosphorous removal, the growth of bacteria is encouraged, through specific biological processes, with the ability to take up and store large amounts of inorganic phosphorous.

In the bioreactor, or aeration tank, adequate mixing is provided between the influent and the returned sludge from the sedimentation tank, with a biomass concentration. This mixture is usually mentioned as *mixed liquor suspended solids* (MLSS) and *mixed liquor volatile suspended solids* (MLVSS).

The design of ASP has to be adequate to the characteristics of the wastewater in order to achieve a good quality effluent. Solids retention time (SRT), food to microorganisms

(F/M), volumetric organic loading rate and hydraulic retention time (HRT) are the most common design parameters.

SRT is in fact the most critical parameter for activated sludge design since it affects the treatment process performance, aeration tank volume, sludge production and oxygen requirements. It represents the period of time in which activated sludge remains in the system and can be calculated with the following Equation 2-1.

$$SRT = \frac{VX}{(Q - Q_w)X_e + Q_w X_R} = \frac{1}{\mu} \quad (2-1)$$

where

SRT = solids retention time	[d]
V = volume	[m ³]
Q = flow rate	[m ³ d ⁻¹]
Q _w = waste sludge flow rate	[m ³ d ⁻¹]
X = biomass concentration	[m ³ d ⁻¹]
X _e = concentration of biomass in the effluent	[m ³ d ⁻¹]
X _R = concentration of biomass in the return line from sedimentation tank	[m ³ d ⁻¹]
μ = specific grow rate	[d ⁻¹]

Depending on the goal treatment, SRT values can vary from 1 day till 50 days. In the Netherlands the wastewater treatment plants (WWTP) were operated with SRT ranging from 14 days to 36 days during the year 2002 (Evenblij, 2006).

The BOD F/M ratio represents the amount of substrate available for the biomass, and according to reported literature values are between 0.04 g substrate/ (g biomass *d) for extended aeration processes and 1.0 g substrate/ (g biomass *d) for high rate processes. The volumetric organic loading rate is defined as the amount of BOD or COD applied to the aeration tank volume per day. Values, expressed in kg BOD or COD/ (m³*d), may vary from 0.3 to more than 3.0 (Metcalf & Eddy, 2003).

The ASP ends in the sedimentation tank where the liquid-solids separation takes place. The settling characteristics of the MLSS must be considered when designing the sedimentation tank to provide adequate clarification of the effluent and solids thickening for the activated-sludge solids. To quantify the settling characteristics of activated sludge, two tests are ordinarily used: the sludge volume index (SVI) and the zone settling rate. For further reading see Metcalf & Eddy (2003), pp. 684-686.

To maintain a given SRT, the excess activated sludge produced each day must be wasted. Usually part of the return sludge from the sedimentation tank is wasted since it is more concentrated and requires smaller waste sludge pumps.

The following processes involving sludge (solids and biosolids) are treatment, reuse and disposal. These are considered the most complex problem in the wastewater field due to the fact that solids and biosolids are by far the largest in volume. The principal methods used are thickening, conditioning, dewatering, and drying, to remove moisture from solids; digestion, composting, and incineration, to treat or stabilize the organic material in the solids.

2.3 Membrane filtration

2.3.1 Membrane filtration process

In wastewater treatment, membrane filtration is a separation process between two phases - solid and liquid. The membrane is the selective barrier that allows the passage of certain constituents and retains other constituents present in the liquid (Cheryan, 1998).

The constituents retained by the membrane form the retentate and those capable of passing through become permeate, see Figure 2-1. The selectivity of a membrane is determined by its pore size, that can be defined in terms of equivalent diameter, commonly in μm (10^{-6} m), or by molecular weight cut-off (MWCO) expressed in Daltons. Koros *et.al.*, (1996) defined MWCO as the “molecular weight of a solute corresponding to a 90% rejection coefficient for a given membrane”.

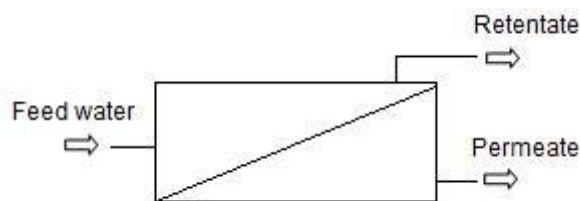


Figure 2-1 - Schematic representation of membrane filtration process

There are four main membrane separation processes: microfiltration (MF), ultrafiltration (UF), nanofiltration (NF) and reverse osmosis (RO), see Table 2.1.

Table 2-1 – Membrane processes overview (Metcalf & Eddy, 2003; Judd, 2006)

Membrane process	Pore size range (μm)	MWCO (Da)	Permeate description	Removed constituents
Microfiltration	0.1-1	500,000	Water + dissolved solutes	TSS, turbidity, protozoan oocysts and cysts, some bacteria and viruses
Ultrafiltration	0.01-0.1	1,000	Water + small molecules	Macromolecules, colloids, most bacteria, some viruses, proteins
Nanofiltration	0.001 – 0.01	100	Water + very small molecules, ionic solutes	Small molecules, some hardness, viruses
Reverse osmosis	0.0001 – 0.001	100	Water + very small molecules, ionic solutes	Very small molecules, color, hardness, sulfates, nitrate, sodium, other ions

2.3.2 Membrane materials

The membranes are required to have certain characteristics in order to guarantee highly efficient filtration, low operational and maintenance costs, and a long-term life. The membrane should provide a high surface porosity, narrow pore size distribution, mechanical strong structure, and a high resistance to thermal and chemical attack (Judd, 2006).

In MBR technology two different materials are used for membrane manufacture – polymeric and ceramic. The most applied in water treatment applications are hydrophilic polymer membranes because of their good wettability and the lesser tendency of hydrophobic components to foul the membrane (Mulder, 1996). Besides that, they are less expensive than ceramic membranes. The most common materials for polymeric membranes are:

- Polyvinylidene difluoride (PVDF)
- Polyethylsulphone (PES)
- Polyethylene (PE)
- Polypropylene (PP)

2.3.3 Membrane configurations

When designing MBRs, three essential membrane configurations can be employed (Mudler, 1996): plate-and-frame/flat sheet, hollow-fiber and (multi)tubular, see Figure 2-2.

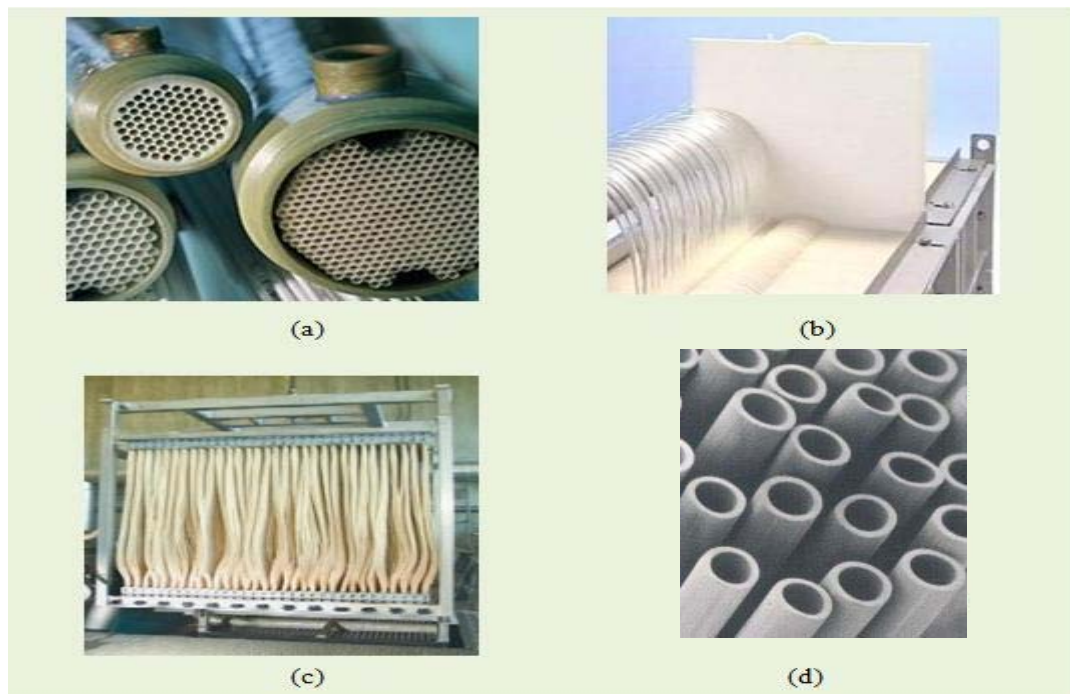


Figure 2-2 – Membrane types: (a) tubular membranes (Berghof); (b) module of flat sheet membranes (Kubota); (c) module of hollow-fiber membranes (Zenon); (d) hollow-fiber membranes(Mitsubishi)

The operation mode relative to the flow is different in each configuration. Flat sheet is operated outside-to-in, multi-tubular is operated inside-out, and hollow-fiber can be operated in both modes. In Table 2-2 the membrane configurations are presented with the respective selectivity application.

Table 2-2 – Membrane configurations (Evenblij, 2006; Judd, 2006)

Configuration	Cost	Turbulence promotion	Application
Flat sheet	High	Moderate	UF, RO
Multi-tubular	Very high	Very good	MF, UF, NF
Hollow-fiber	Very low	Very poor	MF, UF, NF, RO (inside-out)

2.3.4 Membrane process operation

In any membrane process operation there are five major elements influencing the permeate flux, these being the membrane resistance, the operational driving force, the hydrodynamic conditions at the membrane/liquid interface, fouling and subsequent cleaning of membrane surface (Judd, 2006).

Process parameters

The permeate flux (J) is the quantity of material passing through a unit of membrane per unit of time. The SI units are $\text{m}^3\text{m}^{-2}\text{s}^{-1}$, but the typical units are in liters per m^2 per hour (LMH). The permeate flux can be calculated by Darcy's law (Lojkine *et.al*, 1992):

$$J = \frac{\Delta P}{\eta_p R_t} \quad (2-2)$$

where

J = permeation flux	$[\text{Lm}^{-2}\text{h}^{-1}]$
ΔP = transmembrane pressure	$[\text{Pa}]$, or $[\text{bar}]$
η_p = permeate dynamic viscosity	$[\text{Pa}\cdot\text{s}]$
R_t = total filtration resistance	$[\text{m}^{-1}]$

In most water treatment membrane processes the driving force for permeation is trans membrane pressure (TMP). TMP consists in the difference between feedstream pressure and permeate pressure.

The total filtration resistance (R_t) is the sum of the clean membrane resistance (R_m) and a fouling resistance (R_f):

$$R_t = R_m + R_f \quad (2-3)$$

The permeability, which is inversely proportional to total filtration resistance, is a common parameter to characterize the MBR performance. It can be calculated through equation 2-4.

$$P = \frac{J}{TMP} \quad (2-4)$$

where

P = permeability	[Lm ⁻² h ⁻¹ bar ⁻¹]
J = permeation flux	[Lm ⁻² h ⁻¹]
TMP = transmembrane pressure	[Pa], or [bar]

Dead-end and cross-flow operation

Basically two modes of membrane filtration exist: dead-end and cross-flow filtration, see Figure 2-3.

In dead-end filtration all feed water is filtered through the membrane resulting in an accumulation of retained components at the membrane surface (retentate). For cross-flow filtration only a fraction of the feed water that flows along the membrane surface is converted to permeate.

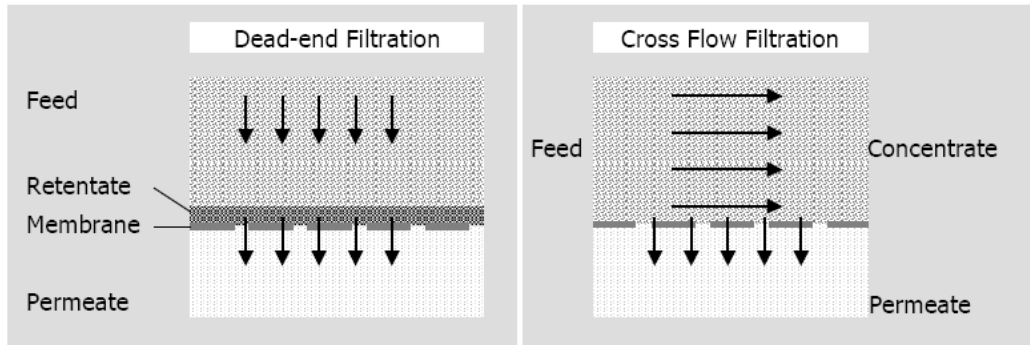


Figure 2-3 –Dead-end and cross-flow filtration (Evenblij, 2006)

Inevitably both operation modes lead to an increase in resistance, though in different ways. In dead-end the resistance increases according to the thickness of the cake formed on the membrane. Consequently, permeability decays rapidly and frequent cleaning is required. In cross-flow operation the deposition in the membrane only remains until the adhesive forces in the cake are disrupted by the continuous cross flow stream and force it to move along the membrane.

When comparing both filtration modes, cross-flow operation can treat water with higher solids content and achieve higher fluxes (since the cross-flow stream minimizes the buildup of constituents in the membrane surface). On the other hand, the circulation of feed water in cross-flow filtration requires higher energy thus raising the operational costs.

2.3.5 Membrane fouling

The increase in filtration resistance over time is caused by membrane fouling and is a natural consequence of the membrane separation process. Membrane fouling has been reported with several definitions.

Van den Berg and Smolders (1990) stated that fouling consists in a long-term process that could be more or less irreversible, in which a flux decline is observed. Also, Cheryan (1998) described the membrane fouling as the decline of flux and emphasizing that all operating parameters are kept constant.

The International Union of Pure and Applied Chemistry (IUPAC) also defined membrane fouling as: “*Process resulting in loss of performance of a membrane due to deposition of suspended or dissolved substances on its external surfaces, at its pore openings, or within its pores*”. (Koros *et.al*, 1996)

However, membrane fouling is widely referred to as a decrease of performance in the separation process, i.e. a flux decline at constant TMP or an increase on TMP for a constant flux (reducing permeability) (Judd, 2006).

Membrane fouling is the main limitation of MBR technology, increasing the operational costs and keeping MBRs less competitive in comparison to conventional wastewater treatment plants. There are three main factors that influence fouling: operating conditions, nature of the membrane, and biomass (Lojkine *et.al*, 1992).

Fouling mechanisms

There are two different components in membrane fouling: reversible and irreversible fouling. Reversible fouling is considered as the loosely bound fouling part in which concentration polarization and cake layer formation are often considered as important reversible fouling mechanisms. Reversible fouling is mainly removed by physical cleaning. On the contrary, irreversible fouling is caused by strong adherence to the membrane such as pore blocking and gel layer formation. Irreversible fouling can be partially removed by chemical cleaning.

During cross-flow filtration different fouling mechanisms may occur (Van den Berg and Smolders, 1990), (Figure 2-4).

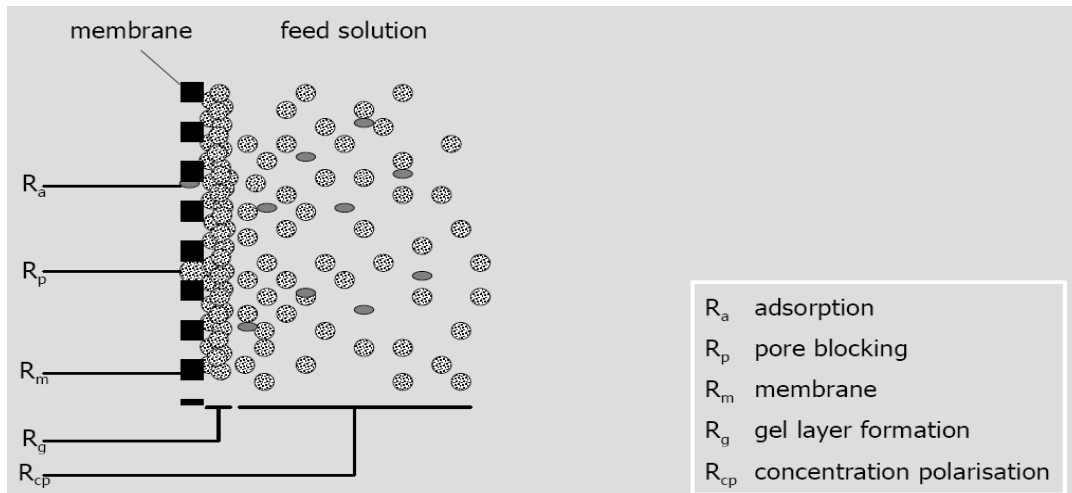


Figure 2-4 – Fouling mechanisms in cross-flow filtration (Evenblij, 2006)

- **Pore blocking**

The pore of the membrane is blocked by particles that were not able to pass through due to particle size or MWCO. The number of pore channels for permeation decreases.

- **Pore narrowing (adsorption)**

Particles and/or substances enter the pore and are absorbed by the pore wall reducing the pore size; as a result, permeability becomes lower.

- **Cake or Gel layer formation**

A layer is formed near the membrane surface with an accumulation of particles and macromolecules. If the constituents are non-interacting, the layer is more permeable –cake layer- and may be removed by increasing TMP or the cross-flow. The cake layer can be removed by physical means such as relaxation of the membrane and back-wash. When an interaction between the particles and the membrane takes place, a cohesive gel layer is formed which is less permeable and more difficult to remove (only by chemical cleaning). Both types of layers will lead to an increase in the total filtration resistance.

- **Concentration polarization**

IUPAC defined concentration polarization (CP) as “*a concentration profile that has a higher level of solute nearest to the upstream membrane surface compared with the more or less wellmixed bulk fluid far from the membrane surface*”.

The origin of the term CP is related to RO applications. Since the pore size is extremely small, there is a back transport of solvent from the permeate side to the feed side leading to an increase in the osmotic pressure. CP promotes the increasing of overall resistance at the membrane/solution interface during membrane filtration.

2.4 Membrane bioreactor technology

2.4.1 MBR configurations

There are two possible configurations relative to the position of the membranes in the MBR process: submerged and sidestream, (Figure 2-5).

In a submerged mode, as the name describes, the membranes are submerged in the aeration tank and the permeate extraction occurs under vacuum to the inside of the membrane. In the sidestream, the membranes are apart from the reactor and sludge is recirculated through the membrane, where permeate extraction takes place from the inside-out. Generally, hollow-fiber and plate and frame modules are use for a submerged MBR and tubular membranes for a sidestream operation.

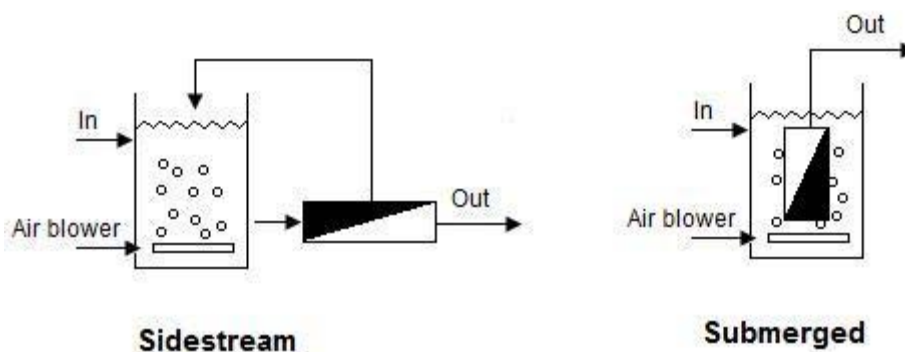


Figure 2-5 – Schematic of sidestream and submerged configurations

The sidestream configuration requires more energy than the submerged configuration since in sidestream high pressures and volumetric flows are imposed when pumping the feed water to the membrane modules. On the other hand, although submerged MBRs have a lesser energy demand, they have an inherently higher fouling propensity compared to sidestream MBRs, since they are operated at higher fluxes (which will lead to lower permeabilities) [Judd, 2006].

2.4.2 MBR history

The first MBR process was introduced in the late sixties, immediately after UF and MF membranes were commercially available. Even though the idea of replacing the sedimentation tank of the conventional activated sludge process (CASP) was attractive, the membrane costs were too high and the filtration performance was compromised due to fouling phenomena.

Only in 1989 the MBR breakthrough happens when Yamamoto *et.al.*, (1989) had the idea to submerge the membranes in the bioreactor, instead of the external (sidestream) configuration used until then. Moreover, the design and operation parameters in MBR were improving with time. In the beginning, MBRs were operated with SRTs that could go up to 100 days and MLSS concentrations above 30 g/L. Nowadays, a lower SRT is applied (10-20 d) with MLSS around 10-15 g/L. Since the operational conditions started to change, better results were achieved in the MBR process, lowering the fouling propensity and decreasing the costs of membrane maintenance (Le-Clech *et.al*, 2006).

In geographical terms, the MBR technology entered the Japanese market in the 1970s. In 1980 the Japanese government invested in the development of a low footprint, high product quality process that would be suitable for water recycling. For this purpose, the Kubota plate and frame membrane was developed. Essentially, the spread of this technology was for small-scale applications (Evenblij, 2006). In the American continent, a hollow-fiber submerged membrane was created by Zenon. In the 1990s the process was extended for WWTP at a larger scale and the USA and Europe registered numerous developments.

Lesjean and Huisjes (2008) reported the existence of about 100 MBRs for municipal WWTP and about 300 for industrial applications in Europe, (Figure 2-6).

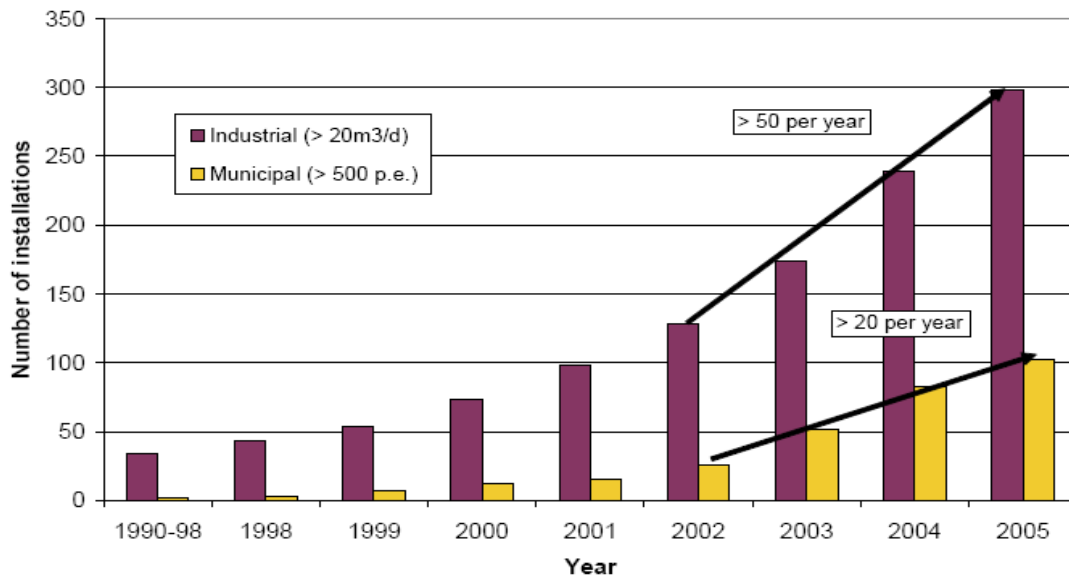


Figure 2-6 – Evolution of municipal and industrial MBR applications in Europe along the period 1990-2005 (Lesjean and Huisjes, 2008)

Naturally, with the market development, new suppliers of MBR filtration systems emerged such as Toray, Mitsubishi, Norit, Kms, etc. See Appendix I for further information.

2.4.3 MBR operating conditions

In a membrane separation process there are three possible ways to operate: at constant TMP, with constant permeate flux or a combination of these two (Evenblij, 2006). At constant TMP, flux will decline over time; with constant flux, higher TMP will be required as the process continues; when a combination of both these processes is applied, good results are obtained diminishing membrane fouling ((Vyas *et.al*, 2002) cited in Evenblij, 2006)).

Aeration (aerobic systems), cross-flow velocity

Most likely, aeration is the most important parameter for MBR design and operation (Judd, 2006). Aeration is necessary for biotreatment, for keeping the mixed-liquor in suspension, and for membrane scouring. A cross flow stream over the membrane surface produced by air bubbling induces a tangential shear stress, which prevents large deposition of particles and increases back transport phenomena. This results in a higher transference rate of liquid through the membrane. Nevertheless, the lateral migration velocity for smaller particles is

much less given that it is proportional to the cube of particle diameter. This implies a stricter fouling caused by fine materials.

Several authors have reported a nearly linear relationship between permeate flux and aeration rate up to threshold value in which no increase in permeability occurs. On the other hand, it has also been reported that intensive aeration may damage the floc structure, reducing floc size and releasing EPS in the mixed-liquor.

Since cross-flow velocity (CFV) is also a function of aeration intensity, a critical value was reported. Liu *et.al*, (2000) stated that when CFV is lower than 0.3 ms^{-1} , the TMP increased sharply, suggesting that sufficient cross flow velocity should be induced to retard membrane fouling.

Solids Retention Time (SRT)

SRT is an important operating parameter impacting on fouling propensity in MBRs. The increase of SRT, and consequent reduction of F/M ratio, leads to an increase of MLSS concentration and a change in biomass characteristics. Extremely low SRTs (down to 2 days) have been tested to evaluate fouling predisposition. The results have shown that the fouling rate increased nearly 10 times when the SRT was lowered from 10 days to 2 days (corresponding to F/M ratio from to 0.5 to $2.4 \text{ gCOD gMLVSS}^{-1} \text{ day}^{-1}$ and MLSS of 7.8 – 6.9 g/l). In practice, the F/M ratio is generally maintained below $0.2 \text{ gCOD gMLVSS}^{-1} \text{ day}^{-1}$ (Le-Clech, 2006).

Long SRTs minimize the excess sludge production but increase MLSS concentration. This has been reported as a main cause for membrane clogging, particularly due to the progressive accumulation in the MBR tank of non-biodegradable materials (like hair and lint), which are not completely removed by the MBR pre-treatment processes. On the other hand, most of the substrate is consumed at higher SRTs to ensure the maintenance needs and the synthesis of storage products. The very low apparent net biomass generation observed can explain the low fouling observed in higher SRT operation [Le-Clech, 2005].

Cho *et.al*, (2005) observed temporal changes of the bound EPS levels when tested in MBR different SRTs - 8, 20 and 80 days. The results showed that the concentration of extracted

EPS was lower for the longer SRT (83–26 mgTOC/gSS for SRT of 8 up to 80 days respectively).

Although considered a key parameter in determining fouling propensity through MLSS and EPS fractions, SRT has most likely less impact on fouling than feedwater quality (Judd, 2006).

Unsteady state operation

Unsteady state can be characterized by variations in the flow input, in the hydraulic retention time (HRT), in the organic loading rates and shifts in the oxygen supply. In MBR operation, unsteady conditions can occur regularly and cause impact on fouling propensity.

From experiment work it was concluded that unsteady operation changed the nature and/or structure (and fouling propensity) of the polysaccharides rather than the overall EPS formation, and therefore could worsen the fouling propensity ((Drews *et.al*, 2005) cited in Judd, 2006)).

Critical Flux (J_c)

There are several definitions for critical flux (J_c). However, this concept was first introduced with the following definition: “*The critical flux hypothesis for MF/UF processes is that on start-up there exists a flux below which a decline of flux with time does not occur; above it, fouling is observed*” (Field *et.al*, 1995).

For real application in MBR the “secondary critical flux”, or “sustainable flux”, is used. Basically, in a “sustainable” flux TMP increases gradually at an acceptable rate until the critical value is reached. What is problematic in MBR operation is to define at which flux should the membrane filtration be operated. To achieve a higher critical flux, a higher shear stress is required, therefore increasing the costs for aeration. On the other hand, lower fluxes require a lower production rate of effluent which reduces its applicability for reuse. Thus, it is important to study the relationship energy costs vs. permeate flux.

2.4.4 Fouling control and mitigation

In MBR operation, in order to achieve a better performance in the membrane separation process, fouling must be controlled and mitigated. Basically, the main strategies used in practice are (Le-Clech, 2006):

- a) Physical cleaning
- b) Chemical cleaning
- c) Optimization of membrane characteristics
- d) Optimization of operating conditions
- e) Pre-treatment of the biomass suspension

a) Physical cleaning

The techniques employed in MBRs for physical cleaning include membrane relaxation while filtration is paused and backwashing (or back flush) in which permeate is pumped in the reversed direction through the membrane. Backwashing is a successful operation to remove most of the reversible fouling caused by pore blocking. The constituents blocking the pore are removed back into the mixed-liquor and clogging near the membrane surface may also be partially loosened or removed by this technique.

When designing backwashing, key parameters such as frequency, duration, the ratio between these two and intensity have to be taken into consideration. The increase of frequency and duration is expected to remove more fouling. However, an optimum relation between these two parameters has to be accomplished. Jiang *et.al*, (2005) stated that less frequent, but longer backwashing (600 s filtration/45 s backwashing) was found to be more efficient than more frequent backwashing (200 s filtration/15 s backwashing).

Membrane relaxation considerably improves the membrane productivity. Under relaxation, back transport of foulants is naturally enhanced. When relaxation is conjugated with air scouring, higher removal efficiencies are obtained.

Depending on the membrane type, different physical cleaning protocols are applied.

b) Chemical cleaning

Chemical cleaning is required since physical cleaning only removes reversible fouling. Different types can be applied such as chemically enhanced backwash (on a daily basis), maintenance cleaning with a higher chemical concentration (weekly), and intensive (or recovery) chemical cleaning (once or twice a year).

The most common cleaning agents are sodium hypochlorite, NaOCl, (for organic foulants) and citric acid (for inorganics). Sodium hypochlorite hydrolyzes the organic molecules, and therefore loosens the particles and biofilm attached to the membrane. For maintenance cleaning, a cycle of 30 min or more is usually carried out every 3-7 days with a moderate reagent concentration of 0.01 wt.% NaOCl (wt. denotes total weight). In recovery cleaning, much more concentrated reagents are employed such as 0.2–0.5 wt. % NaOCl coupled with 0.2–0.3 wt. % citric acid or 0.5–1 wt. % oxalic acid (Le-Clech, 2005).

As well as for the physical cleaning, the chemical cleaning procedure varies according to the membrane type.

c) Optimization of membrane characteristics

Because of the hydrophobic interactions occurring between solutes, microbial cells and membrane material, membrane fouling is expected to be more severe with hydrophobic rather than with hydrophilic membranes. Efforts have been made in trying to increase the hydrophilic properties of a membrane, particularly through chemical modifications. With the introduction of polar groups (from oxygen and nitrogen) on the membrane surface, the membrane hydrophilicity extensively enlarged and better filtration performances and flux recovery were observed.

d) Optimization of operating conditions

Aeration is one of the major factors for energy consumption in MBR operation. Many attempts have been made to optimize designing of airflow rate. The airflow patterns and location of the aerators have been defined as crucial parameters. Besides that, the aeration system has to be designed according to each membrane configuration since the effect of aeration varies according to membrane type.

To guarantee a lower demand of energy, the MBR process should be conducted at a sustainable flux, i.e. a flux at which the TMP increases gradually at an acceptable rate, so that chemical cleaning is not necessary. In this way the operation can have lower costs. Also, different strategies should be studied to find practical solutions in order to maintain the desirable flux.

e) Pre-treatment of the biomass suspension

The addition of coagulants such as ferric chloride and aluminum sulfate (alum) is a common practice used in MBRs to reduce membrane fouling. The alum, when dissolved in water, forms hydroxide precipitates which adsorb suspended particles, colloids and soluble organics. Experiments have shown that the addition of alum resulted in a significant decrease of the carbohydrate fraction of SMP along the filtration process. A lower impact on membrane fouling was observed, probably due to the formation of larger microbial flocs. Although more expensive, ferric chloride showed higher efficiencies when compared to alum. Other coagulant currently used is zeolite which allows the creation of rigid flocs that have lower specific fouling resistance.

Other technique used is the pre-treatment of the feed which is a fundamental step for optimum MBR performance. Different types of sieving can be applied permitting that the influent in the MBR is less compromising to the membrane filtration.

The use of powdered activated carbon (PAC) into biological treatment decreases the level of pollutant, particularly organic compounds. The mixture of PAC with biological suspension in an MBR results in a gradual incorporation of the activated carbon into the biofloc. This way EPS is absorbed into PAC reducing its impact on membrane process.

However, additions of PAC should be done carefully to avoid damage to the membranes.

2.4.5 Comparison between MBR and Conventional Activated Sludge (CAS)

Activated sludge

In activated sludge biological treatment, one of the most notable differences between MBR and CAS operation is the MLSS concentration. While in the CAS aeration tank the solids content can vary in the range 2 to 5 g/L, in MBR it can be up to 15 g/L (Seyssiecq, 2008). When considering an MBR for industrial wastewater treatment, MLSS can go up to 40 g/L (Rosenberger and Kraume, 2002),

Due to this significant difference, the sludge rheological properties will differ. Sludge with higher MLSS is expected to be more viscous. However, in MBR the sludge viscosity is lower than in CAS (Defrance *et.al*, 2000). Since sludge viscosity decreases with increasing shear rate (Rosenberger *et.al*, 2002), this is explained by the higher shear rates applied in MBR (see Section 3.4). Also, lower oxygen transfer efficiencies are a consequence of increasing MLSS.

Treatment efficiency

Since in MBR applications the activated sludge principle is used, the removal efficiencies do not differ substantially when comparing to those of CAS. The removal efficiencies for COD, BOD and SS are high and the effluent is particle free.

In experiments with synthetic feedwater Cicek *et.al*, (2000) found efficiency removals of 98% for COD and for Kjeldahl nitrogen. Adam *et.al*, (2002) stated that in MBR the total phosphorous in the effluent was always lower than 0.2 mg/L for an SRT of 16 to 25 days.

Sludge production

The SRT is a factor that influences the production of sludge. Longer SRTs result in lower sludge production, (Equation 2-1). In MBR the secondary sludge production is lower than in CAS since a higher SRT is applied. However, the primary sludge production is higher due to a higher degree of pre-treatment.

The dewaterability of waste activated sludge from MBRs is much higher when compared to aerobic waste sludge from CAS systems ((Kraume and Bracklow, 2003) cited in Evenblij, 2006).

System footprint

One of the major advantages of an MBR is its reduced system footprint. The substitution of a second clarifier with membranes enables the total rejection of suspended solids without a settling process (Bae and Tak, 2005). This means that an MBR can be operated at higher volumetric loading rates by retaining a high concentration of sludge. Thus, the required space for the aeration tank can be reduced.

Membranes

The most visible difference between CAS and MBR are the membranes. In spite of the many advantages provided by membrane filtration (reduced footprint, higher loading rates, high-quality effluent free of pathogens and most bacteria), the costs for the membranes and for operation and maintenance are still a drawback.

A study made by Davies *et.al*, (1998) compared the costs between two different WWTPs, MBR and CAS, for two different capacities of 2,350 p.e. and 35,500 p.e. (p.e. denotes population equivalent), (Table 2-3).

Table 2-3 – Cost comparison study between MBR and CAS (Davies *et.al*, 1998)

		Capital Costs *	Operating Costs /year *
MBR (Kubota)	2,350 p.e.	613,000	75,373
	CAS	980,204	56,200
MBR (Kubota)	37,500 p.e.	7,292,524	602,101
	CAS	3,642,259	264,730

* Currency not specified

For the purposes of this study, a lifetime of 7 years for the membrane and a total capacity of 2 times Dry Weather Flow (DWF)¹ were defined. The authors concluded that MBR can compete with CAS when the population equivalent is 2,350. For 37,500 p.e. MBR was 2 times more expensive than CAS, in terms of capital and operating costs.

¹ DWF – the average effluent flow during a 7-day period of dry weather, as defined by stringent rainfall limits

However, it is important to remark that the effluent quality obtained in an MBR system is much higher than the one from a CAS, besides the fact that MBR effluent can be reused. This topic was not included in the cost comparison.

Summing up, the main advantages and disadvantages inherent to MBR applications are presented in Table 2-4.

Table 2-4– Main advantages and disadvantages of MBR (adapted from Stephenson *et.al*, 2000)

Advantages	Disadvantages
Small footprint	Membrane fouling
Complete solids removal from effluent	Aeration limitations
Reuse of a high quality effluent	Membrane costs
High loading rate capability	High costs for operation and maintenance
Low sludge production	Process complexity
Rapid start up	
Sludge bulking not a problem	

3 LITERATURE REVIEW ON MEMBRANE FOULING

This chapter aims to review the current literature on membrane fouling in MBRs with particular reference to the effects of mixed liquor suspended solids (MLSS), particle size, extracellular polymeric substances (EPS), and viscosity.

3.1 Mixed liquor suspended solids (MLSS)

Since one of the major features in MBR systems is the possibility to operate at higher MLSS concentrations, this is one of the most investigated parameters. The general trend found in literature is for membrane fouling to increase with increasing MLSS concentrations. Since a higher solids content leads to a higher viscosity, higher shear rates are required to maintain a turbulent regime during membrane filtration. Given that shear stress is fundamental to decrease the fouling propensity in MBR, the MLSS should be a parameter to take into account.

However, no consensus exists (yet) about the influence of solids content in membrane filterability since many different experiments have shown contradictory results. Most likely, the main reason for this is the complexity and variability of the biomass components.

The impact of MLSS concentration was studied by Meng *et.al.*, (2007a). Artificial sludge was used and shifted from 2 g/L till 20 g/L to observe the impact on membrane fouling. In addition, aeration was also investigated with three different intensities (200, 400 and 600 L/h) for each MLSS concentration. The major role played by MLSS concentration on membrane fouling resistance was conclusive. The aeration had small impact on membrane fouling when MLSS was lower than 10 g/L. Thus, in order to operate an MBR, MLSS should be maintained at lower values. Deffrance and Jaffrin (1999), and Bae and Tak (2005) also stated that MLSS was a main contributor for membrane fouling.

Le-Clech *et.al.*, (2003) also studied the effect of MLSS through the flux-step method, which comprehends the concept of critic flux, J_c (Section 2.4.3). In this method the J_c is

defined as the highest flux at which TMP stays steady. In this experiment the flux-step height ranged from 8 to 12 LMH with a 15 min step, and three different MLSS concentrations were investigated: 4, 8 and 12 g/L. The results showed no significant difference when MLSS shifted from 4 g/L to 8 g/L, however, for a MLSS of 12 g/L, J_c showed greater values. Inherent to this study is the fact that an increase in MLSS leads to lower fouling rates resulting in a better filtration performance. Also, the same relationship was observed by Madaeni *et.al*, (1999) (cited in Lousada-Ferreira *et.al*, (2008)).

Other researchers attributed to MLSS a negligible role in membrane fouling. No effect was observed from 3.6 g/L till 8.4 g/L (Harada *et.al*, 1994), from 7.1 g/L till 14.1 g/L (Lesjean *et.al*, 2005) and from 30 g/L till 40 g/L (Yamamoto *et.al*, 1999).

3.2 Particle size

3.2.1 Characterization of the wastewater

In order to have a better understanding of the impact of particle size on membrane fouling, it is primary to characterize the different constituents present in the wastewater according to its particle size.

Several classifications are applied to different fractions in wastewater. In this thesis the classification from Metcalf & Eddy (2003) is used. The category of contaminants is divided in: dissolved ($< 0.001 \mu\text{m}$), colloidal ($0.001 - 1 \mu\text{m}$), supracolloidal ($1 - 100 \mu\text{m}$) and settleable ($>100 \mu\text{m}$).

The role of each fraction in membrane fouling has several interpretations. Bouhabila *et.al*, (2001) stated that the contribution of colloids and solutes to membrane fouling is 75% whilst Bae and Tak (2005) reported 17%, (Figure 3-1).

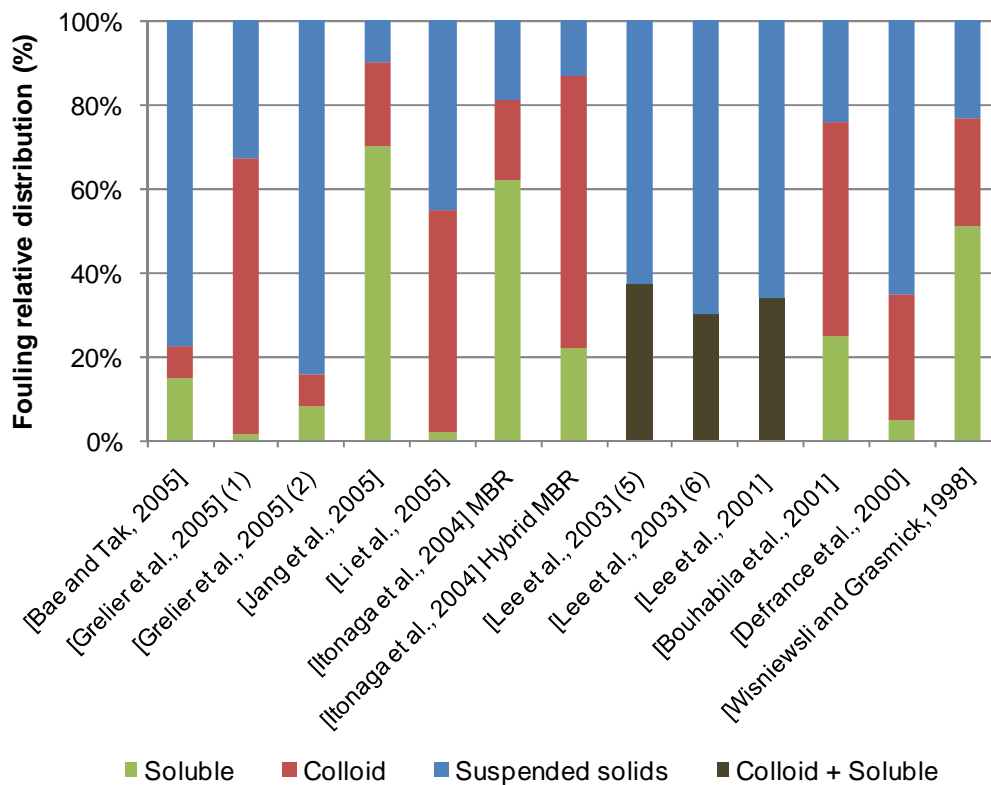


Figure 3-1 –Relative contributions (%) of the different biomass fractions to MBR fouling (adapted from Judd, 2006)

Such variation is probably caused by the operating conditions and biological state of the biomass, and the different fractionation methods.

Despite the divergence of results, the main trend is that the colloidal and soluble fractions are highly important in influencing membrane fouling.

3.2.2 Particle size distribution (PSD) in MBR

Wisniewski and Grasmick (1998) found that 15% of the particles in a biological suspension have a size lower than 100 μm . Also, without recirculation, the size of the flocs varies between 20 μm and up to 500 μm . Moreover, a clear reduction of the particle size was observed when sludge was recirculated. The reducing of the particle size showed a relationship directly proportional to the magnitude of the shear stress and time experiment. Therefore it was concluded that intensive recirculation leads to a floc breakage and subsequently to a modification in the particle distribution. This leads to a decrease of

the settleable fraction and consequently to an increase of the non-settleable fraction, or soluble fraction (polysaccharides, phospholipid, proteins, etc.). Half of the total resistance was due to soluble compounds. Meng *et.al.*, (2006) also stated that the membrane fouling resistance increased as the particle size decreased, mainly due to the deposition of small particles and colloids on the membrane surface.

Leet *et.al.*, (2003) studied the effect of SRT on PSD. SRTs in the range of 20-60 days were applied showing similar floc sizes. Although a slight increase of the floc from 5.2 to 6.6 μm was observed when SRT increased from 20 to 60 days.

As result of a study for particle characterization in MBR, Bae and Tak (2005) reported that in a MBR mixed-liquor most particles existed in a size range between 10 μm and 40 μm , and the mean particle size was 25 μm . The particle size range of the supernatant (or free water) showed a mean diameter of 9 μm . The shear stress was found to be a factor in increasing both the concentration and mean particle diameter of supernatant by breakage of larger particles. A significant role was also attributed to solutes in membrane fouling.

Ivanovic and Leiknes (2008) studied the impact of aeration rates on particle colloidal fraction in the biofilm membrane bioreactor. Results showed a clear increase of particles in the colloidal fraction, particularly below 0.1 μm , with increasing aeration rates. The author outlined the importance of finding the right balance between the sufficient aeration to minimize membrane fouling, while preventing the formation of colloidal particles due to excessive shear forces caused by aeration. Åhl *et.al.*, (2006) also reported a major role of aeration in the formation of more colloidal particles through particle breakage, resulting in an important component of membrane fouling.

Geilvoet *et.al.*, (2007) carried out an experiment aiming at the analysis of the SMP in different fractions and particle counting in the size range 0.4-5.0 μm . The filterability of the sludge was measured according to the DFCm (Section 5.1.7). Results showed a decrease of filterability while an increase of SMP concentrations in the free water was registered. All SMP were found smaller than 0.2 μm and SMP particles in the range 0.2 μm to 1.2 μm were absent. Therefore, the particle distribution in the range size 0.4-5.0 μm was not correspondent to the SMP analyses.

3.3 Extracellular Polymeric Substances (EPS)

3.3.1 EPS background

Extracellular polymeric substances (EPS) are largely appointed as one of the most crucial contributors for membrane fouling (Nagaoka *et.al*, 1996; Rosenberger and Kraume, 2002; Cho and Fane, 2003; Rojas *et.al*, 2005; Al-Halbouni *et.al*, 2008).

EPS is used as a general term which includes all classes of macromolecules such as carbohydrates, proteins, nucleic acids, lipids and other polymeric compounds found at the cell surface or in the intercellular space of microbial aggregates. However, the main components of EPS are proteins (up to 60 %) and polysaccharides (40-95 %) (Flemming and Wingeder, 2001), and both have a natural tendency to form a gel layer which is highly structured (Poele, 2005).

EPS is responsible for the aggregation of bacterial cells in flocs and biofilms, the formation of a protective barrier around the bacteria, retention of water and adhesion to surfaces (Lapidou and Rittman, 2002). EPS also has an important function in microbial survival since it facilitates the interactions between cells and their environment. Due to its heterogeneous and changing nature, EPS can form a highly hydrated gel matrix in which microbial cells are embedded and can therefore create a significant barrier to permeate flow in membrane filtration (Judd, 2006).

EPS in activated sludge can be found in two different ways: cell-associated EPS in which it is closely bound to cells and, dissolved EPS into water phase (free water) which is detached from bacterial cells (Nagaoka and Akoh, 2008). Cell-associated EPS accumulates on the membrane surface as strongly bound EPS, whilst dissolved EPS accumulates as loosely bound EPS.

The dissolved EPS is commonly termed as Soluble Microbial Products (SMP) since Lapidou and Rittman (2002) compared both concepts and concluded that they were indeed identical. SMP are substances produced by micro-organisms that are released into the water phase by cell lysis or excretion. They can also be introduced by the influent, (Figure 3-2).

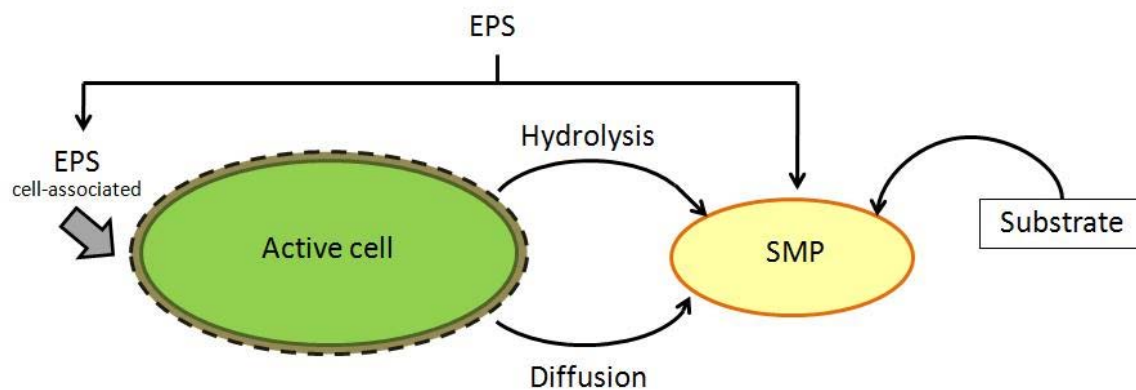


Figure 3-2 –Schematic of EPS and SMP

The conditions that influence the production of EPS and their release into the water phase are still not clear. Some authors have reported the influence of SRT and F/M, the influent C:N:P ratio, insufficient oxygen content, shear stress, temperature, etc. Kuo (1993) listed the main factors that cause SMP production, cited in Evenblij (2006):

- Concentration equilibrium: organisms excrete soluble organic material to establish concentration equilibrium across the cell membrane.
- During starvation bacteria excrete organic material (this could be interpreted as operating MBR for longer SRT and thus lower F/M).
- Increased presence of energy source
- Sudden addition of carbon source and energy source to bacteria starved for carbon and energy may accelerate death to some bacteria, which may result in production of SMP
- If essential nutrients are available in low concentrations, SMP may be produced to scavenge the required nutrients
- To relieve environmental stress, such as temperature changes, osmotic shocks and maybe in response to toxic substances
- During normal bacterial growth and metabolism SMP are produced.

In EPS analysis no standard method exists yet, either for cell-associated EPS or dissolved EPS. This leads to different results and makes the comparison between experiments truly complicated. For a better understanding of the role of EPS on membrane fouling it is urgent to uniform the method of analysis, so that research can progress rapidly.

3.3.2 EPS and membrane fouling

Nagaoka *et.al.*, (1996) studied the influence of EPS in the permeability of the membrane. Three different reactors were used with different composition synthetic feedwater. EPS was measured each 20 days and when the permeate flow had considerably decreased, membrane modules were pulled out of the reactors for cleaning and the amount of EPS attached to the membrane was then measured. They concluded that EPS accumulated both in the mixed-liquor and on the membrane, which might have caused an increase in the viscosity of the mixed-liquor and an increase on the filtration resistance on the membrane.

A study aiming at the comparison of sludge samples from eight different MBR and one conventional WWTP was conducted by Rosenberger and Kraume (2002). No influence of the cell-associated EPS concentrations on the filterability was found. Instead, the composition of the water phase was found to affect mostly the filterability of activated sludge, particularly the dissolved EPS. Also, the high mechanical stress in the MBR and high F/M ratios were found to increase the dissolved EPS concentration. Furthermore, Rojas *et.al.*, (2005) found that only the dissolved EPS had an impact on membrane fouling and not the cell-associated EPS. A different perspective was shown by Al-Halbouni *et.al.*, (2008) which considers that both cell-associated and dissolved EPS have a negative impact on the sludge properties.

Many researchers are trying to evaluate the contribution to membrane fouling of the specific components present in EPS; however, no agreement has been established. The importance of different components was attributed to: polysaccharides (Rosenberger *et.al.*,, 2006; Nataraj *et.al.*, 2008), proteins (Rojas *et.al.*, 2005), and fatty acids from lipopolysaccharides (Al -Halbouni *et.al.*, 2009).

Regarding operating conditions, contradictory results are shown about the influence of SRT in the EPS concentrations and its impact on fouling. Al-Halbouni *et.al.*, (2008) studied the impact of SRT in the EPS content and in the membrane performance. Two pilot-scale MBRs with SRTs of 23 and 40 days, and one full-scale MBR were investigated. The results showed that higher amounts of floc-bound and soluble EPS have a negative impact on sludge properties (settling behavior, dewaterability). The excess production of EPS can be related to season variations in the full-scale MBR and to a low SRT in the pilot

plants. In the pilots, at lower SRT, a high MW fraction of EPS, containing polysaccharides and proteins, was involved in membrane fouling. Despite the different SRT in the pilots, the membrane permeability was found to be similar.

On the other hand, Lee *et.al.* (2003), cited in Rosenberger *et.al.*, (2006), found that when SRT shifted from 20 to 60 days the contribution of the supernatant to overall membrane fouling decreased, while Rojas *et.al.*, (2005) reported the greatest production of EPS at an SRT of 20 days when the SRT was alternated between 10 and 30 days.

Rosenberger *et.al.*, (2006) demonstrated that the non-settleable of the sludge (soluble and colloidal material, i.e. polysaccharides, proteins and organic colloids) was found to impact fouling. It was also found that the SMP concentration was influenced by temperature and stress situations for the microorganisms. This was confirmed by Al-Halbouni *et.al.*, (2008) when they reported that the excess production of EPS could be related to season variations. Also, Lyko *et.al.*, (2008) observed that low temperatures reduced the membrane performance by two mechanisms: increasing permeate viscosity and increasing carbohydrate concentration.

3.4 Viscosity

In wastewater, rheology has been a subject of interest since it is an interesting tool to characterize the hydrodynamics of sludge suspensions, essential for optimization of the different processes in which sludge is operated. Activated sludge viscosity has a major impact on oxygen mass transfer, pressure loss in pipes, transport phenomena near the membrane, as well as, in a further step, sludge conditioning (Roseberger *et.al.*,, 2002).

3.4.1 Rheology theory

Rheology is the science describing the deformation of a body under the influence of stresses. A Newtonian fluid is characterized for the shear stress (stress applied to a surface of a material in a parallel or tangential plan) being linearly related to the shear rate (velocity gradient perpendicular to the direction of shear) according to the Newton equation 3-1 (Seysiecq *et.al.*, 2003):

$$\tau = \mu \dot{\gamma} \quad (3-1)$$

where,

τ – shear stress [Pa]

μ - apparent viscosity [Pa.s]

$\dot{\gamma}$ - shear rate [s^{-1}]

The apparent viscosity in a fluid is defined by the nature and solid concentration, the temperature and the pressure to which it is submitted.

However, sludge suspensions are considered non-Newtonian fluids, i.e. the shear rate being non-linearly related to shear stress. There are two types of models used to describe the behavior of activated sludge:

- shear-thinning model in which a decrease in the material apparent viscosity occurs when shear rate is increased
- plastic model where a yield stress must be reached before flow starts. The value of yield stress corresponds to the stress needed to be applied to overcome the cohesion Van-Der-Walls forces and induce the flow of the suspension

There are several equations to express the behavior of a sludge suspension. However, the most commonly used are the Ostwald and the Sisko for shear-thinning model; the Bingham, the Herschel-Buckley, and the Casson for plastic model (Seyssiecq *et.al*, 2003), (Figure 3-3).

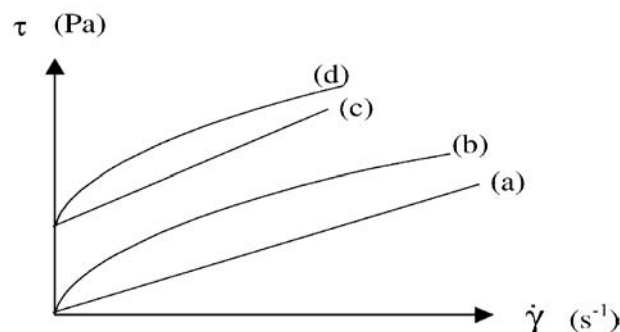


Figure 3-3 – Schematic flow curves for model time-independent materials: (a) Newtonian; (b) Shear thinning; (c) ideal Bingham plastic; (d) actual plastic

Rheometric methods

The apparatus that measures the rheological properties of a fluid is called a rheometer. For sludge, three different categories of rheometers can be used: capillary rheometers, rotational rheometers equipped with concentric cylinders and systemic rheometers (Seyssiecq *et.al*, 2003). In this thesis the sludge measurements were achieved through a rotational rheometer equipped with a concentric cylinder. The advantages of this apparatus are mainly that small sample volumes are required and also their compactness. On the other hand, centrifuge forces and also sedimentation can cause a particle size distribution thus affecting the measurement.

Since for sludge suspensions different rheometers can be used for rheological measurements and also different equations, the comparison of the results between different experiments turns out to be a difficult task. Besides, the sludge is a complex biological system already difficult to categorize.

The rheological behavior of a fluid is usually demonstrated through a rheogram, i.e. the shear stress plotted against shear rate

3.4.2 Viscosity and membrane fouling

Despite the many studies concerning rheology and its impact on membrane performance and membrane fouling, there is still a lack of information, partially due to synthetic wastewater being used in many previous studies and to the complexity of MBR systems (Wu *et.al*, 2007).

It is widely accepted that MLSS is one of the major parameters influencing apparent viscosity in activated sludge, since the increase in solid content leads to an increase in apparent viscosity (Rosenberger *et.al*, 2002; Hasar *et.al*, 2004; Wu *et.al*, 2007; Seyssiecq *et.al*, 2008).

Besides MLSS, temperature has also been reported has an important parameter having an effect on apparent viscosity (Hasar *et.al*, 2004; Wu *et.al*, 2007). Apparent viscosity showed higher values for lower temperatures. Not only the temperature influenced the apparent viscosity but also the shear stress decreased when an increase in temperature was registered (Hasar *et.al*, 2004)

Seyssiecq *et.al*, (2008) developed a study to characterize the rheological properties of an activated sludge with total suspended solids (TSS) ranging from 10 to 35 g/L, and operated in a bioreactor under different stirring and aeration rates. It was concluded that, due to the shearing of air bubbles, apparent viscosities are strongly lowered by the injection of air but almost independent of the quantity of air (in the range 2–6 L/min). However, under high mechanical shear rates (above 100 s^{-1}) the configuration of structural units (i.e. flocs in the case of activated sludge) is only dependent on the mechanical shearing and totally independent of the presence or absence of air. Also, the effect of TSS at constant air flow rate shows that an increase in TSS induces an increase not only in apparent viscosities but also in shear-thinning properties.

It has also been reported that EPS and SMP are responsible for increasing the apparent viscosity (Nagaoka *et.al*, 1996; Rosenberger *et.al*, 2002; Wu *et.al*, 2007)

4 METHODOLOGY

This chapter consists in a description of materials and methods applied to measure the characteristics in the activated sludge such as filterability characterization, particle counting in ranges 2-100 μm and 0.4-5.0 μm , SMP, viscosity and MLSS. The first Sub-chapter 4.1 explains the three different experiments done along the research period. The following Sub-chapter 4.2 is a general approach to the measuring protocol. The next Sub-chapters from 4.3 till 4.8 consist in the description of materials and methods for each applied test.

4.1 Three different experiments

In this thesis, between September 2008 and February 2009, sludge samples from the membrane tank (commonly named blank samples) were collected from five full-scale MBRs: Monheim, Heenvliet, Nordkanal, Ootmarsum and Varsseveld. To study the characteristics of the sludge, several analyses were performed such as filterability, MLSS, particle counting in the ranges 2-100 μm and 0.4-5.0 μm , soluble microbial products (SMP), and viscosity. The most important analysis is the filterability (indicated by ΔR_{20}), measured through the Delft Filtration Characterization method (DFCm) developed by TUDelft (Evenblij *et.al*, 2005).

In order to deepen the study conducted in this thesis, three different experiments were made:

- Blanks Characterization experiment
- Dilutions experiment
- Solids Concentration experiment

In the following Sections the goals of each experiment and the applied methods are described.

4.1.1 Blanks Characterization experiment

The purpose of this experiment is to characterize sludge from full-scale MBRs through the previously referred analyses, and relate the similarities and discrepancies between different treatment plants. In order to understand how the sludge properties can affect the filterability, the correlation between filterability and each analyzed parameter is applied through a regression coefficient.

This was the experiment with the highest number of tests.

4.1.2 Dilutions experiment

The MLSS is one of the most controversial parameters in how it affects filterability and membrane fouling. The goal of this experiment is to study the effect of different solids contents in filterability.

The way to obtain different MLSS was through dilutions with permeate collected in the respective treatment plant. After the measurement of the blank sample (for the Blanks Characterization experiment) two dilutions were made:

- D10p, 10 L of permeate + 20 L of sludge
- D20p, 20 L of permeate + 10 L of sludge

After preparing each dilution, the new “artificial sludge” was submitted to a 30 minute period of aeration to ensure a complete mixture and enough oxygen content for aerobic conditions. Only then were all the analyses performed.

The organization of this experiment is made by sets. A set comprehends the blank, D10p and D20p. It is important to emphasize that the two dilutions cannot be considered as real sludge, so that further conclusions have to be carefully drawn.

4.1.3 Solids Concentration Experiment

The goal of this experiment was to modify the sludge solids concentration by manipulating the operating conditions in a full-scale plant and measuring the filterability for the different

MLSS obtained. By increasing the hydraulic retention time (HRT), and maintaining the permeate flow constant, it was possible to increase the solids content in the membrane tanks.

This experiment only took place at Heenvliet where, for a short period of time, the HRT was able to vary from the normal value. During this period, several sludge blanks were collected and the filterability measured to study the effect of MLSS in filterability.

4.2 General measuring protocol

The majority of the experiments done in this thesis took place at the laboratory of TUDelft. The analyses applied such as particle counting in range 0.4-5.0 μm , SMP, viscosity, and MLSS could not be accomplished outside the laboratory. The only portable apparatus were the Delft Filtration Characterization installation (DFCi) for the filterability test, and the particle counter in range 2 – 100 μm . Therefore, it was necessary to adapt the general measuring protocol to these conditions.

Of all the WWTPs visited, Heenvliet was the nearest one, located approximately 40 km from TUDelft. Since the distance was short and the transport of the sludge from the treatment plant to TUDelft would take around 30 minutes, and the quantity of sample was considerable (40 L), it was assumed that no significant changes in the sludge would take place. For that reason, all experiments with Heenvliet sludge were feasible to do at the laboratory, i.e. “ex situ”. However, to restore the level of oxygen content, the sludge would be aerated for one hour before any experiment.

All the other WWTPs (Monheim, Nordkanal, Ootmarsum and Varsseveld) were, at least, 3 hours from TUDelft which was compromising to the original structure and nature of the sludge, and thus could not be representative of a full-scale MBR. In these cases the DFCi was set up at the treatment plant, “in situ”, as well as the particle counter in range 2 – 100 μm when possible.

For the other tests (particle counting in range 0.4-5.0 μm , SMP, viscosity, and MLSS) sludge samples were collected from the sludge in the bioreactor of the DFCi immediately before the start of the filterability test. For the particle counting 0.4-5.0 μm and SMP, since

free water (defined as water obtained after filtrating through a 7-12 μm pore size paper filter) is required for these measurements, the fractionation test was done “in situ” using a portable vacuum system. The viscosity and MLSS were only possible to measure on the next day. For that reason, the free water samples and sludge samples were saved and stored in a refrigerator in order to reduce the microorganism activity and preserve the original characteristics.

To see the difference between the measurements made “on day” and on the next day, a couple of trials were done where all tests, except the filterability test, were performed on the day of the sludge collection and on the following day. The results were compared and the differences obtained were insignificant, showing that this protocol could be applied conducting to reliable results.

In Monheim and in Nordkanal the DFCi stayed for a week in the treatment plant. Thus, the particles in range 0.4-5.0 μm , SMP and viscosity were not able to be measured and after one week the sludge and free water had a different composition leading to unrepresentative results. Nevertheless, MLSS was obtained through the online sensors in the treatment plant. For Ootmarsum and Varsseveld, since there was only one day of measurements, all the tests were possible.

It was not only in Monheim and Nordkanal that some measurements were not done. Unfortunately, all the apparatus for the different measurements weren't always available due to utilization by other researchers or due to maintenance reasons.

An overview of the type of experiments done and the tests applied can be seen in Table 4-1. In all experiments, the filterability test was done and MLSS was measured, which is why they are not shown.

Table 4-1 – Overview of all experiments between September 08 and February 09

Name	WWTP	Particle	Particle	SMP	Viscosity	Purpose *
		counting 2 – 100 µm	counting 0.4 – 5µm			
Blank 1	Monheim	✓	-	-	-	B.C
Blank 2	Monheim	✓	-	-	-	B.C
Blank 3	Monheim	✓	-	-	-	B.C
Blank 4	Monheim	✓	-	-	-	B.C
Blank 5	Heenvliet	✓	✓	-	-	B.C + Dil.
Blank 6	Heenvliet	✓	✓	-	-	B.C + Dil.
Blank 7	Heenvliet	✓	✓	✓	✓	B.C + Dil.
Blank 8	Heenvliet	✓	-	-	✓	B.C
Blank 9	Heenvliet	-	✓	✓	✓	B.C + Dil.
Blank 10	Nordkanal	-	-	-	-	B.C
Blank 11	Nordkanal	-	-	-	-	B.C
Blank 12	Nordkanal	✓	-	-	-	B.C
Blank 13	Nordkanal	✓	-	-	-	B.C
Blank 14	Nordkanal	✓	-	-	-	B.C
Blank 15	Nordkanal	✓	-	-	-	B.C
Blank 16	Nordkanal	✓	-	-	-	B.C
Blank 17	Nordkanal	✓	-	-	-	B.C
Blank 18	Nordkanal	✓	-	-	-	B.C
Blank 19	Heenvliet	✓	✓	✓	✓	B.C + Dil.
Blank 20	Heenvliet	-	✓	✓	✓	B.C + Dil.
Blank 21	Heenvliet	✓	✓	✓	-	B.C + Dil.
Blank 22	Heenvliet	✓	-	-	✓	B.C + Dil.
Blank 23	Heenvliet	✓	-	-	✓	B.C + Dil.
Blank 24	Ootmarsum	-	✓	✓	✓	B.C + Dil.
Blank 25	Ootmarsum	-	✓	-	✓	B.C
Blank 26	Varsseveld	-	✓	✓	✓	B.C + Dil.
Blank 27	Varsseveld	-	✓	✓	✓	B.C + Dil.
Blanks 1a-5a	Heenvliet	✓	-	-	✓	S.C
Blanks 1b-5b	Heenvliet	✓	-	-	✓	S.C

*B.C – Blanks Characterization; Dil. – Dilutions; S.C – Solids Concentration

4.3 Delft Filtration Characterization installation (DFCi)

The Delft Filtration Characterization installation (DFCi) was developed by Delft University Technology (TUDelft) to study the filtration performance of MBR activated sludge. In order to analyze different activated sludge and obtain comparable data, the Delft Filtration Characterization method (DFCm) was developed as described in Evenblij *et.al*, (2005). This protocol gives the possibility to filtrate sludge samples always under equal hydraulic conditions and link the results only to the characteristics of the sludge.

The most representative element of the DFCi is the membrane that together with

- sludge pump, damper and permeate pump,

- online measuring instruments for pH, temperature, oxygen content, mass balance, pressure and flow
- programmable logic controller (PLC),
- computer to collect the data

are the principal constituents of this installation.

In Figures 4-1 and 4-2 a schematic overview and a picture from the DFCi are respectively represented.

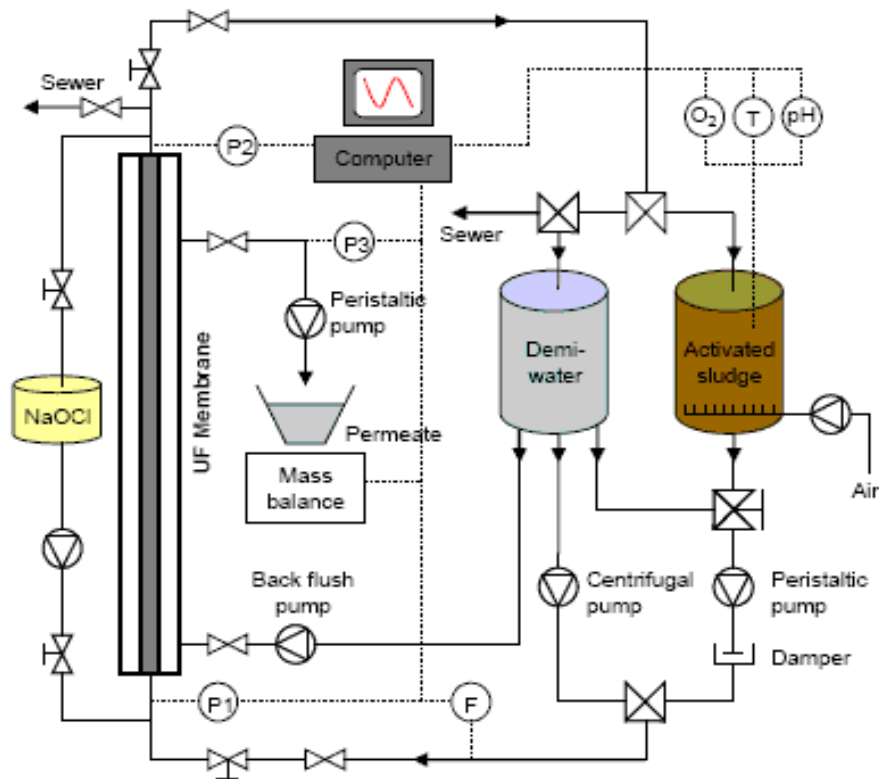


Figure 4-1– Schematic overview of the DFCm (Evenblij, 2006)



Figure 4-2 – DFCi during filtration campaign at Monheim, 2008: front view (left-side) and back view (right-side)

4.3.1 Membrane

The filtration unit has a single tubular X-Flow UF membrane built in Polyvinylidene Fluoride (PVDF) material. The membrane presents the following characteristics: nominal pore size of 0.03 μm , length of 95 cm, diameter of 8 mm, and a surface area of 240 cm^2 . The membrane is placed vertically and operated in upflow side stream configuration. The extraction of permeate is done inside-out. For more details see Appendix II.

4.3.2 Pumps

The installation requires four pumps: sludge pump, permeate pump, water pump and chemical cleaning pump.

Sludge pump - a peristaltic pump is used for the circulation of the sludge with the purpose of not breaking the floc structure of the sludge. Since the pump creates turbulence while

working, and a constant flow is necessary to assure that a crossflow velocity (CFV) of 1 m/s is maintained, a damper was added to the filtration unit to absorb the fluctuations produced.

Permeate pump - the permeate pump, which is connected to the outlet of the membrane module, is also peristaltic to avoid disrupting the structure of permeate when extracted. By controlling the rotational velocity of the pump, it is possible to regulate the desired permeate flux.

Water pump - the water pump is used for a clean forward flush and backflush. In the forward flush, a CFV up to 4 m/s is obtained for a more efficient cleaning. The goal of backflush is to reverse the TMP that results from the filtration test to values near zero. This way each new test is started under the same conditions.

Chemical pump – in order to re-establish the initial resistance of the membrane a chemical cleaning is necessary and is made through a peristaltic pump.

4.3.3 Online measuring instruments

Since the purpose of this installation is to measure sludge filterability, several parameters have to be continually analyzed during the test. The sensors are an important part of the DFCi since they are responsible for measuring several parameters which are fundamental to the membrane filtration. It is important that all the sensors are suitable and accurate otherwise the results could not be entirely representative of the membrane's behavior.

Sludge sensors

During the filtration test there are three parameters being measured online: pH, temperature and oxygen content.

The pH is measured as a reference parameter to compare with other sludge samples.

The temperature is directly related with the formula to calculate the total resistance in the membrane. Total resistance depends on the permeate viscosity, that varies according to temperature. The calculation of the resistance is automatically done by the software for a

temperature of 15°C, and then a subsequent correction is applied to the measured temperature during the filterability test. Equation 4-1 shows how total resistance is calculated.

$$R_t = \frac{TMP}{J} \cdot \frac{\eta_{ref}}{\eta_{act}} \quad (4-1)$$

where,

R_t – total resistance [m^{-1}]

TMP – transmembrane pressure [Pa]

J - flux [$Lm^{-2}h^{-1}$]

η_{ref} – permeate dynamic viscosity at 15°C [Pa.s]

η_{act} – permeate dynamic viscosity for the actual temperature [Pa.s]

The oxygen content is measured to guarantee that the sludge is in aerobic conditions (> 2 mg/l).

4.3.4 Mass balance

The mass balance consists in monitoring the permeate production online, which is fundamental to calculate the permeate flux. It is assumed that the mass of permeate has the same specific weight of water. Through Equation 4-2 it is possible to calculate the flux, J.

$$J = \frac{dM}{dt} \cdot \frac{3600}{A_m \cdot \rho} \quad (4-2)$$

where,

M – mass of permeate [g]

t– time [s]

A_m = membrane area [m^2]

ρ = permeate density [kg/m^3]

4.3.5 Pressure transmitters

The TMP is one of the inherent parameters during the filterability test. The measuring of TMP is done through three pressure transmitters: one on the feed side of the membrane, immediately before the inlet to the membrane tube; one on the outlet of the membrane tube; one in the permeate stream.

The TMP is calculated through Equation 4-3.

$$\text{TMP} = \frac{P_{\text{feed}} + P_{\text{outlet}}}{2} - P_{\text{permeate}} \quad (4-3)$$

4.3.6 Programmable Logic Controller (PLC)

The PLC is the controller of the installation allowing different operation modes such as sludge filtration, water cleaning (forward flush and backflush), recirculation, etc. All the electricity connections from the installation are plugged to the PLC.

4.3.7 Measuring Protocol - DFCm

The filtration characterization test relies on four steps:

1 – **Cleaning the membrane** with a forward flush with demineralised water (demi-water) to remove the cake layer and the cleaning chemicals that remained after the last filtration test. Now the membrane presents the “initial” conditions desired for each test.

2 – **Filtration of activated sludge:** before starting the test, a forward flush is performed to ensure that only sludge runs in the installation. Then recirculation of activated sludge is turned “on” to the sludge vessel (bioreactor). After this, the permeate pump is turned “on” and the test started. The test is performed at least until 20 L/m² of permeate is produced. The main reason for this is that the additional resistance obtained after filtrating 20 L/m² of permeate was previously defined as a comparison point between different activated sludge

samples. The test is performed with a constant flux of $80 \text{ Lm}^{-2}\text{h}^{-1}$ and a CFV of 1 m/s . Eventually, if the TMP reaches a value of 0.70 bar the test is stopped, even if the permeate production is less than 20 L/m^2 .

3 – **Forward flush:** when the test ends a forward flush with demi-water is applied to clean the membrane. Afterwards, in order to restore the “standard” pressure values in the system, a backflush is executed. The vessel in which the activated sludge remains after the filtration test is cleaned properly for the next sludge filtration test.

4- **Chemical cleaning:** After the test is finished a chemical cleaning is carried out with sodium hypochlorite (NaOCl , 500 ppm active chlorine) until the membrane is clean.

4.3.8 Data acquisition and output

The Testpoint software allows the monitoring on the computer of all the data that is being measured online: membrane resistance, TMP, flux, CFV, oxygen content, temperature, and pH. This way, it is possible to have an overview of the filtration test. All the information will be gathered in a single data file for consequent treatment on Microsoft Office Excel.

The filtration test output consists in three figures assembling different information. In Figure 4-3 it is possible to see the additional resistance along the flux extraction, and also the variations of TMP.

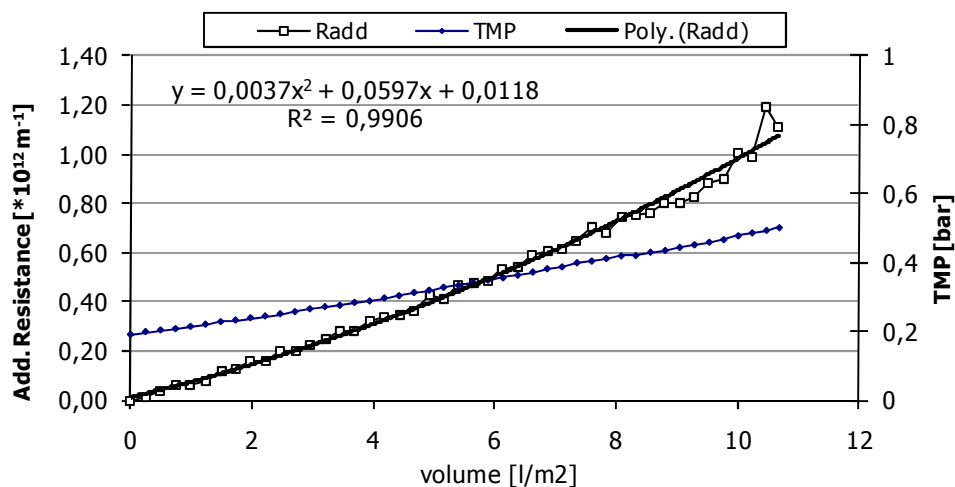


Figure 4-3 - Additional resistance and TMP alongside permeate volume extraction

The output data only presents the evolution of additional resistance, which is the subtraction between total resistance and membrane resistance, along the filtration process. A trendline is applied to the additional resistance data points to characterize the behavior of the sludge filterability through the equation that fits better, usually a second order polynomial equation. Then the calculation of ΔR_{20} is made.

The ΔR_{20} is the parameter used in this work to characterize the filterability of sludge. It is the additional resistance (m^{-1}) after filtration of $20 L/m^2$ of a sludge sample, using a flux of $80 Lm^{-2}h^{-1}$ and a cross-flow velocity of $1 m/s$. This way, all sludge samples are compared under the same membrane and operational conditions. Geilvoet (2009) created a scale to characterize the sludge quality based on parameter ΔR_{20} . According to this scale, sludge can be divided into five different quality groups, see Table 4-2.

Table 4-2 – Sludge quality according to ΔR_{20} values

Excellent	$0 < \Delta R_{20} < 0.05$
Good	$0.05 < \Delta R_{20} < 0.2$
Moderate	$0.2 < \Delta R_{20} < 0.5$
Mediocre	$0.5 < \Delta R_{20} < 1$
Poor	$\Delta R_{20} > 1$

In Figure 4-4, resistance (black line), TMP (blue line) and Flux (red line) are plotted alongside the permeate volume production. It demonstrates the increasing of resistance along the volume production whilst flux is maintained at a constant rate. Although it's not clear, TMP is also increasing.

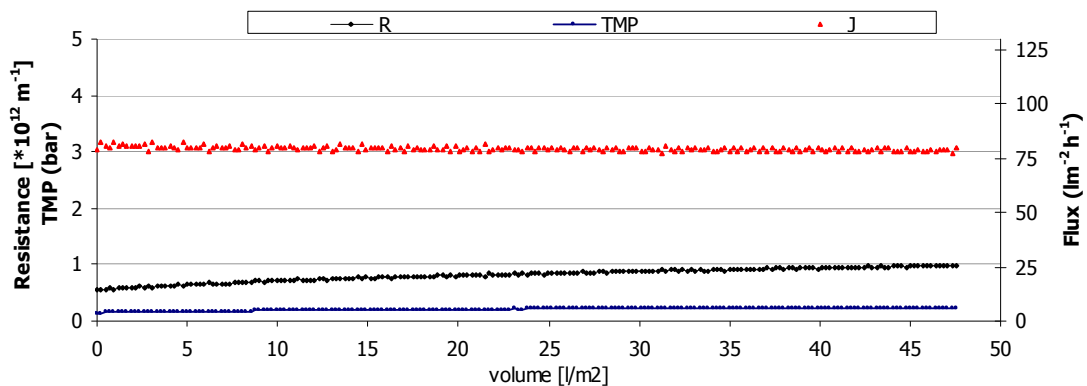


Figure 4-4 – Overview of resistance, flux, and TMP while extracting permeate

The following Figure 4-5 shows the CFV, oxygen content, temperature and pH in the elapsed experience.

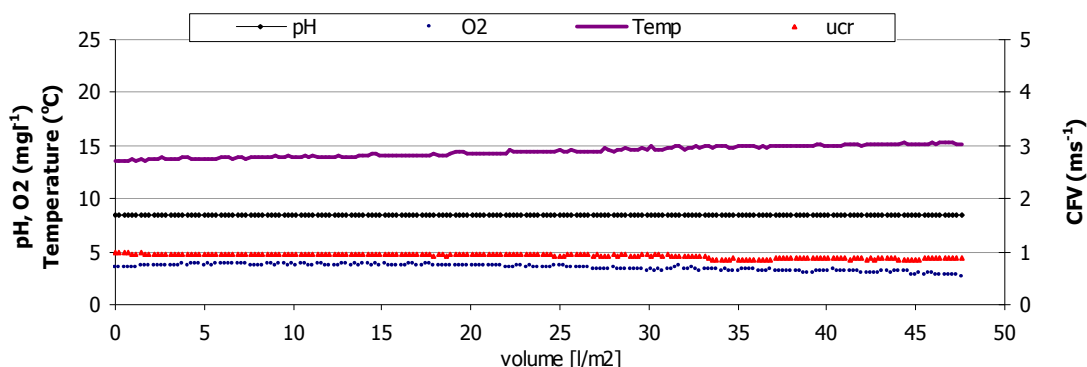


Figure 4-5 – Overview of CFV, pH, oxygen content, and temperature, during a filtration test

4.4 Particle counting in range 2-100 μm

Particle counting aims to characterize the sludge by a particle number distribution, in this case ranging from 2 till 100 μm .

4.4.1 Materials

Particle counting is made using a particle counter Met One PCX.

The particle counter Met One PCX was specifically designed for drinking water applications. It is a pore blocking instrument in which the water is directed into the sensor and funneled through an optical flow cell measuring 750 x 750 microns. Its range comprises from 2 till 100 μm . For calibration, different NIST traceable spheres of known size are used; this information is stored in the memory of the sensor and is used to separate the particle counts into the proper size category (for technical specifications see Appendix III).

The installation, besides particle counting, is composed by the following materials and accessories:

Materials

- Flow controller Krohne DK 47N
- Stirrer and agitator board Protherm pt 100

- Pump Monacor – Netzgerät
- Data Acquisition system: WGS software, computer

Accessories

- Sieve Retsch DIN-150 3310/1 with 100 µm pore size
- Test tube
- Erlenmeyer
- Funnel
- 2 litter bucket

In Figure 4-6 a schematic overview of the particle counting installation is illustrated, and in Figure 4-7 a picture of the installation at laboratory.

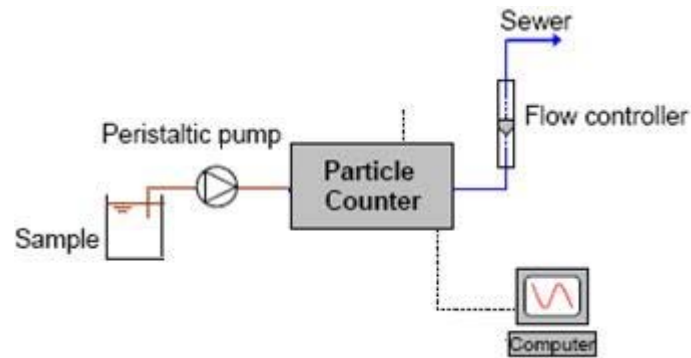


Figure 4-6 – Schematic overview of the particle counting installation 2-100 μm



Figure 4-7 – Particle counting installation at TUDelft laboratory

4.4.2 Measuring protocol

In the particle counting analysis, sludge samples cannot be used directly into the particle counter, otherwise it would contaminate the particle counter due to the high number of particles existing in sludge. Also, the sensor measures up to a maximum particle number of 18 000 particles. Samples with a higher number of particles will provide coincidence errors. Therefore, diluted samples are necessary to perform the test.

Preparation of diluted sludge samples

1 - A sample of sludge is collected from the container where the sludge is being mixed and aerated in the DFC installation, immediately before the filterability test starts.

2 - The sludge is diluted with permeate (collected in the WWTP) in the relation of 1:100 (10 ml of sludge: 1000 ml of permeate).

3 – Subsequently, the solution is sieved using a 100 μm sieve to an Erlenmeyer.

Procedure of Particle counting

1 – The particle counter is turned on as well as the computer

2 – A sample of demi-water is measured according to steps 2a till 2d.

a) a plastic bucket is filled with 2 L of sample and placed in the agitator board with the electromagnetic stirrer. The rotational speed of the stirrer is adjusted to ensure a homogeneous solution and avoid sedimentation.

b) the pump is turned on and the flow is regulated to 6 L/h on the flow meter. Usually there are some air bubbles in the system and so the bucket should be lifted in the air to help release them.

c) when the flow is constant the measurement can start. The software is started and the test begins. For each test the solution is measured twice and the average is then used as final result.

d) after the test is finished the pump can be turned off.

3 – a permeate sample is measured according to step n° 2. After the test, the permeate that remains in the bucket has to be equal or superior to 1000 mL in order to guarantee a dilution in a relation of 10 mL sludge/ 1000 mL permeate.

4 – a sludge dilution 1:100 is measured according to step n° 2

5 – a sample of demi-water is measured to clean the particle counter according to step n° 2.

4.4.3 Data acquisition

The particle counter measures particles through 198 channels with different pore sizes ranging from 2.0 to 100.0 μm . The first channel comprehends particles in a range size of 2.0 μm , the second in a range size of 2.5 μm , and the following ones with 0.5 μm intervals till the range size of 100.5 μm is reached. The particles are measured twice for each test and the average of both countings is the result used.

The particle counting only provides results relative to the number of particles. In addition to the particle number analysis, a particle volume analysis is also calculated. Since it is impossible to predict the real volume of a particle, due to the complex structure of sludge, some assumptions are considered:

- The particle diameter corresponds to the range size channel in which the particle is detected
- The volume of a particle is assumed to be identical to a sphere

In the particle volume analysis the volume of a particle is calculated according to Equations 4-4.

$$V = \frac{1}{6} \cdot \emptyset^3 \cdot \pi \quad (4-4)$$

where,

V – volume of a particle [m^3]

\emptyset – diameter of particle = particle size range [m]

The particle volume of a specific size range is given by the volume of a particle at a certain size range times the number of particles found in that size range.

Calculation of the real number of particles in a sludge sample

Considering that a sludge sample is diluted with permeate in a relation of 1:100, the real number of particles is given by:

$$\eta_{sludge} = [\eta_{sludge (1:100)} - \eta_{permeate} \cdot 0.99] \cdot 100 \quad (4-5)$$

where

η_{sludge} – number of particles in a sludge sample

$\eta_{dilution (1:100)}$ – number of particles in a diluted sludge sample

$\eta_{permeate}$ – number of particles in a permeate sample

The acquired data is then used for correlating filterability, ΔR_{20} , with different particle counting parameters. The parameters defined are:

- cumulative particle number
- maximum particle number
- mean particle size of maximum particle number
- cumulative particle volume
- maximum particle volume
- mean particle size of maximum particle volume

4.5 Particle counting in range 0.4 - 5 μm

Particle counting in range 0.4-5.0 μm is applied to the free water of the sludge.

4.5.1 Materials

Particle counting is accomplished using a particle counter HIAC MicroCount 100 series. The particle counter has a pore blocking sensor appropriate for high purity solutions with sensitivity from 0.4 to 5 μm . The typical flow rate of this apparatus is 100 ml/min and its concentration limit is up to 100,000 particles/mL (for technical specifications see Appendix IV). The installation, in addition to the particle counting, is composed by the following materials and accessories:

Materials

- Flow controller
- Stirrer and agitator board Pump Monacor – Netzgerat
- Peristaltic pump Watson Marlow 205 U
- Data Acquisition system: Particle Vision Online SE, computer

Accessories

- Vacuum filtration unit
- Paper filter Schleicher & Schuell 589/2 with pore size 7-12 μm
- Beaker

In Figures 4-8 and 4-9 an overview and a picture of the particle counting installation are represented respectively.

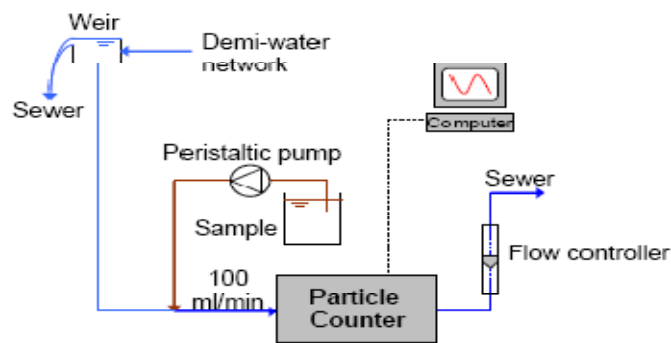


Figure 4-8 – Schematic overview of the particle counting installation in range 0.4-5.0 μm
(Geilvoet *et.al.*, 2007)



Figure 4-9 – Particle counting installation at TUDelft laboratory

4.5.2 Measuring protocol

Fractionation

The free water from the sludge is obtained through fractionation, which consists in the separation of the activated sludge by filtration over a paper filter Schleicher & Schuell 589/2 with pore size 7-12 μm . This process takes place in a vacuum filtration unit.

Procedure of Particle counting

The free water of the sludge sample contains a number of particles higher than the limit imposed by the particle counter. Thus, a dilution sample is prepared with demi-water in a relation of 1:100 (1 sludge/100 demi-water). The demi-water runs by gravity to the installation and, just before entering the particle counter, the free water is added through a

peristaltic pump. The flow controller allows regulating a flow of 100 ml/min. In order to clean and maintain the durability of the installation, a sample of demineralised water is measured before each free water sample.

The particle counting of a sample consists in the following steps:

- 1 – The sludge sample is submitted to vacuum filtration through a Schleicher & Schuell 589/2 paper filter. The filtration is stopped when the free water volume is at least 50 ml, ensuring enough volume for the measurement.
- 2 – The computer is switched on.
- 3 – The valve of the demi-water water network is opened and it starts to run into the installation. The flow is adjusted to 100 ml/min in the flow controller.
- 4 - A sample of demi-water is placed in the agitator board with a stirrer.
- 5 – The pump is switched on and the sample starts running into the particle counter.
- 6 – The software Particle Vision Online SE is started and the particle counting measurement starts. The sample is measured for about 30 minutes.
- 7 – The demi-water sample is replaced with the free water sample and measured for about 30 minutes.
- 8 – If there are more free water samples to measure, a demi-water sample always precedes each new free water analysis.

4.5.3 Data acquisition

The results of the particle counting measurements are expressed as the number of particle countings per ml along different size ranges from 0.4 to 5.0 μm within intervals of 0.1 μm resolution.

For the particle volume analysis, the assumptions made for particle counting in range 2-100 μm referred in Section 4.3.2 are made as well for the particle counting in range 0.4 to 5.0 μm . Also, the same particle counting parameters will be used to observe the

relationship between filterability and particle counting in range 0.4 to 5.0 μm (see Section 4.3.3).

4.6 Soluble Microbial Products (SMP)

The analysis of the SMP is made through photometric methods. The free water from the activated sludge is required, and the analysis is divided in two measurements: proteins and polysaccharides.

4.6.1 Materials

In the SMP analysis the following materials are used:

- Thermo Electron genesys 6 UV-Visible spectrophotometer
- Vortex mixer Genie 2 G-5680
- Cuvetts of 4 cm

4.6.2 Measuring protocol for Proteins

For protein analysis the modified method of Frølund et.al., (1996), based on the method of Lowry et.al., (1951), by Rosenberger (2003), is applied. For the calibration Albumine bovie (BSA), (Acros) fraction V, in a concentration range between 0 – 25 mg/l is used. Afterwards the concentration can be calculated using the BSA calibration curve and the measured difference between the sample and the blank (demi-water).

Reagents

A: 143 mM NaOH and 270 mM Na_2CO_3 in demi-water

B: 57 mM CuSO_4 in demi-water

C: 124 mM Na_2 -tartrate, $\text{C}_4\text{H}_4\text{Na}_2\text{O}_6$, or Na-k-tartrate, $\text{C}_4\text{H}_4\text{NaKO}_6$, in demi-water

D: mixture of reagents A, B and C in the relation of 100:1:1

E: Folin-Ciocalteu phenol reagent I in the relation of 1:1

It is important to state that reagent D has to be prepared on the day of SMP analysis in opposition of reagents A, B, C and E that can be stored for an unlimited period of time.

Method

A sample of 2.5 ml is poured into a round tube together with 3.5 ml of reagent D and mixed in a tube mixer. Afterwards the mixture is stored for 10 minutes in a room at a controlled temperature. Then 0.5 ml of reagent E is immediately added and the mixture has to be mixed fast and powerfully due to the fact that the Folin-Ciocalteu phenol reagent is only stable for a short time in the alkaline environment. The sample-mixtures should then be incubated for 45 minutes at room temperature to make sure that the color complex will be finished before the start of the measurement.

The adsorption is now measured in a 4 cm cuvette at wavelength of 750 nm with a UV-VIS spectrophotometer against a reference sample of demi-water. The formed color complex will be stable for about 45-60 minutes. Each sample is measured twice, and then an average will be used to calculate the concentration in the free water through the calibration curve.

4.6.3 Measuring protocol for Polysaccharides

The polysaccharides analysis is made through Rosenberger (2003) modified method of Dubois et.al., (1956). For the calibration, D(+)-glucose (J.T.Baker), in a concentration range between 0.5-10 mg/l, is used. It will then be possible to calculate the concentration using the polysaccharides calibration curve and the measured difference between the sample and the blank – demi-water.

Reagents

A: 5 % Phenol solution in demi-water

B: 95 – 97 % sulphuric acid

Method

A sample of 4 ml is poured into a round tube and 2 ml reagent A is then added. After mixing properly, 10 ml of reagent B is added and it is again well mixed. After 10 minutes of storing at room temperature a new mixing is required. Subsequently, the mixture is incubated for 30 minutes at room temperature. Then the adsorption is measured in a 4 cm cuvet at a wavelength of 487 nm with a UV-VIS spectrophotometer against a reference sample of demi-water. The formed colour complex will be stable for a long time. Each sample is measured twice, and then an average will be used to calculate the concentration in the free water through the calibration curve.

4.7 Viscosity

The viscosity of the sludge is measured, when possible, for each filtration test. A sludge sample is collected immediately before the start of the filterability test, as it happens for the particle counting 2 – 100 μm and MLSS, see Sub-chapters 5.2 and 5.6 respectively.

The viscosity measurements are always performed at $20\pm 1^\circ\text{C}$ in order to compare different sludge samples. This way it is assumed that the rheological properties of the sludge are due to the solids content and to the pressure forces submitted, see Section 3.4.1.

4.7.1 Materials

The apparatus used for viscosity measurements is a rotational rheometer Anton Paar Physica UDS 200. It allows performing tests with both Newtonian and viscoelastic fluids under controlled “shear rate” ($.0001$ to $5,000\text{ s}^{-1}$, geometry dependent) or controlled “stress” (0.002 mNm - 150 mNm), for technical specifications see Appendix V.

In addition to the rheometer, the installation is composed of:

- Air pressure system
- Thermo heater Jeio Tech RW-0525 G
- Data Acquisition system: US 200/32 v 2.30 software, computer.

In Figure 4-10 a picture of the viscosity installation is illustrated.



Figure 4-10 – Viscosity installation at TUDelft laboratory

4.7.2 Measuring protocol

For a viscosity measurement the following steps are given:

- 1 – Air pressure input: the pressure hose is connected to the wall socket and then a 5 bar pressure is regulated using the pressure adjuster.
- 2 – The power of the rheometer can now be switched on as well as the computer.
- 3 – The protections of the rheometer are removed and the geometry, container and cylinder, are installed. Before installing, the container is filled with a 100 ml sludge sample previously mixed.
- 4 – The thermo heater is turned on and adjusted to 20 °C.
- 5 – The USD 200 software is started and the calibration of the rheometer is done. Now the viscosity test can be carried out. For each test the following shear rates are applied:

Shear rate (s ⁻¹)	5	10	20	30	50	100	250	500	700	1000
-------------------------------	---	----	----	----	----	-----	-----	-----	-----	------

For each shear rate 10 points are measured within a 5 second interval. Then a higher torque is applied to the cylinder in order to achieve the next pre-defined shear rate.

6 – When the test is finished data is collected as a text document for subsequent treatment in Microsoft Office Excel. The results of the tests allow us to know the temperature, shear rate, shear stress, apparent viscosity, speed and torque of each measuring point. Since there are 10 measuring points for each different shear rate, the final value is the average value.

4.8 Mixed Liquor Suspend Solids (MLSS)

The MLSS were measured according to the *Standard Methods*, see Appendix VI.

5 BLANKS CHARACTERIZATION EXPERIMENT

This chapter describes the Blanks Characterization experiment in which filterability of activated sludge from five MBR systems was measured: Monheim, Heenvliet, Nordkanal, Ootmarsum and Varsseveld. In sub-chapter 5-1 a characterization of the five MBRs is made with specific information relative to the operating conditions of each treatment plant. The following sub-chapters present the results and discussion of each analysis, namely filterability, particle counting in ranges 2-100 μm and 0.4-5.0 μm , SMP, and viscosity. In Sub-chapter 5-7 the conclusions drawn are presented. All results are shown in Appendix VII.

5.1 Characterization of five MBR systems

In this sub-chapter, a briefly description of the five MBR systems where sludge was collected for this thesis can be found together with, in Table 5-1, the main differences between the WWTP. The diagrams for each treatment plant are presented in Appendix VIII.

Monheim

The Monheim WWTP is located in Bavaria, Germany. The main treatment process of the plant is an MBR that includes a nitrifying-denitrifying tank and the membrane tanks where the extraction of permeate occurs. The MBR was installed due to the restricted effluent target values, since the effluent is discharged in sensitive surface water.

Heenvliet

This WWTP is situated in Heenvliet, South of Holland. The plant includes a conventional activated sludge system and an MBR that can be operated in series or in parallel. When operating in parallel, the MBR only receives 25% of the influent, whereas the other 75% are received in the conventional system.

Nordkanal

Located in Kaarst, Germany, it is the largest municipal MBR treatment plant in Europe, with treatment capacity of 80,000 p.e (1 p.e. = 54g BOD/d). The biological treatment

consists in aerobic sludge stabilization and a four-channel biological reactor with upstream denitrification for nitrogen removal as well as chemical precipitation for phosphorous removal. The membranes are located in the nitrification tanks.

Ootmarsum

Situated in The Netherlands, this WWTP has a conventional activated sludge system and a sidestream MBR that work in parallel. The effluent is discharged into sensitive surface water.

Varsseveld

This WWTP was the first full-scale MBR in The Netherlands, commissioned at the end of 2004. The volume of water entering in the plant varies hugely: after heavy rainfall, the influent is 3 times more when compared to dry weather conditions.

Table 5-1 – Overview of the main differences in the five WWTP

Parameter	Unit	Monheim	Heenvliet	Noordkanal	Ootmarsum	Varsseveld
WWTP type	...	Full-scale	Full-scale	Full-scale	Full-scale	Full-scale
Location	...	Germany	The Netherlands	Germany	The Netherlands	The Netherlands
Wastewater	...	municipal	municipal	municipal	municipal	municipal
Biological Capacity	p.e. *	9,700	3,333(MBR) + 9,664(CAS) ≈ 13,000	80,000	WWF: 7,000 (MBR) + 7,000 (CAS) = 14,000 / DWF: 9,250 (MBR) + 9,250 (Conv.) = 18,500	23,150
Hydraulic capacity (Average)	m ³ /d	1,820	2,400	WWF: 45,000 / DWF: 16,000	WWF: 1,400 / DWF: 3,600	5,000
Permeate production	m ³ /h	up to 96	100	n.a **	WWF: 150 / DWF: 75	275
Process Configuration	...	Submerged	Submerged	Submerged	Sidestream	Submerged
Membrane type	...	Hollow fibre	Flat sheet	Hollow fibre	Tubular	Hollow fibre
Membrane supplier	...	Zenon	Toray	Zenon	Norit X-Flow AirLift	Zenon
Product name	...	ZeeWeed 500c	Unibrane	ZeeWeed 500c	LPCF	ZeeWeed 500d
Number of lanes	m ²	4 parallel tanks	2 parallel tanks	4 parallel tanks	6 stacks	4 parallel tanks
Total membrane area	m ²	12,320	4,115	84,480	2,784	20,160
Membrane pore size	µm	0.04	0.08	0.04	0.03	0.035
Design Flux (netto/brutto)	LMH	12.0-23	24.3	12.0-23	54	37.5 - 45
MLSS (values from experiments)	g/l	6.9-7.6 (Sept 08)	13-17.7 (Oct 08 - Jan 09)	10.7-11.8 (Nov 08)	7.5-8.9 (Feb 09)	7.6-7.8 (Feb 09)
SRT	days	30	20	25-29	>60	35
Cleaning	-	Mechanical and chemical	Mechanical and chemical	Mechanical and chemical	Drainage stage & Mechanical and chemical	Mechanical and chemical

* 1 p.e. = 54 g BOD/d

** n.a. - not available

WWF - wet weather flow

DWF - dry weather flow

5.2 Filtration characteristics - ΔR_{20} , MLSS and Temperature

5.2.1 Results

In the Blanks Characterization experiment sludge from five MBR systems was collected and different analyses were applied in order to compare different characteristics in the

sludge and link them to filterability when possible. In order to have a clear and well-defined structure, data is organized by chronological event as Table 5-2 shows. This structure will be also used in the *Dilutions* experiments since the dilutions are originated from a blank sample.

Table 5-2 - Experiments carried out in the period of September 08 – February 09

Blank samples									
Name	WWTP	Sample	Date	T °C	MLSS (g/L)	Sludge age (d)	ΔR_{20} ($\times 10^{12} m^{-1}$)	R ²	
blank 1	Monheim	MT	08-09-08	19.0 *	7.6	30	0.067	0.86	
blank 2	Monheim	MT	09-09-08	19.0 *	7.1	30	0.092	0.98	
blank 3	Monheim	MT	10-09-08	20.1 *	6.9	30	0.094	0.95	
blank 4	Monheim	MT	11-09-08	19.9 *	7.0	30	0.098	0.93	
blank 5	Heenvliet	MT	22-10-08	19.8	17.7	20	0.025	0.63	
blank 6	Heenvliet	MT	29-10-08	19.5	14.3	20	0.047	0.24	
blank 7	Heenvliet	MT	05-11-08	19.5	14.1	20	0.036	0.85	
blank 8	Heenvliet	MT	10-11-08	19.5	15.1	20	0.042	0.37	
blank 9	Heenvliet	MT	20-11-08	20.2	13.0	20	0.066	0.47	
blank 10	Nordkanal	MT	26-11-08	15.0 *	11.0	25-29	0.234	0.74	
blank 11	Nordkanal	MT	26-11-08	16.2 *	11.8	25-29	0.418	0.92	
blank 12	Nordkanal	MT	26-11-08	15.4 *	11.7	25-29	0.391	0.87	
blank 13	Nordkanal	MT	27-11-08	15.5 *	10.7	25-29	0.278	0.90	
blank 14	Nordkanal	MT	27-11-08	17.2 *	11.1	25-29	0.398	0.95	
blank 15	Nordkanal	MT	27-11-08	16.7 *	11.0	25-29	0.382	0.86	
blank 16	Nordkanal	MT	28-11-08	15.2 *	10.7	25-29	0.320	0.83	
blank 17	Nordkanal	MT	28-11-08	17.5 *	10.7	25-29	0.266	0.89	
blank 18	Nordkanal	MT	28-11-08	17.5 *	11.0	25-29	0.389	0.80	
blank 19	Heenvliet	MT	17-12-08	23.7	15.1	20	0.096	0.92	
blank 20	Heenvliet	MT	18-12-08	22.9	15.1	20	0.070	0.91	
blank 21	Heenvliet	MT	07-01-09	14.5	16.4	20	0.221	0.99	
blank 22	Heenvliet	MT	21-01-09	12.1 *	17.0	20	0.183	0.95	
blank 23	Heenvliet	MT	23-01-09	12.3 *	16.1	20	0.246	0.88	
blank 24	Ootmarsum	MT	05-02-09	8.2 *	8.9	> 60	2.674	0.99	
blank 25	Ootmarsum	MT	05-02-09	8.2 *	7.5	> 60	2.258	1.00	
blank 26	Varsseveld	MT	12-02-09	10.8 *	7.8	35	4.248	0.99	
blank 27	Varsseveld	MT	12-02-09	10.8 *	7.6	35	4.104	0.98	
				Max	23.7	17.7	> 60	4.248	1.00
				Min	8.2	6.9	20	0.025	0.24

* Temperature "in situ"

All MBRs, except Heenvliet, were located at a considerable distance from TUDelft, thus not all the analysis were feasible since most of them had to be performed at the laboratory in TUDelft.

During the experiments period, the MLSS concentrations from sludge blanks ranged between 6.9 g/L and 17.7 g/L. Heenvliet presents the higher MLSS concentrations, 13.0 - 17.7 g/L, followed by Nordkanal, with values around 11.0 g/L. Ootmarsum and Varsseveld showed lower values of around 8.0 g/L, as well as Monheim where the lowest MLSS concentration was observed with more or less 7.0 g/L

In terms of filterability, values obtained for ΔR_{20} reside in the interval of $0.03 \times 10^{12} \text{m}^{-1}$ - $4.25 \times 10^{12} \text{m}^{-1}$, see Figure 5-1.

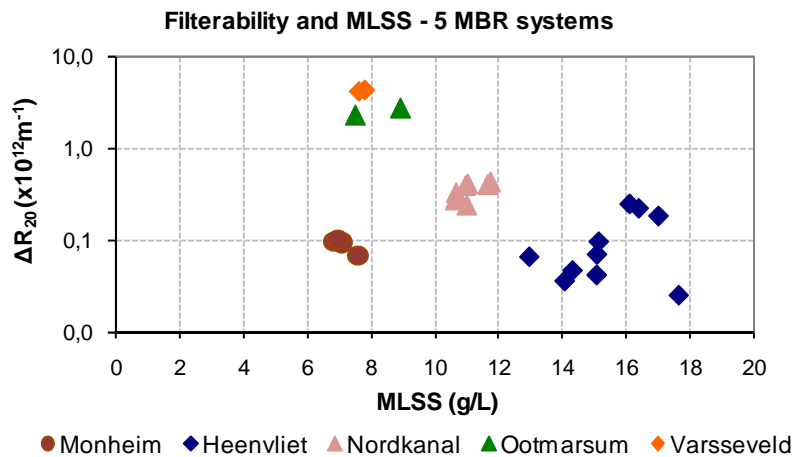


Figure 5-1 –Filterability plotted against MLSS according to each WWTP

According to the scale created by Geilvoet (2009) (see Table 4-2 in Section 4.3.8), the quality of the sludge tested varied between excellent, good, moderate and poor. No mediocre sludge was observed. In Figure 5-1 it's possible to see that sludges from Monheim, Heenvliet and Nordkanal have the best filterability, moderate - excellent, as opposed to Ootmarsum and Varsseveld with very poor filterability.

However, it is important to mention that sludge samples were collected at different WWTPs in different months, which implies different temperatures when performing the filterability tests. Not only was the test temperature affected by the seasonal variations but also by whether the DFCi was placed “in situ” or “ex situ”:

- a) “in situ” – directly in the WWTP where the sludge temperature is considered similar to the external temperature
- b) “ex situ” - at laboratory in TU Delft where the temperature of the sludge is the same as in the room.

Only the sludge from Heenvliet was, sometimes, tested at the laboratory since the distance between the treatment plant and TUDelft was not compromising to the reliability of the test (see Sub-chapter 4.2).

In Figure 5-2 the temperature from all experiments is plotted along the time with the respective filterability values.

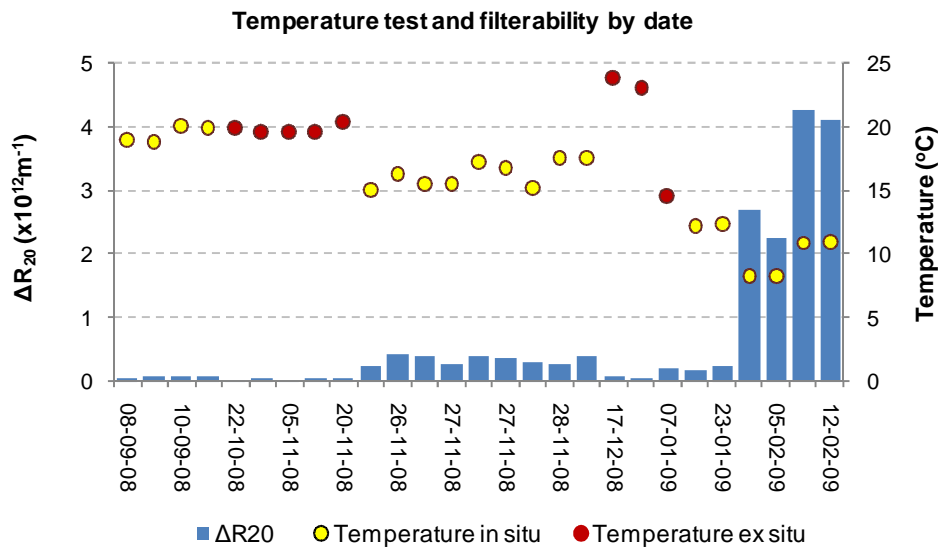


Figure 5-2 – Temperature and ΔR₂₀ by experiment date

In general, higher temperatures correspond to lower values of ΔR₂₀, which indicates a better filterability. However, the lowest temperature of 8.2°C registered on February 5th doesn't match the highest ΔR₂₀ which is verified when temperature is 10.8°C in February 12th. The main reason why we should pay more attention to “in situ” temperature values is because, while in “ex situ” the sludge experiences a quick change of temperature (from the treatment plant to the lab), “in situ” the sludge is considered stabilized and more representative of the real conditions in which MBRs are operated.

5.2.2 Correlating filterability with MLSS and Temperature

When plotting filterability in terms of quality sludge instead of the WWTP where sludge was collected, a more clear perception is given regarding the relation between MLSS and filterability. In Figure 5-3 it can be seen that, when the sludge quality is good, a large range of MLSS can coexist, 7.6 – 17.0 g/L. Also, for sludge with moderate quality, a considerable high interval of solids content occurs (10.7-16.4 g/L). Besides that, sludges of different quality can have similar MLSS. For instance, blanks of good and poor quality are observed when MLSS is approximately 8.0 g/L.

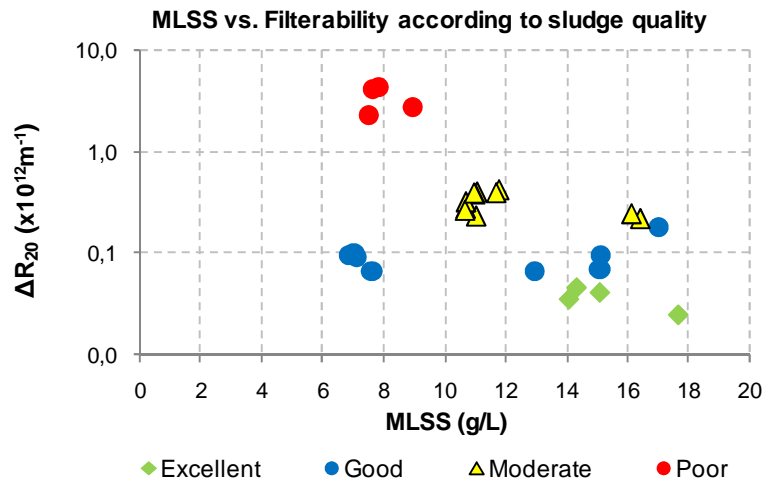


Figure 5-3 –Filterability plotted against MLSS according to sludge quality

When considering all the collected data, no correlation between MLSS and filterability is found. Harada et.al., (1994), Rosenberger and Kraume (2003), and (Lesjean et.al.,, 2005) have reported the same.

In relation to temperature, since higher temperatures corresponded in general to lower values of ΔR₂₀, a mathematical correlation between temperature “in situ” and filterability was made throughout a polynomial equation, see Figure 5-4.

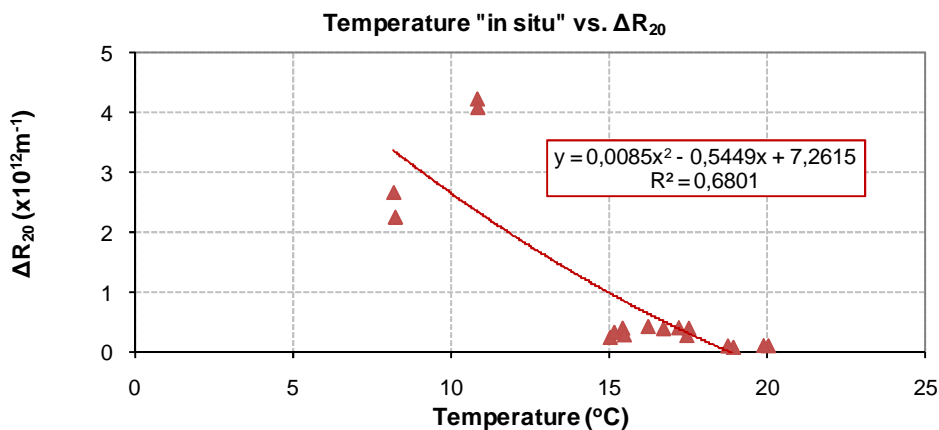


Figure 5-4 – Temperature “in situ” vs. ΔR₂₀

The correlation found is relatively high with a correlation factor of 0.68. This might indicate that temperature has a role in filterability. Geilvoet et.al., (2007a) and Lyko et.al., (2008) monitoring different full-scale MBRs also found an influence of temperature (seasonal variations) on filtration performance, where lower temperatures

corresponded to a worse filterability. The latter author attributes this relationship to the increase of the permeate viscosity and carbohydrate concentration at lower temperatures.

5.3 Particle counting in the range size of 2-100 μm

The particle size characterization in range 2-100 μm includes blank samples from Monheim, Heenvliet and Nordkanal. In Table 5-3 the particle counting parameters are presented according to the type of analysis.

Table 5-3 – Results from particle counting analysis in the range 2-100 μm

	Name	Particle number analysis				Particle volume analysis			
		Cumulative Nr (/ 100 mL)	Max Nr (/ 100 mL)	Max (%) *	Mean size max	Cumulative Vol (ppb)	Max Vol (ppb)	Max (%) *	Mean size max
Monheim	Blank 1	1.11E+06	2.12E+04	1.91	5.0	1.21E+07	1.60E+05	1.32	35.5
	Blank 2	1.07E+06	1.96E+04	1.83	5.0	1.26E+07	1.59E+05	1.27	34.5
	Blank 3	1.03E+06	1.88E+04	1.83	5.0	1.74E+07	1.57E+05	0.90	36.5
	Blank 4	1.08E+06	1.76E+04	1.63	5.0	1.56E+07	1.87E+05	1.20	39.0
Heenvliet	Blank 5	1.12E+06	1.34E+04	1.20	25.0	3.98E+07	3.99E+05	1.00	51.0
	Blank 6	1.02E+06	1.26E+04	1.24	26.0	3.28E+07	3.29E+05	1.00	49.0
	Blank 7	1.09E+06	1.37E+04	1.26	25.0	3.46E+07	3.53E+05	1.02	49.0
	Blank 8	1.09E+06	1.31E+04	1.20	26.0	4.09E+07	4.10E+05	1.00	51.0
	Blank 9	9.73E+05	1.19E+04	1.22	26.0	3.36E+07	3.45E+05	1.03	51.0
	Blank 19	1.05E+06	1.28E+04	1.22	25.0	2.82E+07	2.58E+05	0.91	70.5
	Blank 21	1.03E+06	1.26E+04	1.23	25.0	2.52E+07	2.27E+05	0.90	66.5
	blank 22	1.13E+06	1.41E+04	1.25	18.0	3.11E+07	2.82E+05	0.91	75.0
Blank 23	1.11E+06	1.39E+04	1.25	18.0	3.08E+07	3.07E+05	1.00	69.5	
Noordkanal	Blank 12	7.46E+05	1.19E+04	1.59	5.0	2.82E+07	2.62E+05	0.93	73.5
	Blank 13	7.32E+05	1.19E+04	1.63	5.0	3.01E+07	2.81E+05	0.93	66.5
	Blank 14	7.70E+05	9.81E+03	1.27	6.0	3.06E+07	2.83E+05	0.92	70.5
	Blank 15	8.38E+05	1.29E+04	1.54	5.0	4.01E+07	3.95E+05	0.99	51.0
	Blank 16	8.64E+05	1.87E+04	2.17	5.0	4.00E+07	3.91E+05	0.98	51.0
	Blank 17	7.81E+05	1.37E+04	1.76	3.5	3.49E+07	3.48E+05	1.00	51.0
	Blank 18	7.51E+05	1.03E+04	1.37	3.5	3.36E+07	3.34E+05	0.99	51.0

* Percentage of maximum relatively to the cumulative

5.3.1 Characterization of the particle size and volume distributions

Particle number analysis

The results showed a different particle size distribution (PSD) for each WWTP. To have a clear perception and to allow a possible comparison of the different PSDs, only one representative blank from each treatment plant was chosen and plotted in Figure 5-5 (for all PSD see Appendix VII).

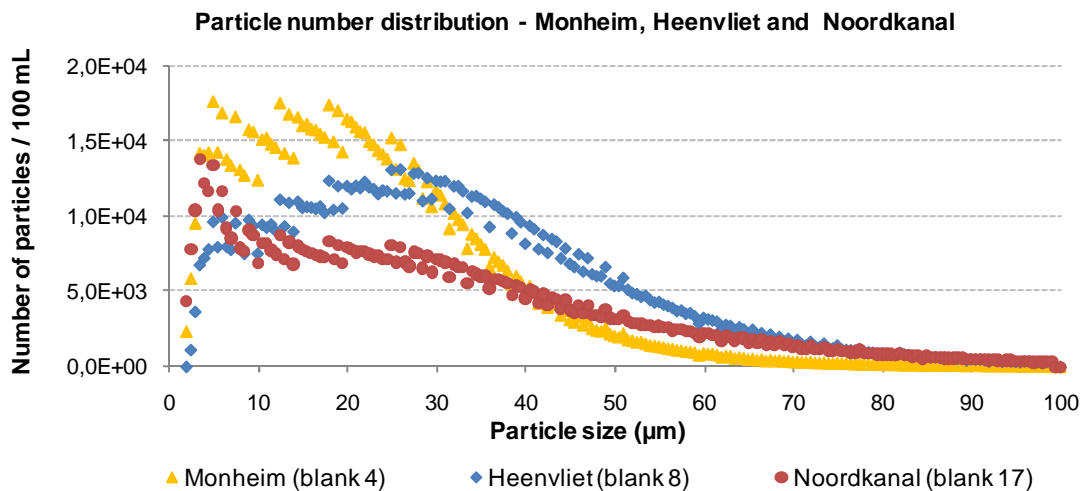


Figure 5-5 – Particle number distribution representative of different full-scale MBR

From Figure 5-5 it is visible that, for all distributions, in general, the higher particle number occurs for smaller particle sizes.

Of all three different PSDs, Monheim presents the highest particle number, in the interval 3-28 µm, and also the lowest, approximately from 50 till 100 µm. In Heenvliet the higher particle number exists when the particle size ranges from 15 till 35 µm. For particle sizes above 30 µm, Heenvliet presents the higher number of particles when compared to the others. For Nordkanal, the most particles are situated in a compact interval of 3-6 µm and from there the particle number decreases gradually.

In the interval 99.5-100.5 µm no particles were counted. The reason for this is probably related with the sieving (100 µm) used in the measuring protocol (see Sub-chapter 4.4). Even with the cleaning of the sieve after each test, most likely an accumulation of materials within the pores took place reducing the pore size of 100 µm. This might also explain why from 2 µm till 87 µm 99% of the cumulative particle number is represented in all blank samples. Therefore particle counting analysis and further correlations will only be made with values within the interval 2-87 µm.

In relation to cumulative particle number values are found between 7.32E+06 particles /100 mL and 1.15E+06 particles /100 mL. From Figure 5-6 it is possible to see that the Nordkanal presents the lowest values, around 7.8E+05 particles /100 mL, whilst Monheim

and Heenvliet have values around $1.1E+06$ particles /100 mL (35% higher than Nordkanal).

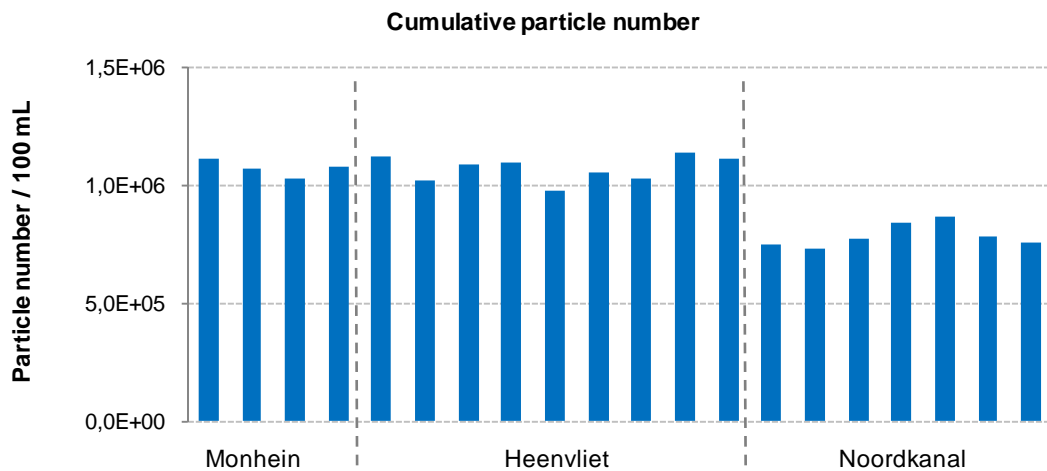


Figure 5-6 –Cumulative particle number of different WWTP

The maximum particle number per particle size represents in average 1.5 % of cumulative particle number. The values for maximum particle number are found between $2.0E+04$ particles /100 mL and $9.83E+04$ particles /100 mL. Heenvliet and Nordkanal both present an average of $1.3E+04$ particles /100 mL while in Monheim it is slightly higher, $1.8E+04$ particles /100 mL.

The results for the particle size of maximum particle number showed divergent values. In Monheim and Nordkanal the maximum particle number occurs at small size: $5.0 \mu\text{m}$ for Monheim and between $3.5 \mu\text{m}$ and $6 \mu\text{m}$ for Nordkanal. In Heenvliet a different behavior is observed since the particle size of maximum particle number varies between $18 \mu\text{m}$ and $26 \mu\text{m}$, see Figure 5-7.

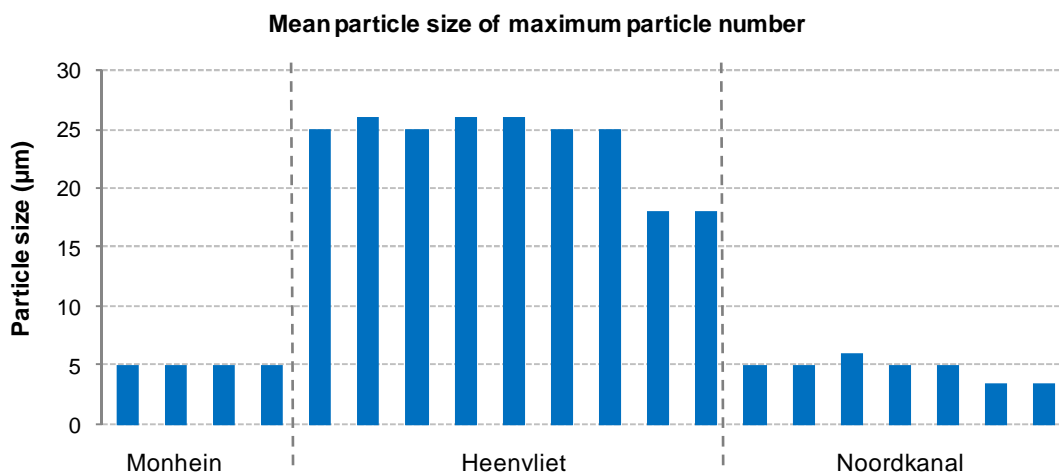


Figure 5-7 - Mean particle size of maximum particle number per WWTP

As said in Sub-chapter 3.2, the PSD of a sludge sample can be influenced by the operating conditions in MBR, namely severe aeration, intensive recirculation and SRT.

In relation to the aeration intensity, usually expressed as specific aeration demand (SADm), values are around $0.4 \text{ m}^3 \text{ m}^{-2} \text{ h}^{-1}$ for Heenvliet and Noordkanal. No data is available from Monheim, but since it's a Zenon system, it is expected to have similar values to Noordkanal (a Zenon system as well). Thus, aeration does not explain the differences observed. The values found for SRT are quite different: 20 days for Heenvliet, 25-29 for Noordkanal, and 30 for Monheim. The differences found in the mean particle size for maximum particle number can be due to the SRT, since Noordkanal and Monheim have similar SRTs. One possible explanation is that for higher SRT a higher recirculation is required for the activated sludge, leading to floc breakage and subsequently to a modification in the particle distribution (Wisniewski and Grasmick, 1998). However, SRT is also dependent of the membrane tank volumes, which were not possible to compare.

Particle volume analysis

In Figure 5-8, the cumulative particle volume distributions for each WWTP are represented. In Monheim the values are much lower when compared to the other two WWTPs, and also a different pattern is observed which is similar to a “mountain”. The highest peak is reached when particle size is near $37 \mu\text{m}$.

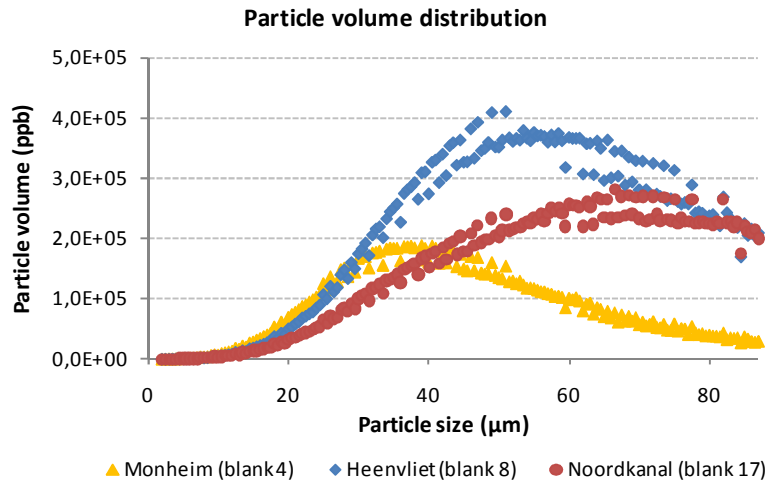


Figure 5-8 – Particle volume distribution representative of different full-scale MBR

For Heenvliet and Noordkanal distributions an identical pattern is evident, though the particle volumes are much higher for Heenvliet. The highest peak of particle volume is at 51 µm for Heenvliet and 70 µm for Noordkanal. After these peaks are reached there is a slight decrease along the following particle sizes.

The cumulative particle volumes for the blank samples are situated between 1.2E+07 and 3.7E+07 ppb (ppb – one part per billion: denotes one part in 10⁹ parts). Heenvliet has the higher values, an average of 3.3E+07 ppb, followed by Noordkanal with an average of 2.5+07 ppb and finally Monheim with 1.4+07 ppb, see Figure 5-9.

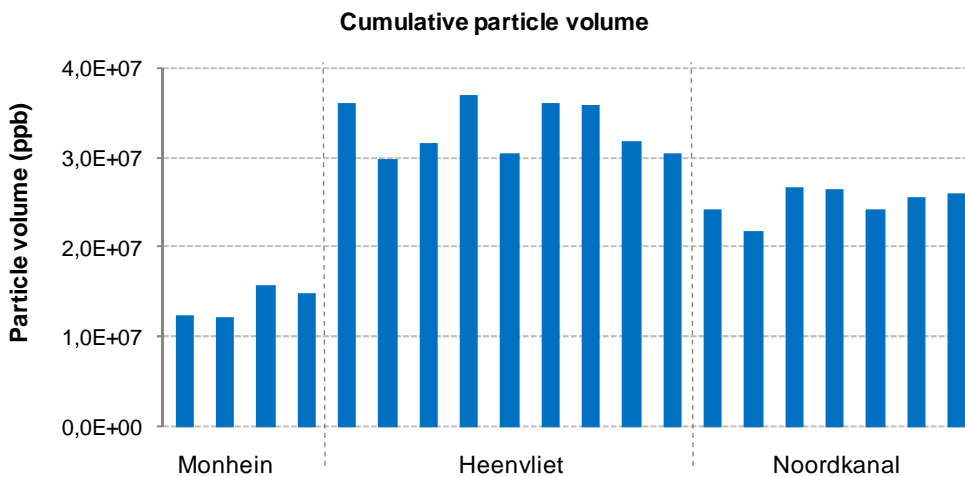


Figure 5-9 – Cumulative particle volume per WWTP

For the maximum particle volume, values ranged from 1.6E+05 ppb till 4.1E+05 ppb. The distribution of maximum particle volume is practically the same observed for cumulative particle volume.

Each WWTP presents a different mean particle size of maximum particle volume. Monheim and Nordkanal present some variations along their values in opposite to Heenvliet where they are significantly constant - only 2 samples out of 9 had different values, see Figure 5-10.

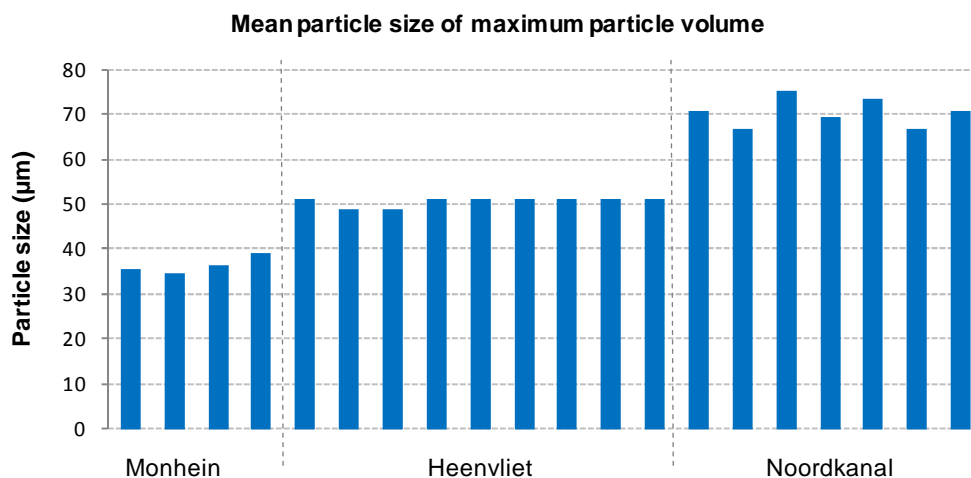


Figure 5-10 – Mean particle size of maximum particle volume

On average, the mean particle size of maximum particle volume is 36 µm for Monheim, 51µm for Heenvliet and 70 µm for Noordkanal.

5.3.2 Correlation between filterability with particle counting in range 2-87 µm

From Figure 5-11 it is possible to see the cumulative particle number per group quality with the associated filterability. When the sludge quality is excellent and good, the cumulative particle number is more or less the same and filterability does not vary significantly. However, in moderate sludge two different patterns are observed: a smaller group of blanks with a lower cumulative number (corresponding to Noordkanal blanks), and two blanks with higher cumulative numbers (Heenvliet). This is due to their different origin.

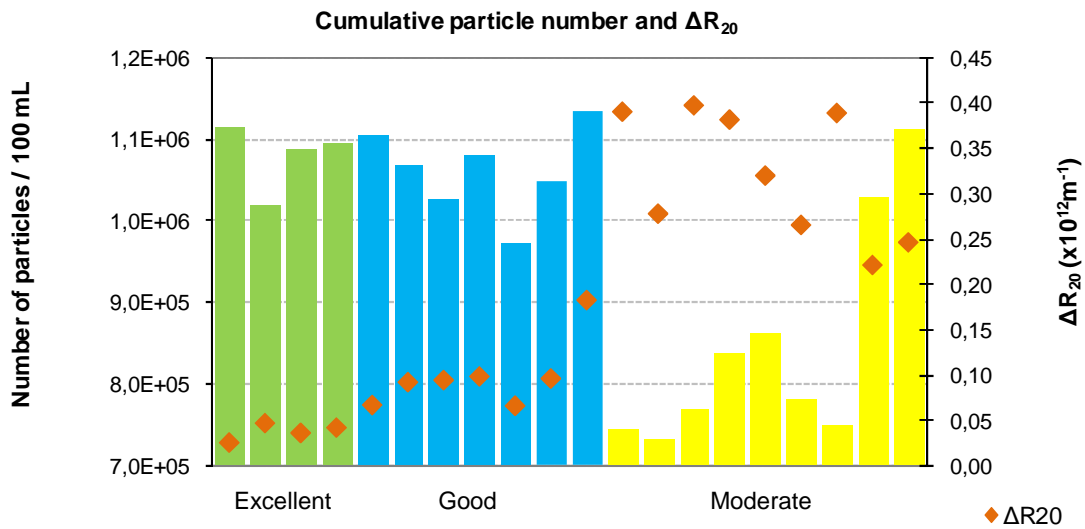


Figure 5-11 – Cumulative particle number and ΔR_{20} by group quality

The last two blanks in the moderate group have similar cumulative numbers as the ones seen in sludge of excellent and good quality. This means that the difference in filterability cannot be explained by the cumulative particle number.

No relationship between cumulative particle number and ΔR_{20} was found.

When correlating the filterability with cumulative particle volume no correlation is found either. Blanks with excellent and moderate quality presented cumulative particle volumes in the same range of values.

For maximum particle number all blanks have on average more or less the same maximum particle number, $1.4E+04$ particles /100 mL. From the presented groups, only inside the group with good quality there are some more emphasized oscillations for the maximum particle number but with no relationship with filterability. No correlation between maximum particle number and filterability was found.

In relation to the maximum particle volume, no relationship with filterability seems to exist either since to identical maximum particle volumes correspond different ΔR_{20} , and for different maximum particle volumes similar ΔR_{20} coexist.

When correlating the mean particle size for the maximum particle number with filterability no relationship is found; however, the particle size for the maximum particle volume has shown a correlation with filterability.

From Figure 5-12 it can be verified that, in general, when the mean particle size of maximum particle volume is high, the additional resistance in the membrane is also high, though not in a linear pattern.

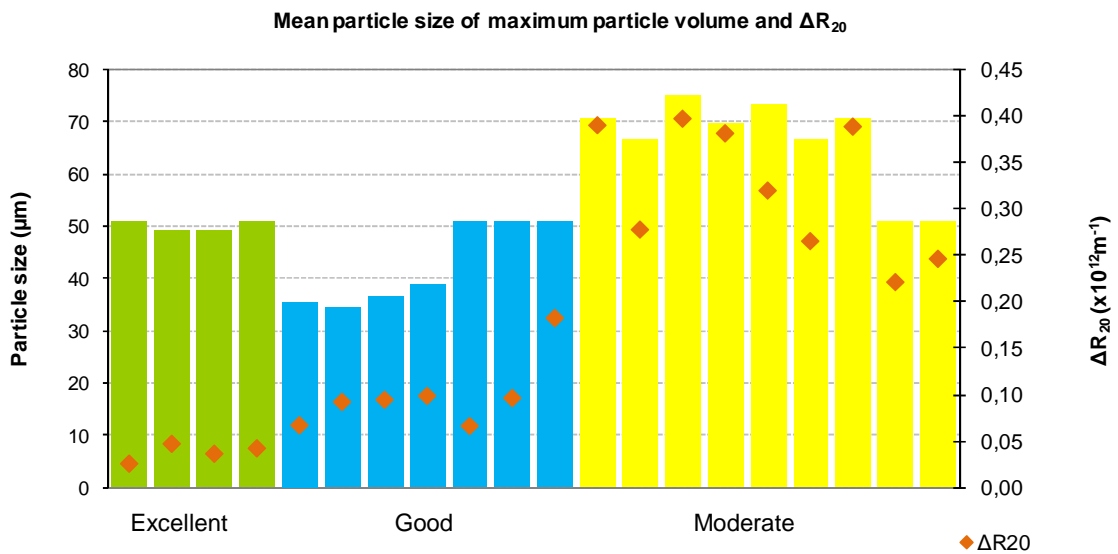


Figure 5-12 – Mean particle size of maximum particle volume per group quality

To evaluate how significant this relation is, a mathematical correlation throughout a polynomial equation is applied, as Figure 5-13 illustrates.

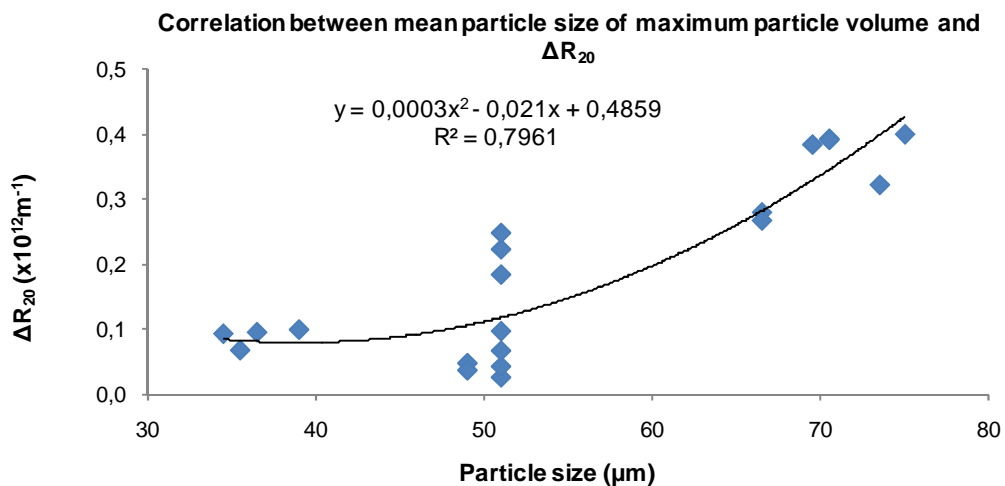


Figure 5-13 – Mean particle size of maximum particle volume vs. filterability

A correlation factor of 0.80 was found showing a strong correlation between mean particle size of maximum particle volume and filterability. Though for particle size around 50 μm ΔR_{20} values differ from $0.03 \times 10^{12} \text{m}^{-1}$ till $0.25 \times 10^{12} \text{m}^{-1}$.

This relationship suggests that filterability decreases for higher particle sizes of maximum particle volume.

5.4 Particle counting in the range size of 0.4-5 μm

The particle counting analysis in the range of 0.4-5 μm was performed on blank samples from Heenvliet, Ootmarsum and Varsseveld. In Table 5-4 an overview of the results is presented.

Table 5-4 – Results from particle counting analysis in the range 0.4-5 μm

	Name	Particle number analysis				Particle volume analysis			
		Cumulative Nr (/ mL)	Max Nr (/ mL)	Max (%) *	Mean size max	Cumulative Vol (ppb)	Max Vol (ppb)	Max (%) *	Mean size max
Heenvliet	Blank 5	4.40E+06	3.15E+06	71.6%	0.45	2.90E+02	1.50E+02	51.9%	0.45
	Blank 6	1.87E+06	1.32E+06	70.5%	0.45	1.24E+02	6.29E+01	50.6%	0.45
	Blank 7	2.44E+06	1.77E+06	72.4%	0.45	1.67E+02	8.42E+01	50.5%	0.45
	Blank 9	2.16E+06	1.65E+06	76.0%	0.45	1.46E+02	7.85E+01	53.9%	0.45
	Blank 19	7.74E+05	6.57E+05	84.9%	0.45	6.79E+01	4.61E+01	67.9%	0.45
	Blank 20	2.00E+06	1.45E+06	72.4%	0.45	1.40E+02	6.92E+01	49.3%	0.45
	Blank 21	1.15E+07	8.25E+06	71.9%	0.45	7.04E+02	3.93E+02	55.9%	0.45
Ootmarsum	Blank 24	6.58E+06	4.17E+06	63.3%	0.45	4.89E+02	1.99E+02	40.7%	0.45
	Blank 25	3.85E+06	2.65E+06	68.8%	0.45	2.83E+02	1.26E+02	44.7%	0.45
Varsseveld	Blank 26	1.86E+07	1.32E+07	71.0%	0.45	1.19E+03	6.29E+02	52.9%	0.45
	Blank 27	1.97E+07	1.38E+07	70.2%	0.45	1.27E+03	6.61E+02	52.0%	0.45

* Percentage of maximum relatively to the cumulative

5.4.1 Characterization of the particle size and volume distributions

Particle number analysis

The PSD, as Figure 5-14 reveals, shows that Heenvliet and Ootmarsum have an identical pattern while Varsseveld demonstrates a major difference, more precisely when the particle size is 0.45 μm .

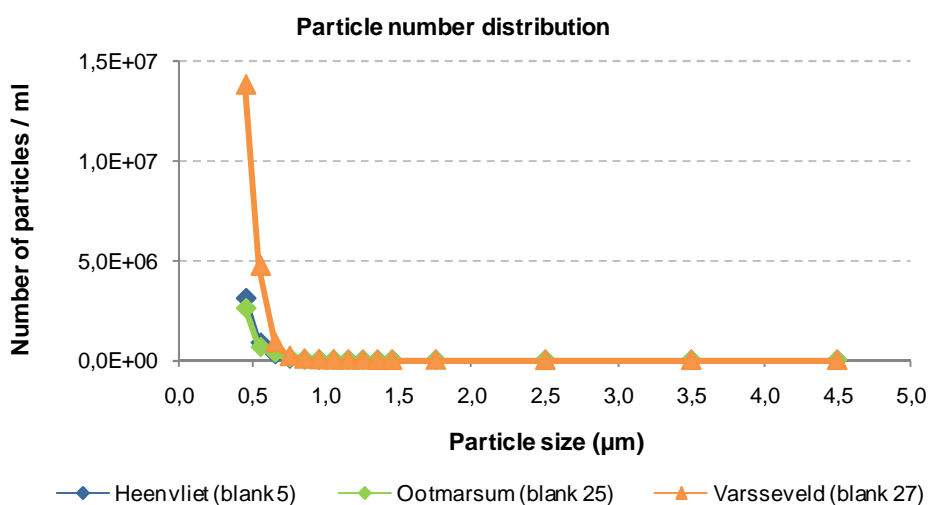


Figure 5-14 – Particle number distribution in the range 0.4-5 µm (representative blanks)

All blanks show a PSD where the number of particles is decreasing as the particle size increases. It is also visible that higher particle numbers occur from 0.45 till 1.0 µm. This was confirmed by the analysis of all blanks, which revealed that 99% of the cumulative particle number is represented in the interval of 0.4-1.0 µm. For that reason further analyses will only include the particles in this range.

The Figure 5-15 illustrates the cumulative particle number according to each treatment plant.

Varsseveld presents a much higher particle number than the other two treatment plants, on average 5 times more than Heenvliet and 4 times more than Ootmarsum.

Values are more inconstant in Heenvliet than in Ootmarsum and Varsseveld, varying between 1.9E+06 and 1.2E+07 particles/ mL. This could be due to seasonal variations since in Heenvliet samples were measured between October and January, while Ootmarsum and Varsseveld measurements only correspond to the same day (see Table 5-1). In Ootmarsum and Varsseveld values are on average 5.2E+06 particles /mL and 1.9E+07 particles /mL, respectively.

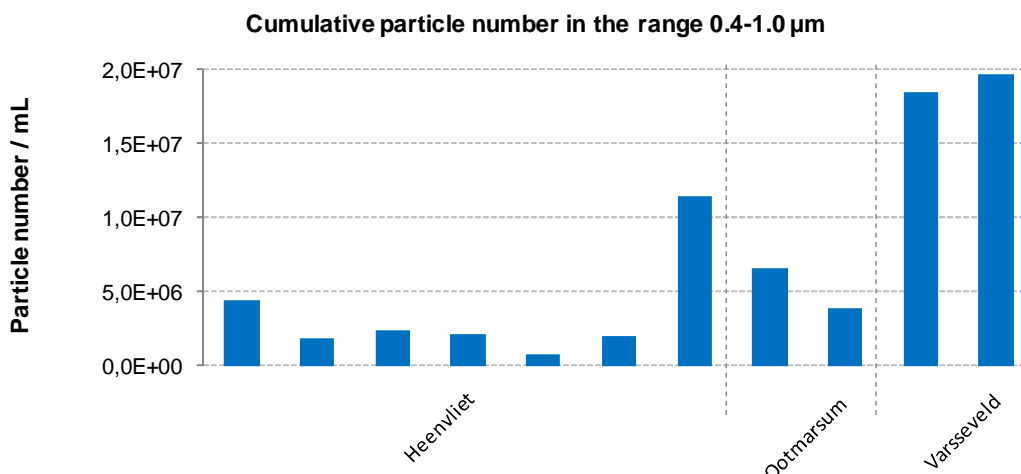


Figure 5-15 – Cumulative particle number in the range 0.4-1.0 μm

When analyzing the maximum particle number all blanks demonstrated an equal distribution as showed for the cumulative particle number. This can be easily explained by the maximum particle number being on average 70% of the cumulative particle number.

The mean particle size for maximum particle number is the same for all blanks - 0.45 μm.

Particle volume analysis

The particle volume distributions have shown that higher particle volumes are found for smaller particle sizes. From Figure 5-16 it is once again clear the similarity between Heenvliet and Ootmarsum distribution, and the discrepancy observed in Varsseveld.

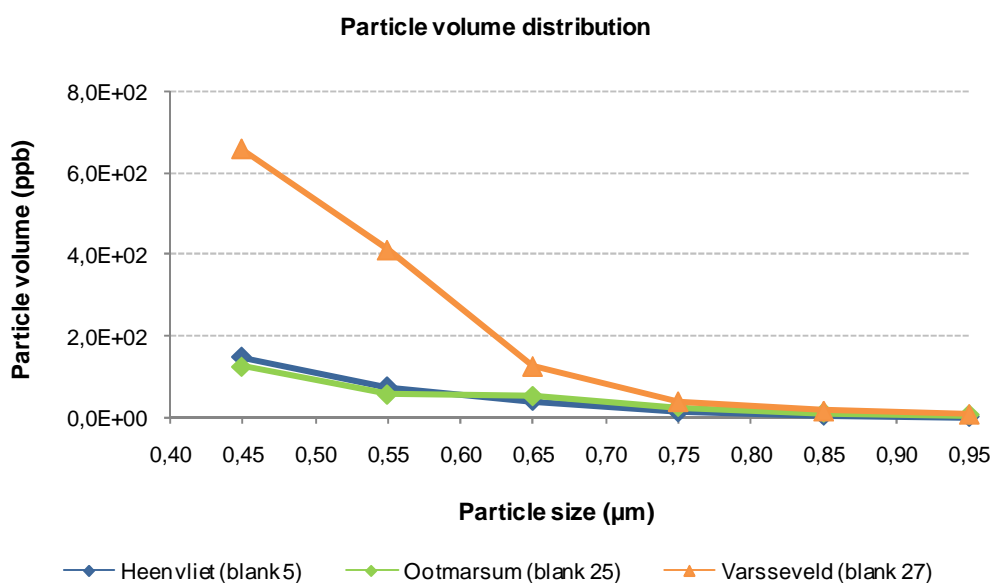


Figure 5-16 - Particle volume distribution in the range 0.45-1.0 μm

The cumulative particle volume showed, on average, values of $2.3E+02$ ppb, $3.9E+02$ ppb and $1.2E+03$ ppb for Heenvliet, Ootmarsum and Varsseveld, in that order.

In relation to maximum particle volume, this includes on average 50% of the cumulative particle volume. The values varied from $4.6E+01$ till $3.9E+02$ ppb in Heenvliet, $1.3E+02$ till $2.0E+02$ ppb in Ootmarsum, and from $6.3E+02$ till $6.6E+02$ ppb in Varsseveld.

All the samples show their maximum particle volume for a particle size of $0.45 \mu\text{m}$.

5.4.2 Correlation between filterability and particle counting in range $0.4\text{-}1.0 \mu\text{m}$

The analysis of particle counting in range $0.4 - 1.0 \mu\text{m}$ comprises sludge with excellent, good, moderate and poor quality.

The cumulative particle number has not revealed a clear behavior along the quality groups. On one hand, sludges of excellent and good quality have similar particle numbers that are lower than moderate and poor sludge, see Figure 5-17. On the other hand, there are some contradictions: the blank with moderate quality presents a higher particle number than two blanks of poor quality; blanks 5 (excellent) and 24 (poor) have identical cumulative particle numbers, however a large gap in filterability distinguishes them - $0.3 \times 10^{12}\text{m}^{-1}$ and $2.7 \times 10^{12}\text{m}^{-1}$, respectively.

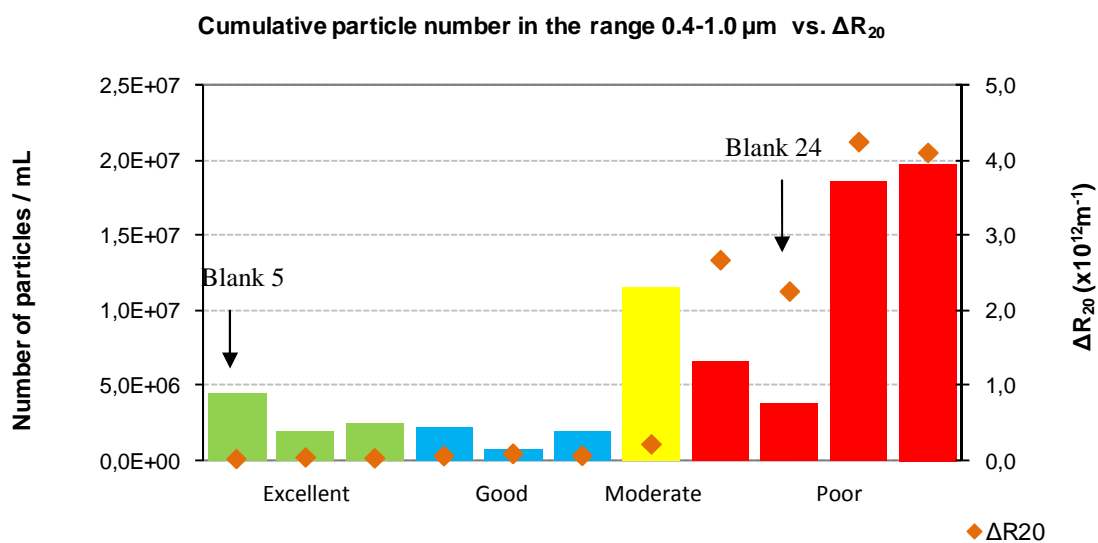


Figure 5-17 - Cumulative particle number and ΔR_{20} by group quality

Nevertheless, in overall results a main tendency seems to exist in which higher particle numbers match higher resistances in the membrane filtration. A correlation factor of 0.67 was found.

In relation to the maximum particle number, since it represents 70% of the cumulative particle number, the correlation obtained is practically the same ($R^2=0.66$)

In the particle volume analysis the results are quite the same as for the particle number analysis. Still, the correlation between cumulative particle volume and filterability is slightly higher than for cumulative particle number, $R^2 = 0.72$.

Benschop (2008) also investigated this relationship at TUDelft with the same methodology and apparatus but only with Heenvliet sludge. A high correlation between cumulative particle volume in the range 0.4-1.0 μm and filterability was found, where higher particle volumes corresponded to higher resistances in the membrane i.e. worst filterability.

When only looking at the results for Heenvliet presented on this thesis, the same correlation is also found for the cumulative particle volume and filterability, with a high correlation factor of 0.97. Moreover, the other particle counting parameters have shown a high correlation with filterability as well, see Table 5-5.

Table 5-5 – Correlation factors between filterability and particle counting in range 0.4-1.0 μm for Heenvliet

	Correlation factor, R^2
ΔR_{20}, Cumulative Nr.	0.98
ΔR_{20}, Maximum Nr.	0.97
ΔR_{20}, Cumulative Vol.	0.97
ΔR_{20}, Maximum Vol.	0.96

These high correlations show that particles in range 0.4-1.0 μm might help to estimate the additional resistance in the membrane and can thus be useful to predict membrane fouling. However, according to the results obtained, the only clear correlation is for Heenvliet sludge (from excellent to moderate quality). This means that the correlations found can

only be valid for Heenvliet sludge and/or to sludge with quality from excellent to moderate.

5.5 Soluble Microbial Products

5.5.1 SMP results

The results of SMP are represented by the protein and polysaccharide concentrations. Table 5-6 shows the SMP results concentrations together with other characteristics according to the sludge quality.

Table 5-6 – SMP results: protein and polysaccharide concentrations

	Name	WWTP	Date	T °C	MLSS (g/L)	ΔR_{20} ($\times 10^{12} m^{-1}$)	Proteins (mg/L)	Polysaccharides (mg/L)
Excellent	blank 7	Heenvliet	05-11-08	19.46	14.08	0.036	11.32	4.81
Good	blank 9	Heenvliet	20-11-08	20.21	12.96	0.066	12.80	3.48
	blank 19	Heenvliet	17-12-08	23.70	15.15	0.096	12.38	5.274
	blank 20	Heenvliet	18-12-08	22.92	15.10	0.070	11.32	3.60
Moderate	blank 21	Heenvliet	07-01-09	14.46	16.41	0.221	15.48	8.90
Poor	blank 24	Ootmarsun	05-02-09	8.18	8.94	2.674	12.03	14.05
	blank 26	Varsseveld	12-02-09	10.83	7.83	4.248	20.97	17.14
	blank 27	Varsseveld	12-02-09	10.84	7.64	4.104	21.89	18.30

It is visible that in every blank the protein concentration is higher than the polysaccharides except for Ootmarsum where polysaccharide concentration is 2 mg/L higher than the proteins. None of the previous researchers at TUDelft obtained a concentration of polysaccharides higher than the proteins for the same sludge sample. Therefore, the protein concentration in Ootmarsum will not be considered as a valid measurement and consequently will not be used for further correlations with other parameters.

The protein concentration varied between 11.3 mg/L and 21.9 mg/L whilst polysaccharide concentrations have lower values between 3.5 mg/L and 18.3 mg/L.

In Heenvliet the polysaccharide concentrations are below 5.5 mg/L whilst protein concentrations are at least double – Proteins represent 71% of the total SMP.

In Varsseveld is where the protein and polysaccharide concentrations are higher when compared to the other WWTPs (both above 17 mg/L). Although the protein concentrations are higher than the polysaccharides, they diverge slightly – Proteins are only 55% of SMP.

The analysis of the retention of proteins and polysaccharides by the membrane was possible since the SMP from the extracted permeate during the filterability test was also measured. It showed different behaviors for proteins and polysaccharides. On average, the membrane retained 43% of proteins and 80% of polysaccharides, which means that proteins breakthrough is 3 times higher than that of polysaccharides. Similar values were also observed by Geilvoet et.al., (2007) for the DFCi with the same pore size membrane.

In Figure 5-18 protein and polysaccharide concentrations are plotted according to WWTP with the respective temperature for each measurement.

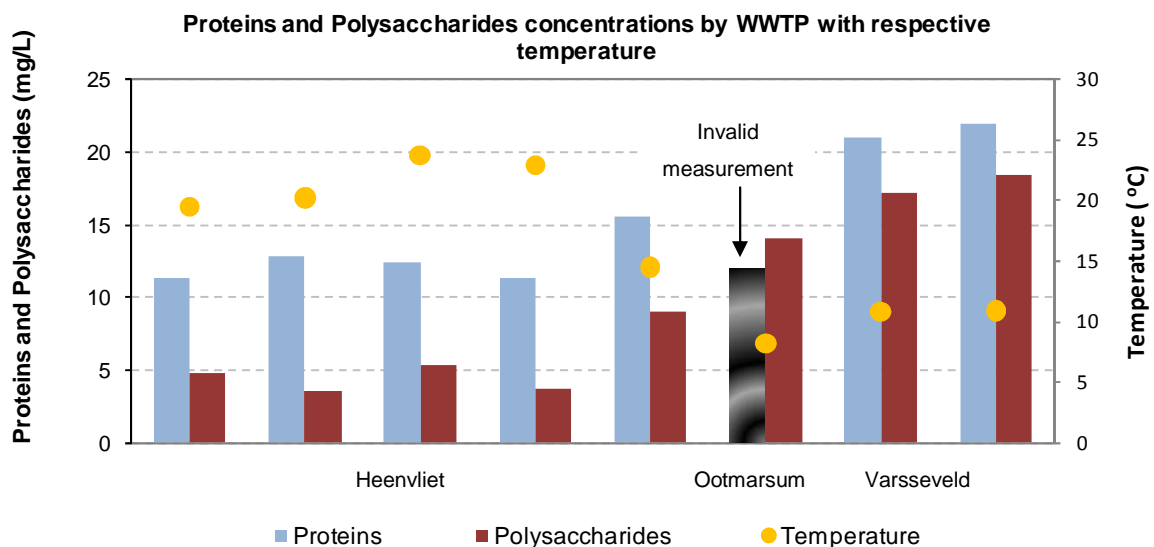


Figure 5-18 - Proteins and polysaccharides by WWTP with respective temperature

Looking at Figure 5-18, it can be seen that higher temperatures correspond to lower SMP concentrations. Further along, a correlation between SMP and temperature will be made to evaluate how significant this relationship is.

5.5.2 Correlating filterability with SMP

The concentrations of the proteins and polysaccharides are plotted in Figures 5-19 and 5-20 against ΔR_{20} with the respective correlation factor obtained.

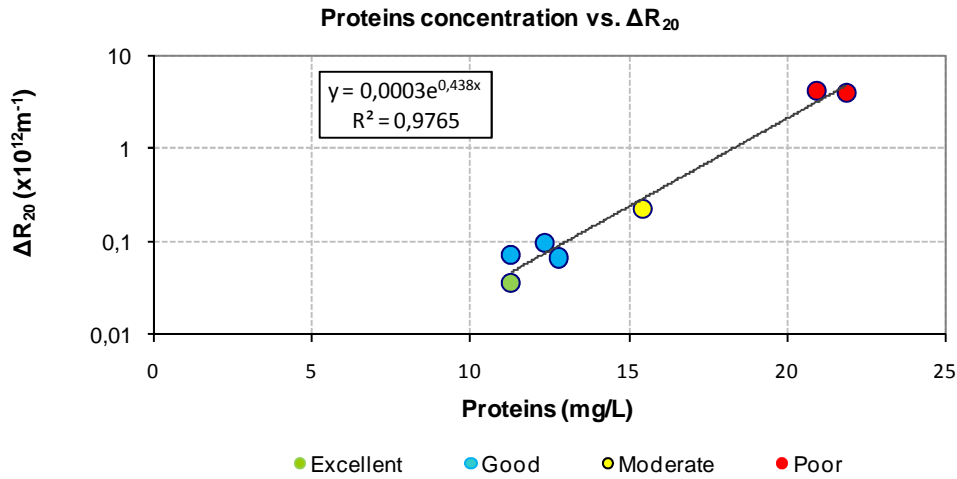


Figure 5-19 – Protein concentrations plotted against ΔR_{20}

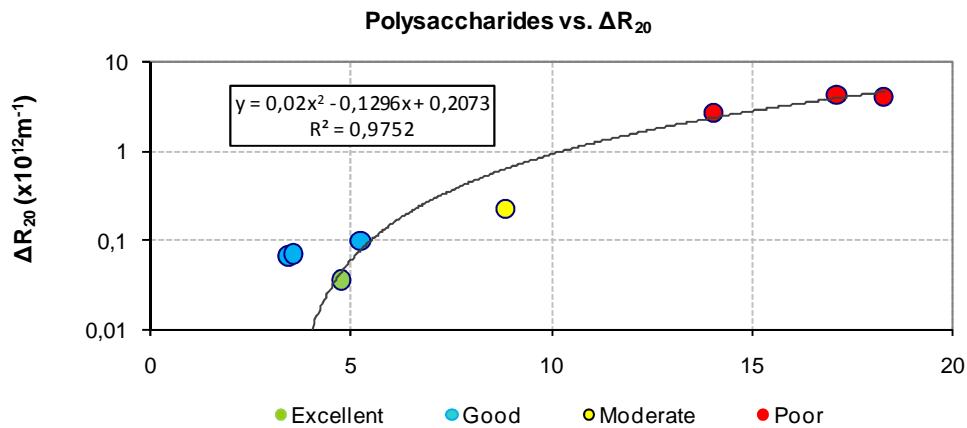


Figure 5-20 – Polysaccharide concentrations plotted against ΔR_{20}

A correlation between filterability and SMP concentrations was found.

From Figures 5-19 and 5-20, both relationships for proteins and polysaccharides were demonstrated throughout a mathematical correlation with very high correlation factors – $R=0.98$ for both. However, different regressions were applied for a better approximation of

each behavior: for proteins an exponential equation was applied and for polysaccharides a second order polynomial equation was used.

It is clear that higher concentrations of proteins and polysaccharides correspond to a higher additional resistance in the membrane. This conforms with many authors that have reported EPS as one of the most significant contributors for membrane fouling (Nagaoka et.al., (1996), Rosenberger and Kraume (2003) and Al-Halbouni et.al., (2008)). However, it is not clear yet how proteins and polysaccharides affect the filtration process. Even when looking at the breakthrough of proteins ($\approx 60\%$) and polysaccharides (20%), no conclusions can be drawn since different fouling mechanisms may be involved.

A correlation between SMP and temperature was also found.

Looking at Figure 5-21 it can be seen that higher temperatures correspond to lower SMP concentrations. Both correlation factors for proteins and polysaccharides are significantly high ($R^2=0.98$ for proteins and $R^2=0.84$ for polysaccharides). This suggests that temperature might have a role in the release of SMP into the sludge. Also, Al-Halbouni et.al., (2008) and Lyko et.al., (2008) stated that one of the factors that have an influence on the production of SMP is the temperature. This can be explained by the fact that at lower temperatures the kinetics of the degradation of SMP is lower than at higher temperatures or/and also that the dropping of temperature rises the stress level in the microbial cells leading to a bigger release of SMP.

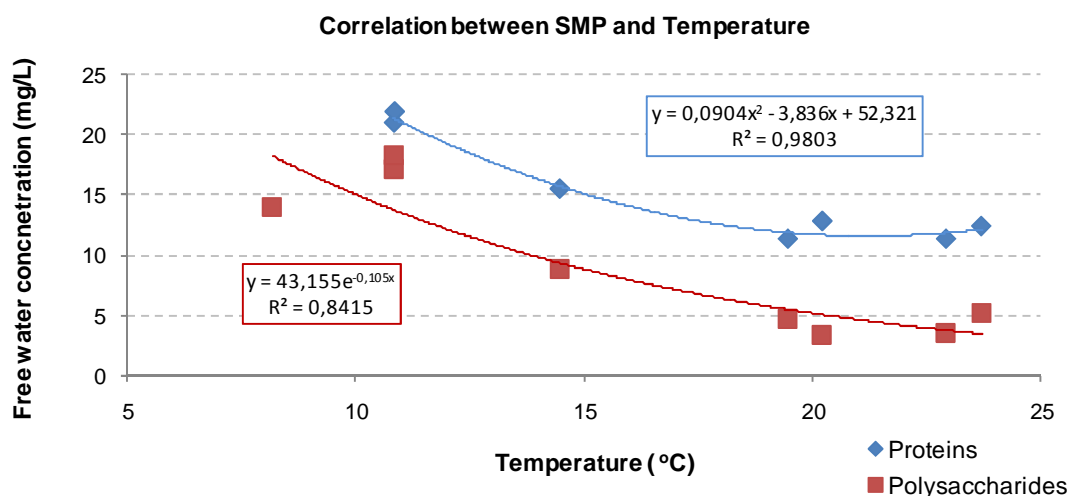


Figure 5-21 – Proteins and polysaccharides plotted against temperature

As demonstrated in Section 5.2.2, a correlation between filterability and temperature was observed ($R^2 = 0.68$). Since filterability is related to SMP concentrations, and SMP related to temperature, a relationship between these three parameters seems to exist.

Since a moderate relationship between filterability and particle counting in range 0.4-1.0 μm was found (see Section 5.4.2), a correlation between SMP and particles in this range was applied. In Table 5-7 the correlations obtained are presented.

Table 5-7 – Correlation factors between SMP and particle counting parameters in range 0.4-1.0 μm

	Particle number		Particle volume	
	Cumulative	Maximum	Cumulative	Maximum
Proteins	0.98	0.99	0.98	0.99
Polysaccharides	0.73	0.71	0.76	0.71

A relationship was established between particle counting in range 0.4-1.0 μm and SMP.

When SMP concentrations are higher, a higher number of particles is also associated. This is especially valid for proteins, which present much higher correlation factors than polysaccharides. This however doesn't mean that SMP particles are contained in the range from 0.4 μm till 1.0 μm . Evenblij and van der Graaf (2004) reported that EPS particles are mainly present with particles of smaller size than 0.1 μm . Also Geilvoet *et.al.*, (2007) stated that in the range of 0.2 μm till 1.2 μm no SMP particles are present.

However, this correlation might indicate that a higher number of particles in the range 0.4-1.0 μm correspond to a higher number of particles in the submicron range, range where SMP particles coexist. Therefore, the particle counting in range 0.4-1.0 μm may be a useful tool to estimate and predict the SMP concentrations and to enlarge the knowledge on membrane fouling.

5.6 Viscosity

The viscosity measurements were performed for all blanks of temperature 20 ± 1 °C with different shear rates applied, from 5s^{-1} till 1000s^{-1} . Besides apparent viscosity, shear stress

was also obtained and used to produce rheograms consisting of the shear rate plotted against shear stress.

5.6.1 Results

The viscosity results showed that for all samples, at a certain shear rate, a modification on the sludge structure occurred. As the shear rate increases, a decrease on the apparent viscosity is expected (Hasar et.al.,, 2004), however, there is a turning point where apparent viscosity starts to raise whilst shear rate continues to increase. This phenomenon was mostly observed at a shear rate of 500 s^{-1} but it was also noticed at shear rates of 700 s^{-1} and 250 s^{-1} . Therefore, the viscosity analysis will only focus on shear rates in the range $5\text{-}150 \text{ s}^{-1}$, which ensures that the original floc structure remains the same for all blanks.

All blanks show a non-Newtonian behavior since the shear rate is non-linear related to the shear stress, see Figure 5-22.

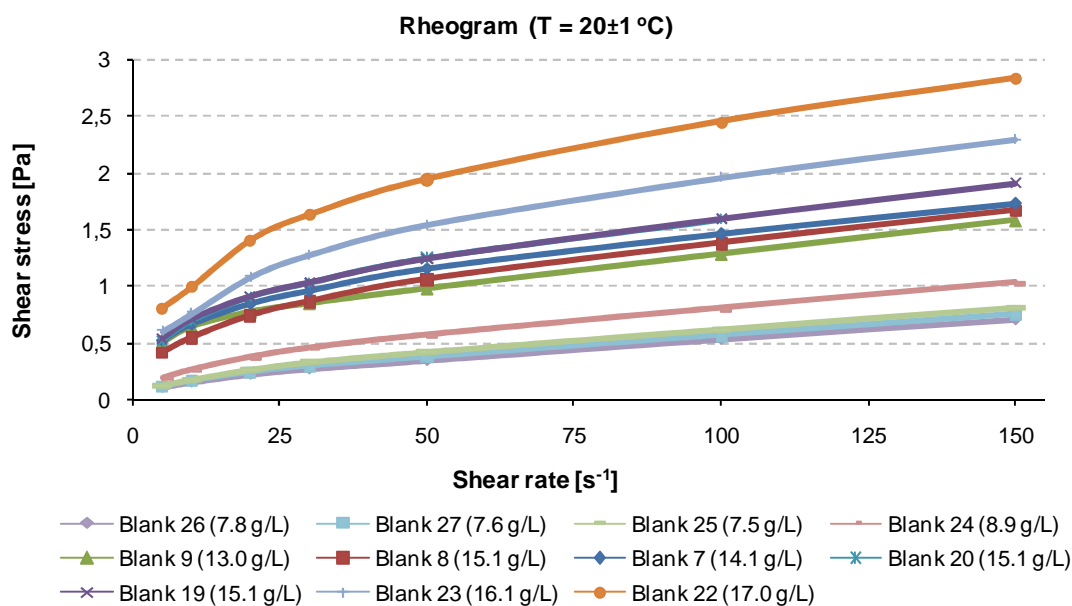


Figure 5-22 – Rheogram for all blanks with the respective MLSS concentration

The maximum shear stress listed corresponds to blank 22 with the higher MLSS (17.0 g/L) and the minimum is registered for blank 26 with an MLSS equal to 7.8 g/L. As Figure 5-22 demonstrates, blanks 25 and 27, with an MLSS of 7.5 g/L and 7.6 g/L correspondingly, have higher values of shear stress when compared to blank 26, which has a higher MLSS

of 7.8 g/L. The same also happens with blanks 7 and 8 where the latter has a higher MLSS (1.1 g/L more) and presents lower shear stress values.

The reason for these results is probably related with the very small differences in MLSS concentration among the samples, in spite of the high precision of the rheometer. For this reason the results obtained are considered valid and reliable for further use.

In Figure 5-23, it is possible to see that blanks with lower MLSS also have lower apparent viscosities, and as shear rate increases the apparent viscosity decreases. This is a characteristic of shear thinning fluids.

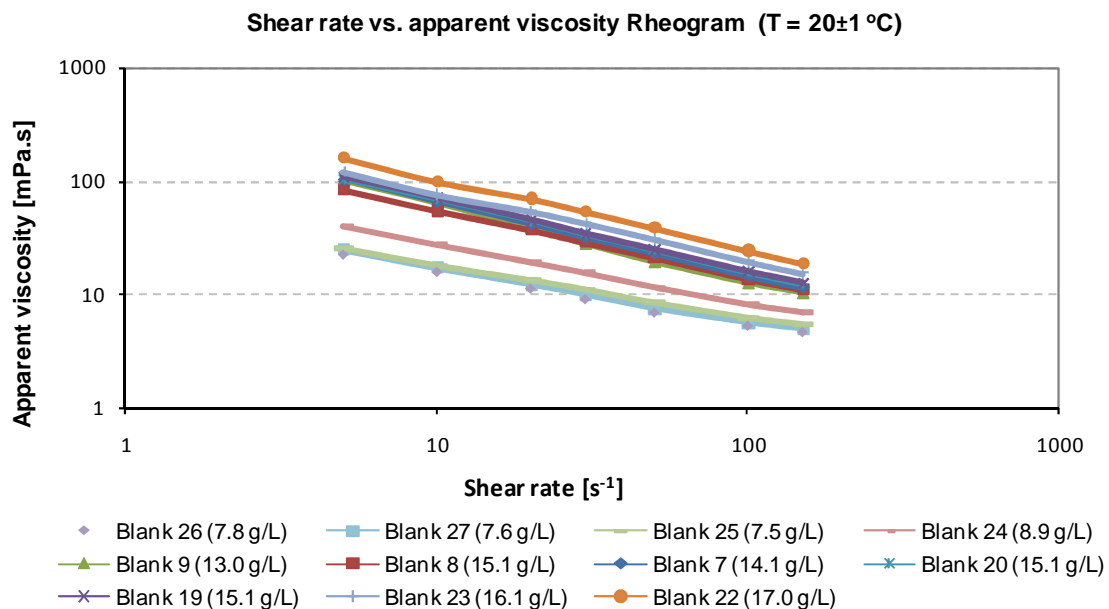


Figure 5-23 – Apparent viscosity per blank samples

5.6.2 Correlating viscosity

The relationship between apparent viscosity and MLSS was found with the same significant correlation factor for all shear rates ($R=0.95$) showing that the solids content is a major factor in apparent viscosity as literature states (Rosenberger et.al., 2002; Hasar et.al., 2004; Seyssiecq et.al., 2008).

Many authors have studied the influence of MLSS on apparent viscosity with sludge from a full-scale MBR and developed mathematical models for rheological simulations.

Rosenberger *et.al.*, (2002) created a model based on Ostwald equation whilst Laera *et.al.*, (2007) developed a Bingham model. Both models allow estimating apparent viscosity through solids content.

A comparison between the results obtained with the rheometer and the ones calculated with the two different formulas was made. Major divergences were found. The apparent viscosity through Rosenberger’s formula was sometimes half of the apparent viscosity obtained from the rheometer, and none of the shear rates values were similar. For Laera’s formula the same was verified but in the inverse way and with higher proportions since values were sometimes triple the rheometer values (See Appendix VII). These results indicate that the mentioned formulas are not applicable for all MBR activated sludge samples.

As an example of the divergence between the values a sample was chosen and plotted in Figure 5-24 with the different apparent viscosities.

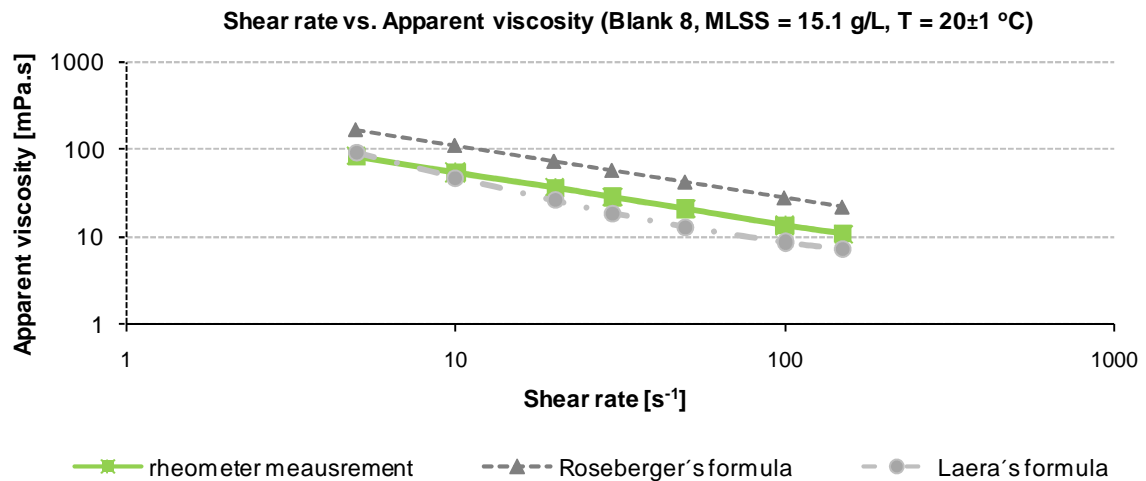


Figure 5-24 – Apparent viscosity from the rheometer measurements and Rosenberger’s and Laera’s formulas

These major differences observed are due to the complexity and variety of the components that constitute an activated sludge sample. An equation is always an approximation to reality and does not include all the relevant parameters for an activated sludge sample. For that reason the apparent viscosity obtained through the rheometer is more accurate and reliable than the one calculated through equations.

For the correlation between filterability and viscosity a shear rate was chosen to equally compare all blanks. At 100 s^{-1} , it is assured that the original structure from the sludge has not changed, and thus it will be used for comparison. In Figure 5-25 the filterability is plotted together with apparent viscosity.

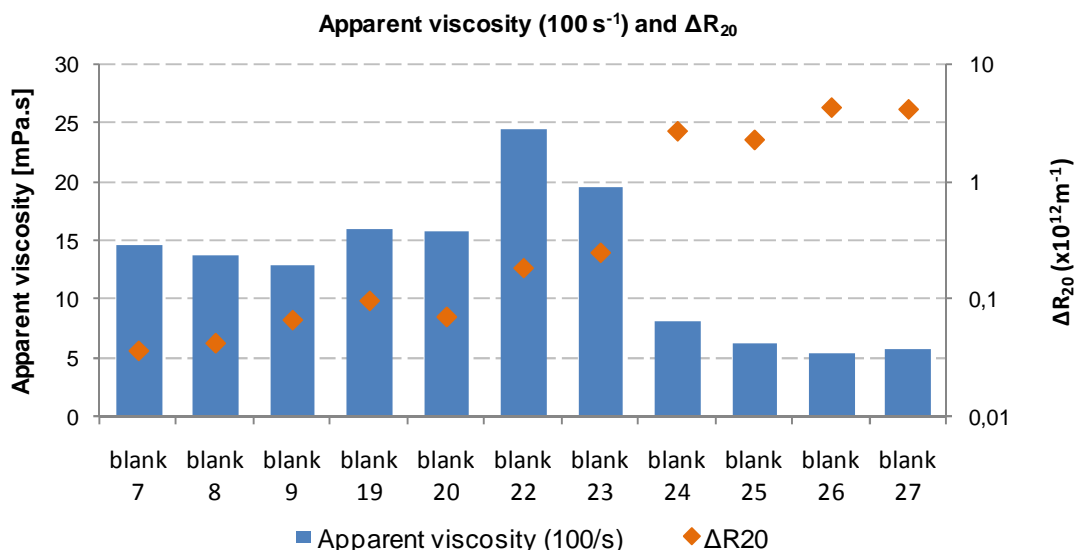


Figure 5-25 – Apparent viscosity (100 s^{-1}) and filterability

No correlation between filterability and apparent viscosity is found.

Higher apparent viscosities would be expected for blanks with higher values of ΔR_{20} . This is not observed since blanks 24-27 have the lowest apparent viscosities and the highest ΔR_{20} values. This suggests that apparent viscosity is not a major parameter influencing filterability.

5.7 Conclusions

The Blanks Characterization experiment goal was to study the characteristics of sludge in full-scale MBRs in order to evaluate their effects on membrane filterability and membrane fouling. Five MBR systems were analyzed: Monheim, Heenvliet, Nordkanal, Ootmarsum and Varsseveld. Each blank, in addition to the filterability test, was submitted, when possible, to different tests such as particle counting in range 2-100 μm , particle counting in range 0.4-5.0 μm , EPS, and viscosity.

The filterability of the activated sludge varied from 0.03 till $4.25 \times 10^{12} \text{m}^{-1}$, i.e. from excellent to poor quality. However, no sludge with mediocre quality was observed. The MLSS concentrations varied from 6.9 till 17.7 g/L, and the temperature between 8.2 and 23.7°C.

No correlation between filterability and MLSS was found. Sludge blanks with good and extremely poor quality were observed at $\text{MLSS} \approx 8 \text{g/L}$. This suggests that MLSS does not play a fundamental role in membrane fouling.

The seasonal variations, temperature differences, seemed to have an impact on membrane filterability ($R^2=0.68$). At lower temperatures, higher resistances in the membrane were found.

For the particle counting in range 2-100 μm , it was observed that 99% of particles exist in the range 2-87 μm . The particle counting in range 2-100 μm revealed a different PSD for each WWTP. This was probably due to the different SRT, probably implying different recirculation ratios, applied in each treatment plant. No correlation between filterability and particles in range 2-100 μm was found, except for the mean particle size of maximum particle volume with a correlation factor of 0.80. The floc size of the maximum particle volume varied between 34.5 and 75 μm , and higher resistances corresponded to a bigger floc size.

For the particle counting in range 0.4-5.0 μm , it was observed that 99% of particles exist in the range 0.4-1.0 μm . When correlating the filterability with particle counting parameters, a main tendency was present in which the blanks with highest number of particles were the ones with the worst filterability. This was even clearer when only analyzing sludge from Heenvliet with excellent to moderate quality, since all correlations were found with correlation factors above 0.96. This means that particles in this range have an effect on membrane filterability. However, since this is only clear when analyzing Heenvliet sludge samples, the conclusions drawn have to be careful when extrapolation is made for all MBR sludge samples. Overall, particle counting in range 0.4-1.0 μm can be a useful tool to predict membrane fouling.

A high relationship between filterability and SMP was found with a correlation factor of 0.98 (proteins and polysaccharides). A higher concentration of SMP led to a worst filterability. Also a relationship between SMP and temperature was found with high significance ($R^2=0.98$ for proteins and $R^2=0.84$ for polysaccharides). A strong correlation between SMP and particle counting parameters in range 0.4-1.0 μm was also found. Even though SMP particles are considered as being smaller than in the observed range, particle counting in range 0.4-1.0 μm seems to be a good indicative of the SMP levels in the activated sludge.

This suggests that a three-way relationship exists between filterability, SMP and temperature. The temperature seems to influence the release of SMP into the activated sludge, and SMP concentrations seem to be a major factor influencing membrane filterability. Therefore, SMP and temperature might play a major role in membrane filterability, and in a long-term operation, have an impact on membrane fouling.

The apparent viscosity of the activated sludge showed to be highly influenced by the MLSS concentration. No correlation between filterability and apparent viscosity was found.

6 DILUTIONS EXPERIMENT

This chapter describes the Dilutions experiment in which activated sludge from Heenvliet, Ootmarsum and Varsseveld was used. The sub-chapters present the results and discussion of each test applied, namely filterability, particle counting in ranges 2-100 μm and 0.4-5.0 μm , SMP, and viscosity. In Sub-chapter 6-6 the conclusions drawn are shown. All results can be seen in Appendix IX.

6.1 Filtration characteristics - MLSS and ΔR_{20}

6.1.1 Results and Discussion

In Table 6-1 the filtration characteristics from the dilutions experiments are presented.

Table 6-1 – Filtration characteristics from Dilutions experiment

		WWTP	Sample	Date	MLSS (g/L)	ΔR_{20} ($\times 10^{12} \text{m}^{-1}$)	R^2
Set 1	blank 5	Heenvliet	MT	22-10-08	17.7	0.025	0.63
	D10p				9.5	0.101	0.98
	D20p				4.5	0.020	0.13
Set 2	blank 6	Heenvliet	MT	29-10-08	14.3	0.047	0.24
	D10p				7.5	0.081	0.86
	D20p				3.7	0.031	0.70
Set 3	blank 7	Heenvliet	MT	05-11-08	14.1	0.036	0.85
	D10p				9.2	0.104	0.96
	D20p				4.2	0.068	0.94
Set 4	blank 9	Heenvliet	MT	20-11-08	13.0	0.066	0.47
	D10p				7.3	0.183	0.98
	D20p				5.3	0.099	0.91
Set 5	blank 19	Heenvliet	MT	17-12-08	15.1	0.096	0.92
	D10p				10.4	0.326	0.98
	D20p				2.2	0.156	0.98
Set 6	blank 20	Heenvliet	MT	18-12-08	15.1	0.070	0.91
	D10p				8.5	0.330	0.99
	D20p				3.7	0.162	0.98
Set 7	blank 21	Heenvliet	MT	07-01-09	16.4	0.221	0.99
	D10p				9.8	1.096	1.00
	D20p				4.7	0.500	0.99
Set 8	blank 22	Heenvliet	MT	21-01-09	17.0	0.183	0.95
	D10p				12.3	1.878	0.94
	D20p				4.6	0.839	0.96
Set 9	blank 23	Heenvliet	MT	23-01-09	16.1	0.246	0.88
	D10p				6.0	0.814	0.99
	D20p				2.6	0.404	0.96
Set 10	blank 24	Ootmarsum	MT	05-02-09	8.9	2.674	0.99
	D10p				5.9	1.232	0.99
	D20p				4.2	0.640	0.99
Set 11	blank 26	Varsseveld	MT	12-02-09	7.8	4.248	0.99
	D10p				5.1	2.343	0.97
	D20p				2.8	1.005	0.99
Set 12	blank 27	Varsseveld	MT	12-02-09	7.6	4.104	0.98
	D10p				6.5	2.541	1.00
	D20p				2.0	1.333	0.99

*D10p = 10L of permeate + 20L sludge; D20p = 20L of permeate + 10L sludge

In Table 6-1 the values of MLSS and ΔR_{20} from each dilution set are visible. Since D10p and D20p are done following the same procedure, it would be expectable that sets with the same blank MLSS concentration would have similar MLSS in the prepared dilutions. However, this wasn't always the case, with differences occurring between the dilutions, for instance when comparing set 7 and set 9. The MLSS concentration in sets 7 and 9 is respectively 16.4 g/L and 16.1 g/L for blank, 9.8 g/L and 6 g/L for D10p and 4.7 g/L and 2.6 g/L for D20p. This happens because the measuring of volumes, for sludge and permeate, is not always precise, which leads to differences in the final solids content.

In Figure 6-1 all sets are plotted with the respective MLSS and ΔR_{20} .

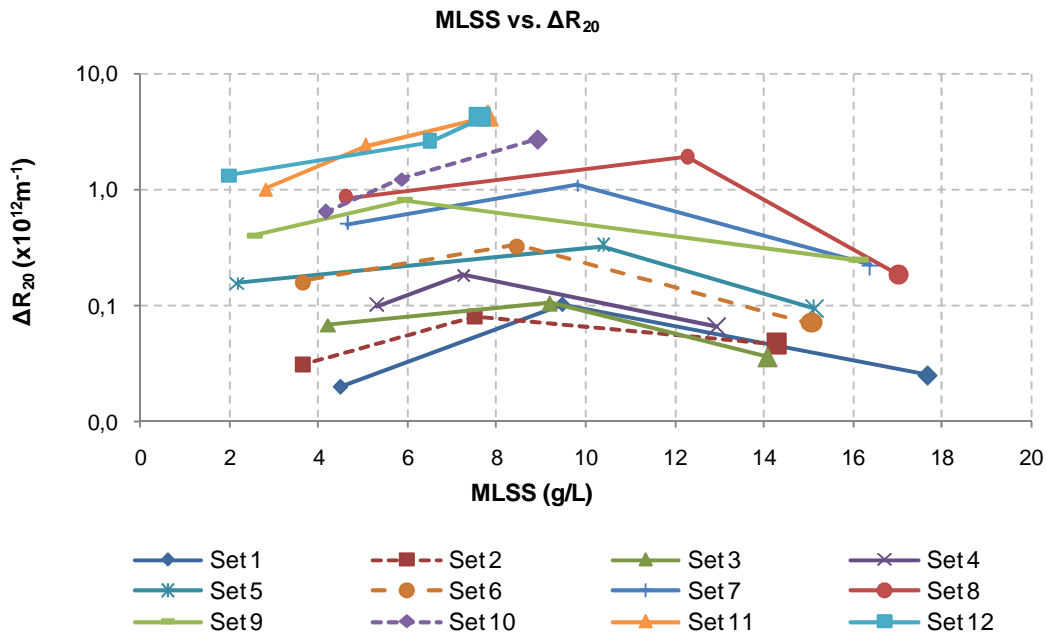


Figure 6-1 – MLSS plotted against ΔR_{20} by set

Observing Figure 6-1 it is seen that the behavior along the sets is not always the same, with two different patterns existing according to ΔR_{20} values:

- Group A: $D10p > blank$
It is the most frequent situation, where two sub-groups are observed:
 - A1 - $D10p > D20p > blank$, which occurs in seven cases out of nine;
 - A2 - $D10p > blank > D20p$, only valid for sets 1 and 2.

- Group B: $blank > D10p > D20p$
It is only applied for sets 10, 11 and 12.

From now on, to simplify, the reference to these two different patterns will be according to groups A and B.

Looking to Figure 6-2, the most eye-catching difference between these two patterns is related to the blank solids concentration. In group A, all blanks show an MLSS superior to 10 g/L as opposed to blanks from group B, where MLSS is inferior to 10 g/L.

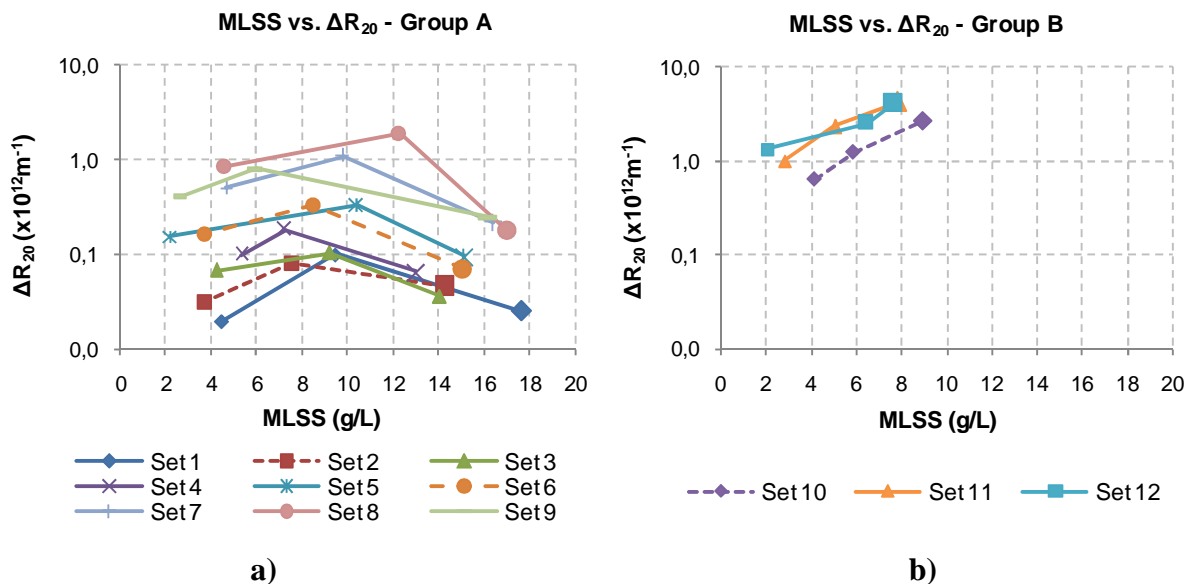


Figure 6-2 MLSS plotted against ΔR_{20} – Group A (a) and Group B (b)

This situation was also observed before by Lousada-Ferreira (2008). Temperature could also be a main factor influencing these two diverged behaviors since the sets from group B have much lower temperatures (between 8.2 and 10.8 °C). However, in the results from the previous author temperature did not show a relevant influence.

No direct correlations between MLSS and filterability were found.

When correlating filterability with D10p no relationship is found. The same is observed for the relationship filterability – D20p. Although, in group B, when MLSS decreases along the set, an increase in filterability is observed. It can only be said that if the original blank

has an MLSS above 10 g/L, a worst filterability is expected in dilution D10p. If the original blank has an MLSS below 10 g/L, an improvement on filterability is observed along the set, i.e, as MLSS decreases.

In order to obtain a possible explanation for these results, more information from particle counting, SMP and viscosity is required.

6.2 Particle counting in the range size 2-100 μm

For the particle counting in range 2-100 μm only sets from group A were analyzed. All conclusions to be drawn are only valid for this group. All results from particle counting are presented in Appendix IX.

6.2.1 Particle counting characterization

Particle number analysis

In Section 5.3.1, it was referred that 99% of the cumulative particle number was within the interval 2-87 μm . The same was observed for D10p and D20p, thus the subsequent analysis will be done for this range.

All sets presented a change in the particle number distribution for each dilution, when compared to the PSD of the blank. In general, diluted samples present a higher number of particles for smaller sizes when compared to blank samples. Set 8 is a good and representative example of all sets, see Figure 6-3.

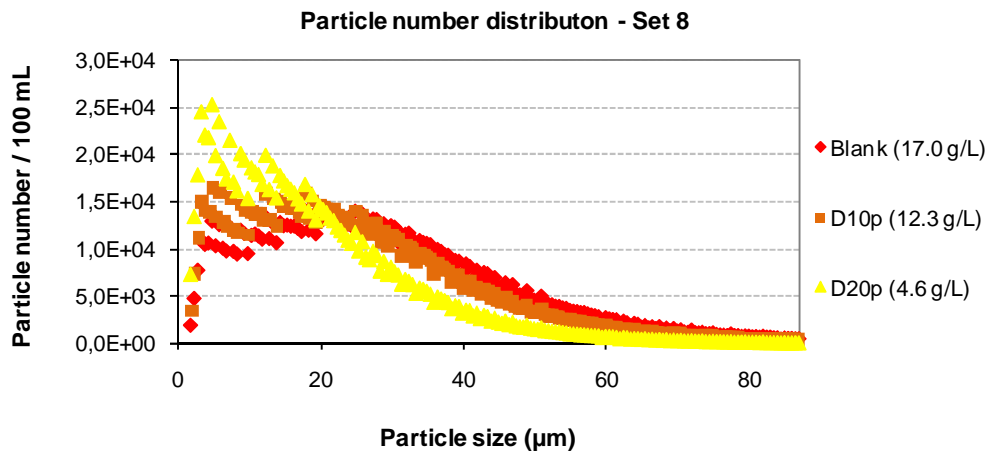


Figure 6-3 — Particle number distribution (Set 8)

Figure 6-3 reveals a shift to the left of the particles along the dilution set. Thus the number of smaller size particles increases along the set, i.e., from the most to the less concentrated sample.

In relation to the cumulative particle numbers, no clear pattern is observed. D10p shows both higher or lower number of particles than the blank sample. D20p showed lower values than the blank for all sets, though in each set a different ratio D20p/blank is observed.

The effect of each dilution in the PSD is clearer when looking at the mean particle size of maximum particle number. In general, along the set the particle size of the maximum number is decreasing, showing that in dilution a floc breakage takes place - deflocculation. Both dilutions show lower particle sizes for the maximum number when compared to the blank, however, D10p does not always have higher values than D20p. In sets 4 and 8, both dilutions have equal values and in set 9 D20p is slightly higher than D10p, see Figure 6-4.

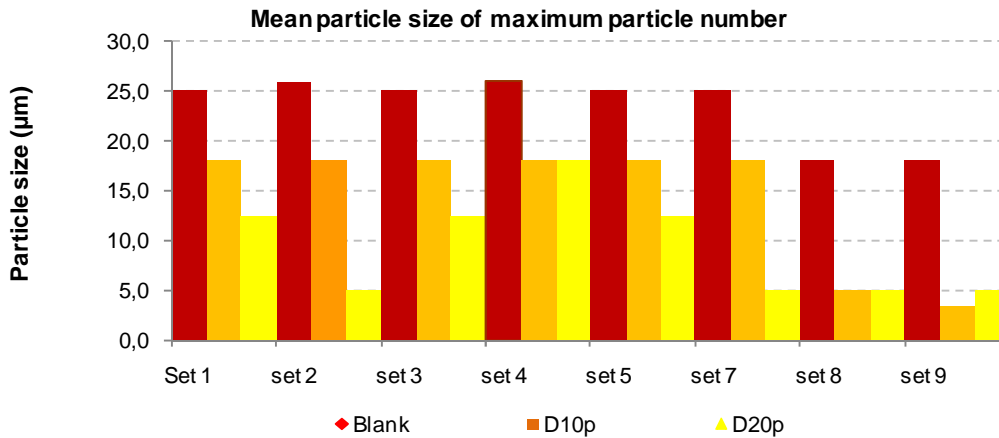


Figure 6-4 — Mean particle size of maximum particle number (all sets)

Particle volume analysis

In the analysis of the particle volume distribution the process of deflocculation is more obvious. The floc size is shifting from 50-60 µm (blank) to 35-45 µm (D20p), see Figure 6-5. This is also clear when comparing the mean particle size for maximum particle volume: 51 µm (blank), 49 µm (D10p) e 39.5 µm (D20p).

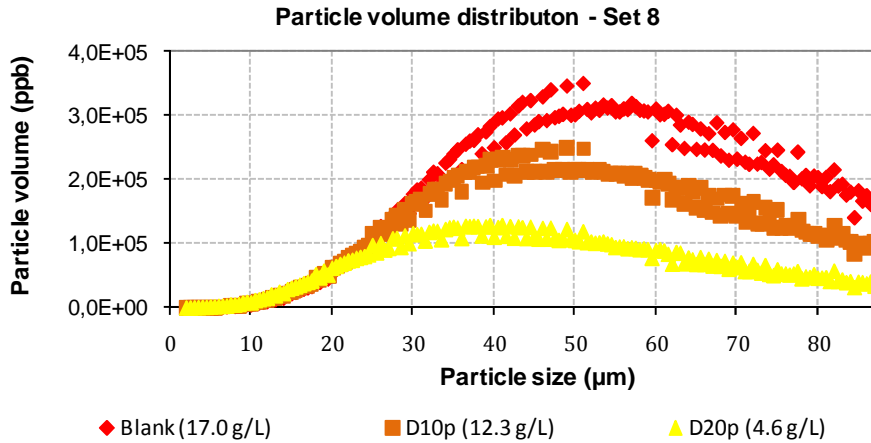


Figure 6-5— Particle volume distribution (Set 8)

6.2.2 Correlation between filterability with particle counting in range 2-87 µm

Although in the particle counting analysis the deflocculation process can be easily observed along the set, no correlation was found between filterability and particle counting in the range 2-87 µm.

However, there is one exception regarding the mean particle size for the maximum particle volume. Previously, in Section 5.3.2, a correlation between filterability and mean particle size of maximum particle volume was found for blank samples with a correlation factor of 0.80. When applying the same correlation to the dilutions, a correlation factor of 0.96 is found for D20p. Dilution D10p did not show any relationship with filterability.

The particle counting parameters did not explain the variations in filterability observed along the sets.

6.3 Particle counting in the range size of 0.4-5.0 μm

The results from particle counting in range 0.4-5.0 μm comprehend sets from groups A and B (see definition in Section 6.1.1). All results are found in Appendix IX.

6.3.1 Characterization of the particle size and volume distributions

Particle number analysis

The results obtained show that particle number is, generally, decreasing along the set as it happens with the solids concentration. In Figure 6-6 the typical distribution along the set is illustrated by Set 1. However, two exceptions exist: set 5, in which blank and D10p have the same cumulative particle number, and set 6 where D10p presents almost 20% more particles than the blank.

As observed in the particle counting results for blanks (Section 5.4.1), it was also noticed that the particles in range 0.4-1.0 μm are still 99% of the cumulative particle number for both dilutions D10p and D20p.

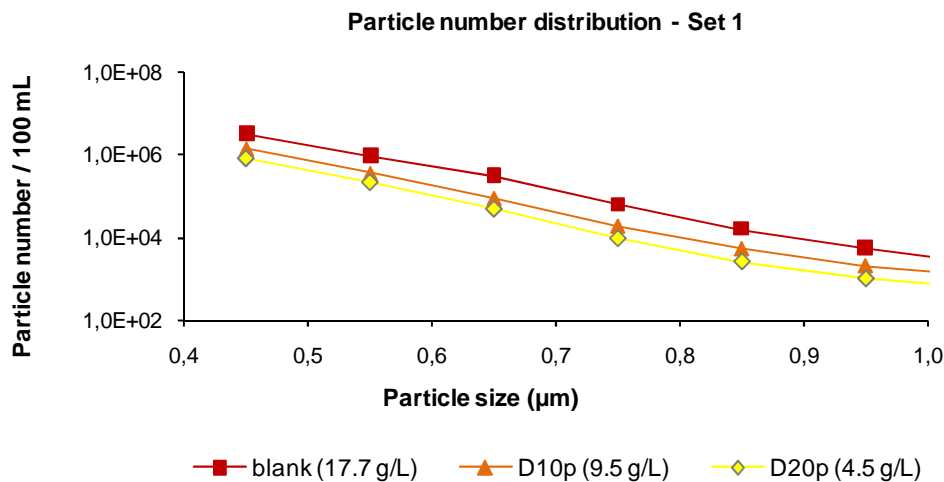


Figure 6-6— Particle number distribution (Set 1)

In relation to the maximum particle number, it represents on average 75% of the cumulative particle number for D10p and D20p, and occurs for a mean particle size of 0.45 µm. The only exception is set 2 where both dilutions present their maximum number when the particle size is 0.55 µm.

Particle volume analysis

In the particle volume distribution, a decrease along the set is observed. Only Set 6, as it happens for the particle number, has a cumulative particle volume higher in D10p than in the blank. The maximum particle volume shows the same behavior along the sets since it is on average 51% for blank, 65% for D10p and 53% for D20p.

The maximum particle volume has a mean particle size of 0.45 µm for all sets, except for set 2 where both dilutions have a particle size of 0.55 µm.

6.3.2 Correlation between filterability and particle counting in range 0.4-1.0 µm

In figure 6-7 the cumulative particle number of each set is plotted together with the respective ΔR_{20} .

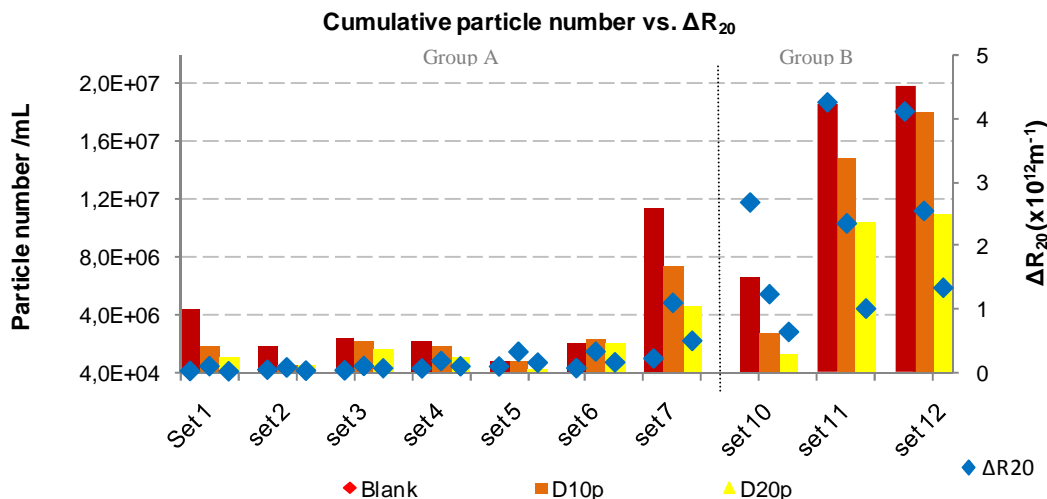


Figure 6-7 — Cumulative particle number in the range 0.4-1.0µm vs. ΔR₂₀, by set and group

The results obtained for each group regarding particle counting in range 0.4-1.0 µm are divergent.

In group A no relationship between filterability and particle counting is observed. For group A the D10p, which has always a worst filterability than the blank, shows a lesser number of particles than the blank for most sets. However, in this group the values for particle number and ΔR₂₀ varied in a very small interval when compared to the range of values presented in Group B, which may explain the enormous difference within the groups.

When looking at group B, a relationship is found since higher resistances are associated to higher cumulative particle numbers for blanks, D10p and D20p.

The behaviors observed in groups A and B may be explained by the quality of the blank. If the quality is excellent, good or moderate, the number of particles and respective ΔR₂₀ along the set suffers minimal variations that cannot lead to a clear interpretation. If the sludge presents a poor quality, the particle number and ΔR₂₀ values undoubtedly show differences for each sample type - blank, D10p and D20p.

However, when all values from dilutions D10p are considered together and linked to filterability, a strong relationship between cumulative particle number and filterability is

found (R=0.90). Also, the same relationship is found for dilutions D20p, though slightly lower with R=0.84. Both correlations are higher than the one for blank samples (R=0.78), see Figure 6-8.

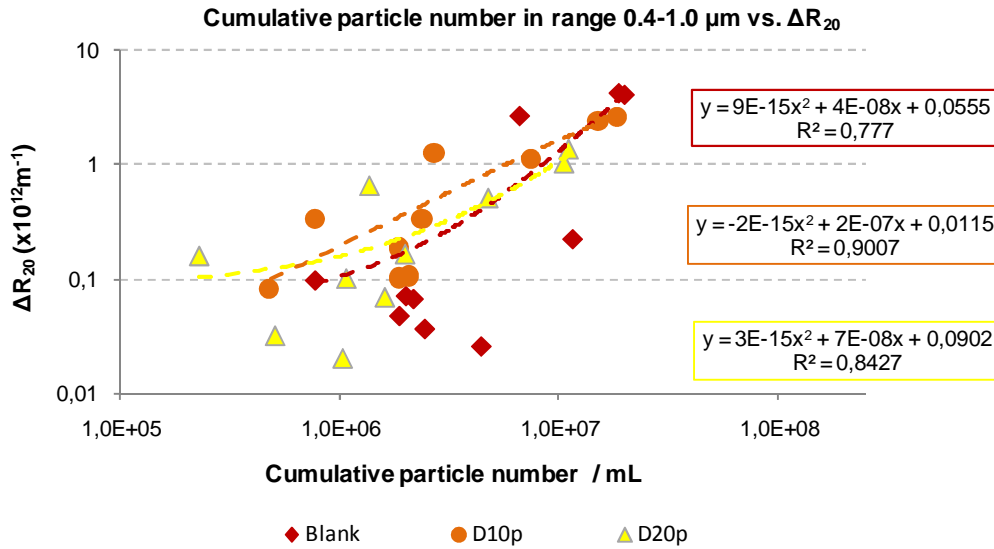


Figure 6-8 — Cumulative particle number in the range 0.4-1.0μm vs. ΔR₂₀

Also, significant correlations were found regarding the other particle counting parameters, see Table 6-2.

Table 6-2 – Correlations between filterability and particle counting parameters

	Blank	D10p	D20p
ΔR ₂₀ , Cumulative particle number	0.78	0.90	0.84
ΔR ₂₀ , Maximum particle number	0.76	0.89	0.85
ΔR ₂₀ , Cumulative particle volume	0.81	0.80	0.81
ΔR ₂₀ , Maximum particle volume	0.76	0.89	0.84

Although D10p and D20p have shown high correlations between filterability and particles from 0.4 μm till 1.0 μm, it has to be noted that these dilutions are artificial sludge and therefore all the results have to be carefully interpreted. Although the dilutions correlations cannot be extrapolated to real sludge samples, the results are, at least, consistent for each dilution type and can be helpful to support other behaviors observed with real sludge.

6.4 Soluble Microbial Products

6.4.1 Results

In order to evaluate how the SMP concentrations have varied along the set, dilutions D10p and D20p were also submitted to SMP analysis. Table 6-3 presents the concentrations obtained in mg/L from the measurement of proteins (PT) and polysaccharides (PS).

Table 6-3 – Protein (PT) and polysaccharide (PS) concentrations in mg/L by set

		Blank		D10p		D20p	
		PT	PS	PT	PS	PT	PS
Group A	Set 3	11.3	4.8	11.0	3.4	11.2	4.5
	Set 5	12.4	5.3	10.1	6.2	10.8	3.4
	Set 6	11.3	3.6	11.5	3.3	10.1	2.3
	Set 7	15.5	8.9	12.0	6.8	11.9	4.7
Group B	Set 11	21.0	17.1	17.5	10.9	14.4	9.5
	Set 12	21.9	18.3	15.5	8.3	19.1	14.1

Looking to Table 6-3, it's possible to see that SMP concentrations varied differently along the sets. There are sets where SMP concentrations decrease from the blank to D20p; sets where concentrations remained identical; and sets where D10p presented higher concentrations than the blank.

In order to have a better understanding of SMP evolution along each set, a comparison between the D10p and D20p was made in relation to the initial blank concentration, see Figure 6-9.

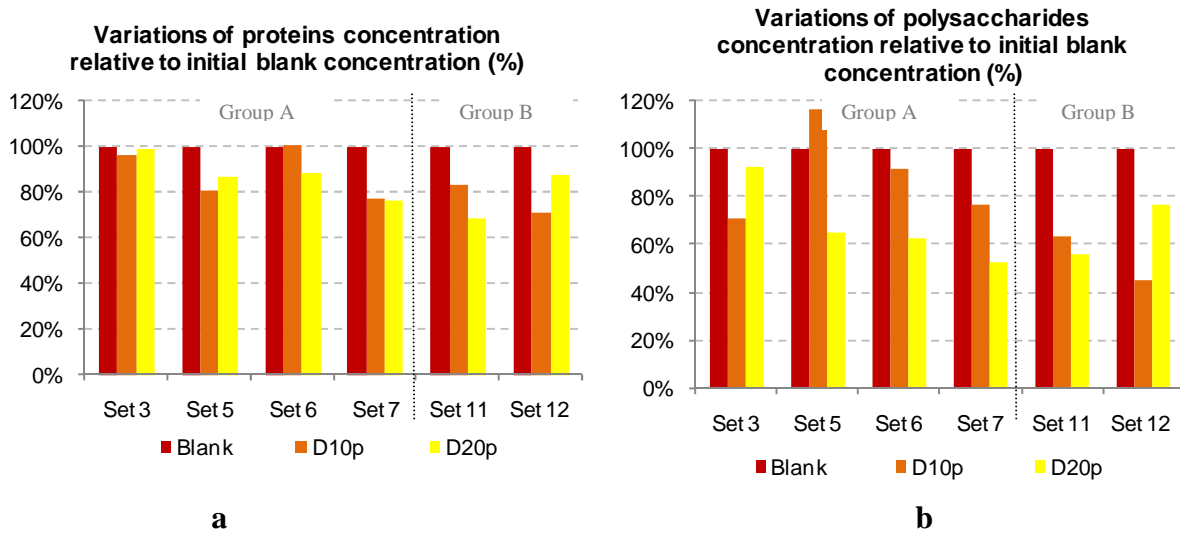


Figure 6-9 — Variation of protein (a) and polysaccharide (b) concentrations compared to blank initial concentration (%)

In Figure 6-9 the differences between protein and polysaccharide evolution along each set are clear. In proteins, values are more constant especially for group A. Variations observed were only of 10% to 30% compared to the blank initial concentration. In all sets, D10p and D20p have lower concentrations than the respective blank except set 6 where blank and D10p have nearly the same concentration. However, between both dilutions sometimes D20p has a higher concentration than D10p.

In polysaccharides, larger variations are observed. In Set 5, D10p has a concentration of almost 20% more than the blank. On the other hand, there are sets where dilutions have only half of the blank concentration. All sets except set 5 have a lower concentration in D10p and D20p than in the blank. However, when comparing dilutions only, sets 3 and 12 have a higher polysaccharide concentration in D20p than in D10p.

Overall, it can be said that in the majority of the set dilutions have lower concentrations of proteins and polysaccharides than the blanks. Yet between dilutions no pattern can be established.

The protein and polysaccharide breakthrough had some variations for both dilutions as well, see Table 6-4.

Table 6-4 – Proteins (PT) and polysaccharides (PS) retained in the membrane (average values)

	Retained PT	Retained PS
Blank	47.2%	76.3%
D10p	29.2%	70.1%
D20p	29.9%	58.9%

From Table 6-4 it is visible that, in average, D10p and D20p had a higher breakthrough of proteins and polysaccharides when compared with the blank. Dilutions D10p and D20p have the same percentage of retained proteins, nearly 30%, which is 17% lower than the blank retention. In polysaccharides, blank and D10p have almost the same retention percentage, 76% and 70% respectively, though in D20p the polysaccharide retention is 59%.

Since the membrane pore size in the filtration test was the same for all sets, this may suggest that a change in the protein and polysaccharide concentrations affects the breakthrough process. It may be related with the fact that at lower concentrations the layer built on the membrane surface is not so dense and is more permissive so that more SMP flocs can pass through the membrane; and/or that a modification in the sludge structure occurred in which the sludge flocs incorporated less SMP, becoming therefore more easy to breakthrough the membrane.

6.4.2 Correlating filterability with SMP

In Figures 6-10 and 6-11, protein and polysaccharide concentrations from each set are plotted with the respective ΔR_{20} .

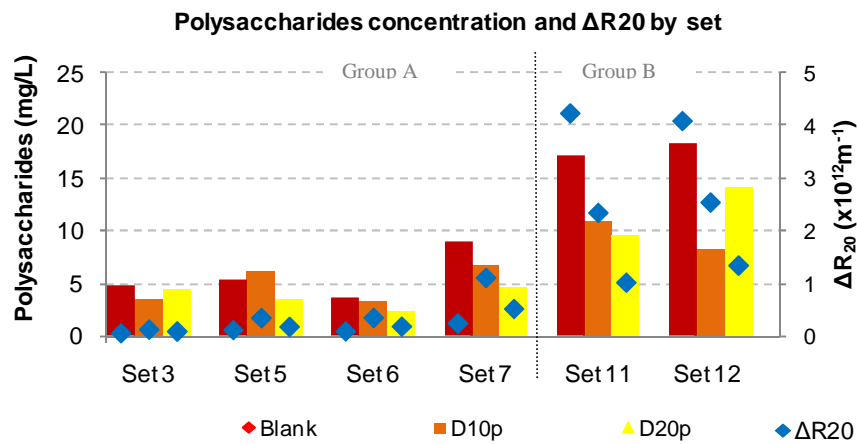


Figure 6-10 – Protein concentration and ΔR_{20} by set

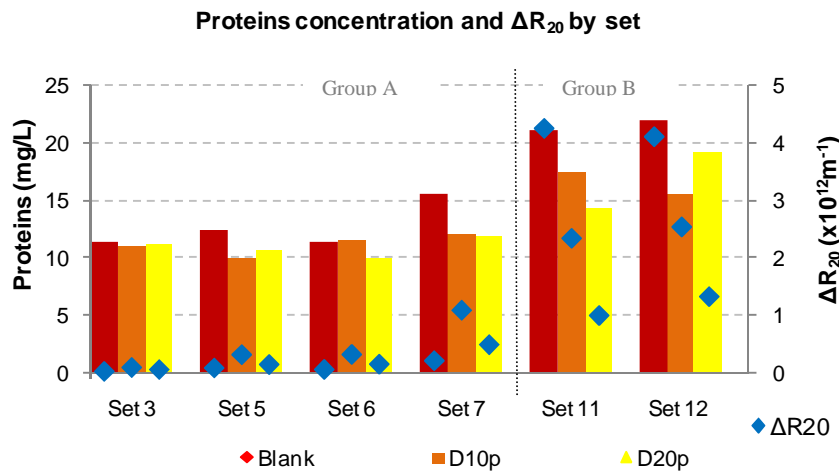


Figure 6-11 – Protein concentration and ΔR_{20} by set

Figures 6-10 and 6-11 show that filterability is not explained by protein or polysaccharide concentrations along the sets. For instance in sets 11 and 12, both from group B, two different patterns are seen. In set 11 proteins and polysaccharides decrease along the set as ΔR_{20} does, however in set 12 the D20p has a higher protein and polysaccharide concentration than D10p, and yet the latter has a higher ΔR_{20} .

In the meanwhile, a trend is present where higher resistances in the membrane filtration correspond to higher SMP concentrations. In sequence of the correlations between SMP and the blanks analysis found in Section 5.5.2, the same correlations, ΔR_{20} with SMP and SMP with cumulative particle number in range 0.4-1.0 μm , are applied separately to both dilutions. The results are presented in Table 6-5.

Table 6-5– Correlation factors for proteins and polysaccharides according to dilution type

		ΔR_{20}	Cumulative particle number 0.4-1.0 μm
Blank	Proteins	0.98	0.98
	Polysaccharides	0.98	0.73
D10p	Proteins	0.90	0.68
	Polysaccharides	0.78	0.89
D20p	Proteins	0.94	0.84
	Polysaccharides	0.92	0.91

The correlation factors are considerably high for the relationship between ΔR_{20} and SMP in both dilutions – above 0.90, except for polysaccharides in D10p ($R=0.78$). The same is true for the correlation between SMP and cumulative particle counting 0.4-1.0 μm however in a smaller degree. The correlations factors varied from 0.68 till 0.91 for D10p and D20p.

Although SMP do not entirely explain the resistances found in the membrane filtration along each set, the high correlations show that in each type of sample i.e. blank, D10p and D20p, the performance in membrane filtration can be attributed to SMP concentrations. The particles from 0.4 μm till 1.0 μm showed a strong relationship with SMP, the same verified before in the blanks analysis, although in reported literature SMP is not present in the range of 0.2 μm till 1.2 μm (Geilvoet *et.al.*, 2007). Nevertheless, particle counting in range 0.4-1.0 μm might be a valuable tool to help predicting SMP concentrations in sludge.

6.5 Viscosity

6.5.1 Results

The viscosity was measured along the sets at constant temperature, $20 \pm 1^\circ\text{C}$. As said in Section 5.6.1, the blank analysis had only comprehended shear rates from 5s^{-1} till 150s^{-1} , in order to maintain the original floc structure. The dilutions D10p and D20p have shown that in some cases the apparent viscosity at 150s^{-1} turned out to be higher than at 100s^{-1} . To guarantee that all dilutions are compared at equal conditions, the range of shear rates is between 5s^{-1} and 100s^{-1} .

All sets showed that apparent viscosity decreases along the set just as the solids content. In all sets, a non-Newtonian behavior was observed for each sample type. In Figure 6-12 it is possible to observe the viscosity results from Set 3, which is representative of all sets.

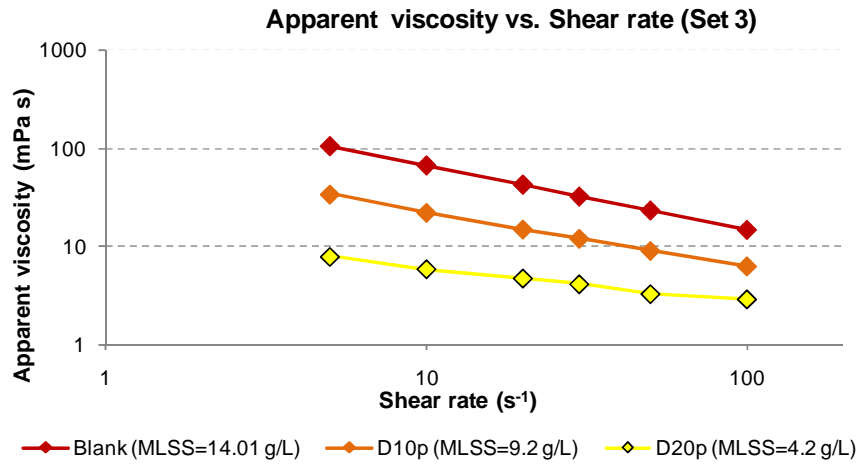


Figure 6-12 – Shear rate vs. apparent viscosity for Set 3 (T=20 ±1°C)

D10p and D20p results were analyzed separately to identify how apparent viscosity varied inside of each dilution type. In Figure 6-13 shear rate is plotted against apparent viscosity for D10p.

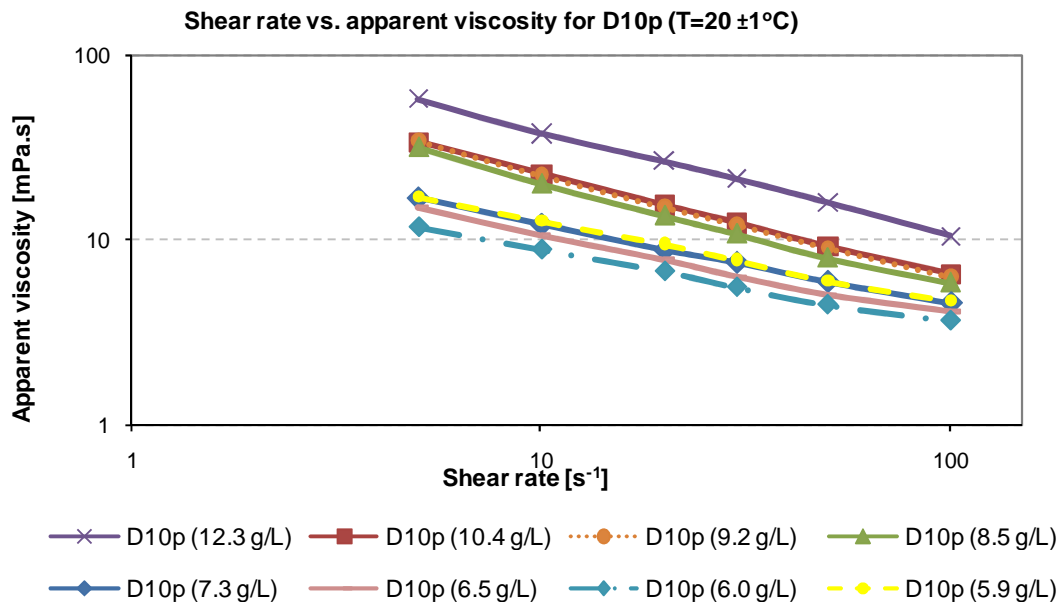


Figure 6-13 – Shear rate vs. apparent viscosity for D10p (T=20 ±1°C)

According to Figure 6-13 it is possible to see that, in general, higher MLSS correspond to higher apparent viscosities. Though there are some contradictions. The apparent viscosity is the same for samples with MLSS of 9.2 g/L and 10.4 g/L; the same is verified for samples with 5.9 g/L and 7.3 g/L. The differences are quite small, so it is not surprising that this happens. However, it cannot be ignored that other parameters might have influenced viscosity, even if they aren't the most significant (like solids content, shear rate and temperature).

When looking at Figure 6-14, all D20p show identical apparent viscosity. It is visible that two samples with the same MLSS, 4.2 g/L, have slightly different apparent viscosities. Also samples with MLSS in the interval 3.7-2.0 g/L present practically the same apparent viscosity. This is probably due to the fact that the range of MLSS is very small, varying from 2.0 till 5.3 g/L. However, there is also the possibility that other parameters influenced viscosity.

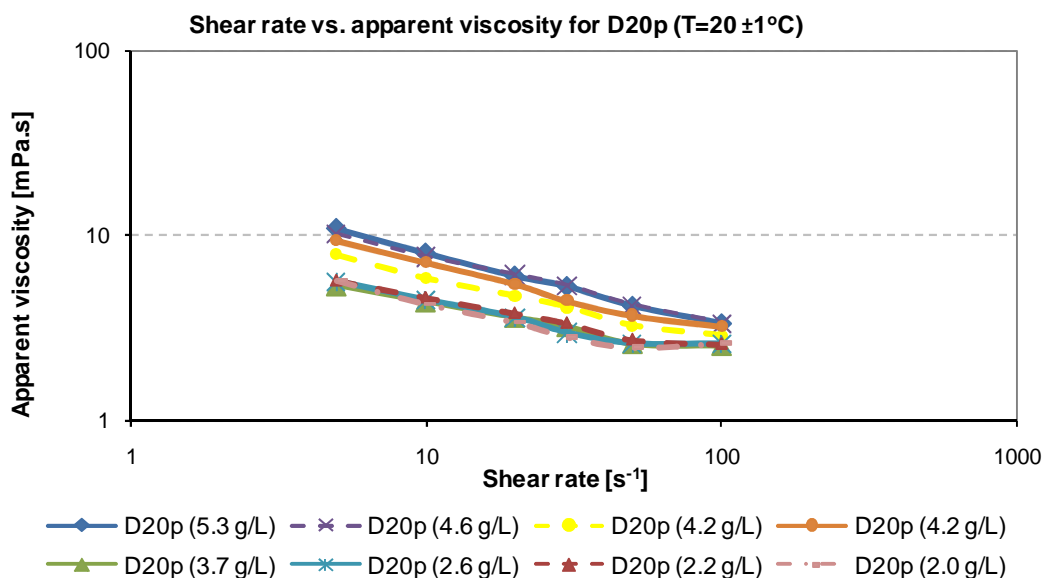


Figure 6-14 – Shear rate vs. apparent viscosity for D20p (T=20 ±1°C)

6.5.2 Correlating viscosity

To identify how MLSS affects the apparent viscosity, a correlation was made firstly for each set, and then for both dilutions at each shear rate. Inside each set a very strong relationship between apparent viscosity and MLSS was found, where all sets presented a

correlation factor ≈ 1 . When considering each dilution type, D10p and D20p, the results showed a different behavior, see Table 6-6.

Table 6-6– Correlation factors between MLSS and apparent viscosity, according to dilution type

Shear rate (s^{-1})	D10p	D20p
5	0.94	0.14
10	0.95	0.16
20	0.95	0.22
30	0.95	0.22
50	0.95	0.22
100	0.95	0.23

In dilution D10p it is clear that MLSS has a significant impact on apparent viscosity since correlation factors varied between 0.94 and 0.95 for all shear rates. The strength of this relationship was found to be the same as observed in blanks with a correlation factor of 0.95 (see Section 5.6.2). Although D10p is an artificial sludge, this shows that the same coherence in terms of apparent viscosity is verified as in real sludge.

On the contrary, D20p did not show any relationship between MLSS and apparent viscosity given that the higher correlation factor was 0.23 at $100s^{-1}$. This occurs probably due to the solids content that only varies from 2.0 g/L till 5.3 g/L, which is a very small interval. However, contrary to D10p samples, it may also be possible that viscosity in D20p samples might be influenced by other parameters.

For the correlation between filterability and viscosity, values at a shear rate of $100 s^{-1}$ were used. In Figure 6-14 the apparent viscosity is plotted together with ΔR_{20} for D10p and D20p.

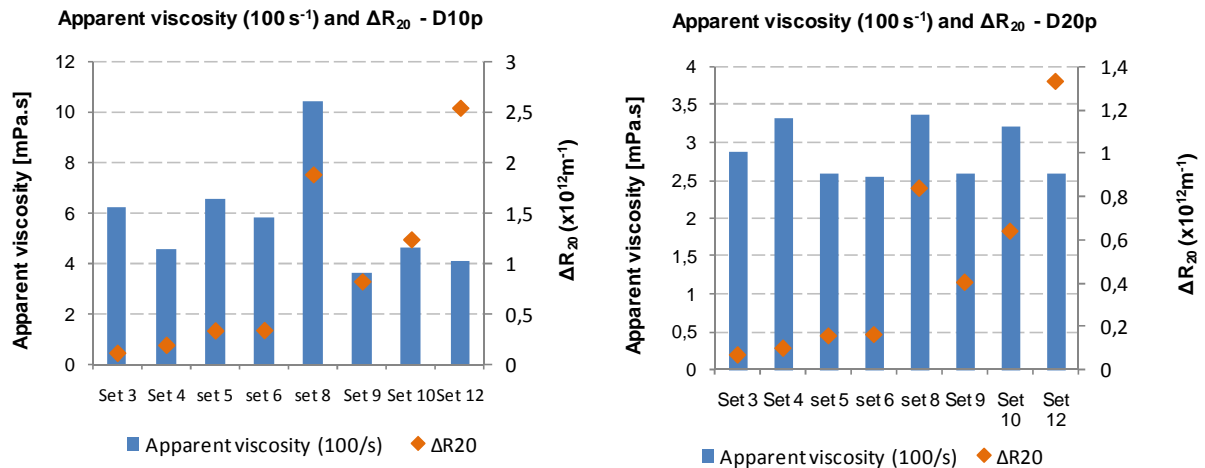


Figure 6-15 - Apparent viscosity (100 s^{-1}) and filterability – D10p (left-side) and D20p (right-side)

The results show that apparent viscosity does not have a major influence in filtration performance. In D10p, the highest resistance in the membrane showed one of the lower viscosities. For D20p, sets 5 and 12 have both the same apparent viscosity and the difference in ΔR_{20} goes from 0.16 till $2.0 \times 10^{12} \text{ m}^{-1}$.

No correlation was found between filterability and viscosity for both dilutions D10p and D20p.

6.6 Conclusions

The *Dilutions* experiment was carried out with sludge samples from three full-scale MBR systems: Heenvliet, Ootmarsum and Varsseveld. This experiment had as main purpose to study the MLSS effect on membrane filterability.

The change of the MLSS concentration from the original sludge sample was made in an artificial way, through two dilutions with permeate: D10p (10L permeate + 20L sludge) and D20p (20L permeate + 10L sludge). The analyses were divided in 12 sets, in which a set is composed by blank, D10p and D20p. Besides the filterability test, other tests were applied when possible: particle counting in range 2-100 μm , particle counting in range 0.4-5.0 μm , EPS, and viscosity.

The filterability along the set was expressed by two groups of different behavior when considering the ΔR_{20} values:

- Group A: $D_{10p} > \text{blank}$, which coincides when the blank MLSS is superior to 10 g/L.

This group can be divided in two sub-groups: $D_{10p} > D_{20p} > \text{blank}$ (7 sets) and $D_{10p} > \text{blank} > D_{20p}$ (2 sets)

- Group B: $\text{blank} > D_{10p} > D_{20p}$, which coincides when the blank MLSS is lower than 10 g/L.

When correlating filterability with MLSS no relationship is found for group A. In this group, the highest resistance in the membrane is always verified for D_{10p} , which is the sample from the set having the mean MLSS concentration. For group B, a correlation is found where filterability improves as MLSS concentration decreases. However, no explanation is found for these two different behaviors. It can only be stated that, when the blank MLSS is superior to 10 g/L, higher resistances are expected for the following dilutions; when the blank has an MLSS concentration lower than 10 g/L, filterability improves from the most concentrated to the most diluted sample.

For particle counting in range 2-100 μm no relationship with filterability was found, except for the mean particle size of maximum particle volume (correlation previously observed in the *Blanks Characterization* experiment). However, this correlation was not valid along the set, but only valid when considering D_{20p} . A bigger floc size of the maximum particle volume seems to be linked to a worst filterability. When considering D_{10p} no relationship was observed.

The particle counting in the range 2-100 μm did not explain the variations in filterability observed along the sets.

As in *Blanks Characterization* experiment, it was observed for the particle counting in range 0.4-5.0 μm that 99% of particles exist in the range 0.4-1.0 μm .

For particle counting in range 0.4-1.0 μm a relationship with filterability is observed only for group B. Along the set, the particle number decreases while filterability also decreases. This suggests that a higher number of particles in this range leads to an increase of the membrane resistance. For group A, the variation of the particle number along the set is minimal when compared to group B, thus a clear interpretation is difficult to make. However, when the dilutions in groups A and B are considered separately, D10p and D20p, a relationship between filterability and cumulative particle number is found for both dilutions: $R^2=0.90$ for D10p and $R^2=0.84$ for D20p. Both correlations are higher than the one for blank samples ($R^2=0.78$).

In the SMP analysis, the relationship between filterability and SMP is not clear along the sets. Nevertheless, a trend is present where higher resistances in the membrane filtration correspond to higher SMP concentrations. In the meanwhile, when considering D10p and D20p separately, high correlations are found between filterability and SMP. A relationship was also observed between particles in range 0.4-1.0 μm and SMP, though at a lower level.

Although SMP concentrations do not entirely explain the resistances found in the membrane filtration along each set, when considering separately the blank, D10p and D20p, performance in membrane filtration can be attributed to SMP concentrations.

From the viscosity measurements, D10p showed that its apparent viscosity is highly influenced by the MLSS concentrations ($R^2 \sim 95$). The opposite occurs for D20p, where no correlation between apparent viscosity and MLSS is found. When correlating filterability with viscosity no relationship is observed.

The *Dilutions* experiment showed that some of the results were coherent with other behaviors observed in the *Blanks Characterization* experiment. Although the dilutions are considered artificial sludge, it is important to observe identical patterns as in “real” sludge, contributing to reinforce the statements relative to sludge from a full-scale MBR.

7 SOLIDS CONCENTRATION EXPERIMENT

During the period from January 20th – 23rd the DFCi was transferred from TUDelft to Heenvliet WWTP for filterability tests “in situ”. The solids concentration experiments were carried out on January 20th and 22nd. Besides the filterability test, particle counting in range 2-100 μm and viscosity measurements were applied.

In the two days of experiments, the HRT from the Membrane Tank (MT) was shifted from 17 hours, at normal operation, to 30.8-40.8 hours, during a period of approximately three hours. After that, the MBR was again submitted to the normal operation conditions where the HRT was gradually regularized to its standard value. HRT is controlled by the wastewater feedstream into the MT. The feedstream was gradually reduced implying an increase of the HRT. During this period of three hours, sludge samples were collected from the MT and filterability tests performed.

The particle counting in range 2-100 μm and viscosity measurements were only made at TUDelft on the day following the filterability tests, due to the localization of Heenvliet WWTP. To avoid microbiological activity and to preserve as much as possible the characteristics of the sludge at the time of collection, sludge was saved and stored in a refrigerator. The results from both tests are considered reliable and truly representative of the sludge tested since a previous trial was done with positive results. In this trial sludge was collected from Heenvliet and viscosity was measured, as well as particle counting done, in the same day of collection. Sludge was saved and both tests repeated again in the next day. The differences observed only diverged in about 0.2% for both tests.

It is important to state that this experiment is not truly representative of continuous operation since the characteristics of the sludge are constantly changing and are not in a steady-state mode.

All results are presented in Appendix X.

7.1 Filterability

7.1.1 Results

During the period in which the HRT was modified, several sludge samples were collected to see the effect caused on membrane filterability. However, the first blank of each day was measured whilst the HRT was still “normal”, i.e. the MBR was under steady-state operation.

In Table 7-1 the results obtained from the filterability test are presented.

Table 7-1 – Main results from the filterability tests performed on January 20th and 22nd

Name	Time (hh:mm)	T °C	MLSS (g/L)	ΔR_{20} ($\times 10^{12} \text{m}^{-1}$)
blank 1a	09:36	11.4	14.3	0.520
blank 2a	10:15	11.4	15.1	0.321
blank 3a 20-01-2009	10:47	11.6	16.0	0.232
blank 4a	11:24	11.5	17.2	0.128
blank 5a	11:55	11.5	17.5	0.131
blank 1b	09:54	12.2	15.2	0.640
blank 2b	10:21	12.1	14.9	0.592
blank 3b	10:48	12.1	17.1	0.449
blank 4b 22-01-2009	11:15	12.2	16.2	0.412
blank 5b	11:46	12.2	16.3	0.335
blank 6b	12:18	12.2	16.5	0.302
blank 7b	12:50	12.1	18.2	0.346

The results obtained are organized according to the day of experiment.

Experiment on 20-01-09

The MT was operated with a different HRT during 2h20 minutes. The MLSS increased from 14.3 g/L till 17.5 g/L, as expected, at the same time as ΔR_{20} decreased from 0.52 till $0.13 \times 10^{12} \text{m}^{-1}$. The temperature for the filterability tests was in average 11.5 °C.

The results from day 20th are shown on a column chart concerning ΔR_{20} values with associated MLSS, see Figure 7-1.

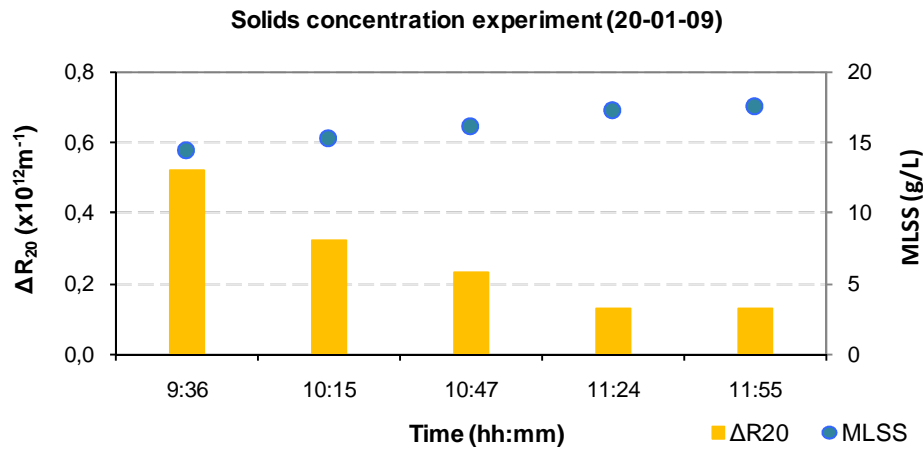


Figure 7-1 – ΔR_{20} and MLSS in January 20th

As Figure 7-1 shows, there was a significant decrease of additional resistance in the membrane along time, i.e. while HRT increased.

Experiment on 22-01-09

This experiment had a duration of almost three hours. The MLSS concentration shifted from 14.9 g/L till 18.2 g/L and ΔR_{20} from 0.64 till 0.30 $\times 10^{12} \text{m}^{-1}$. The average temperature during the experiment was 12.2 °C.

In Figure 7-2 the results from day 22nd are shown with the evolution of MLSS and ΔR_{20} during the experiment.

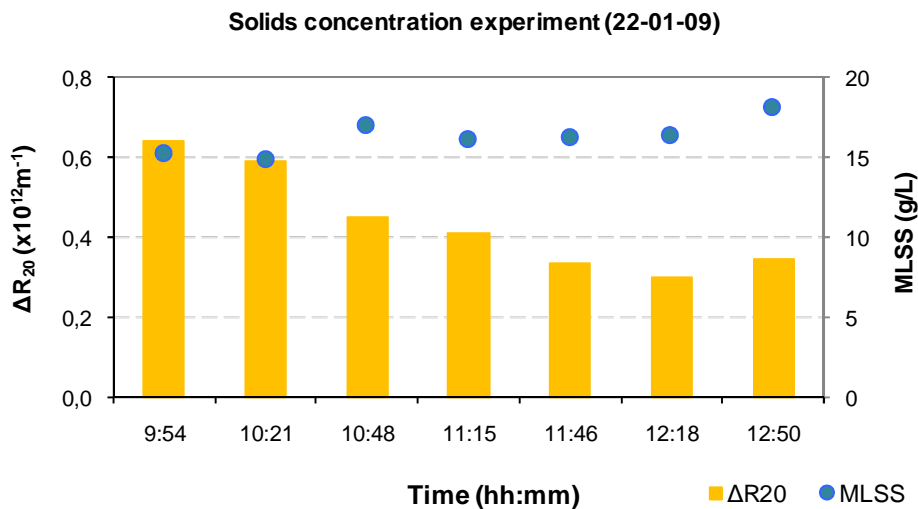


Figure 7-2 – MLSS and ΔR_{20} in January 22nd

The results obtained on January 22nd show the same trend observed on January 20th, although in a more inconstant way. The initial blank was measured with an MLSS of 15.2 g/L. Due to the change of HRT, the following sample would be expected to have a higher MLSS concentration. On the contrary, MLSS decreased slightly to 14.9 g/L and at the same time there was an improvement on filterability from 0.64 till 0.59 $\times 10^{12} \text{m}^{-1}$. The subsequent samples showed that MLSS was increasing in a non-linear way while filterability was improving along time. However, the lowest ΔR_{20} does not match the higher MLSS like it happened on day 20th.

7.1.2 Correlating filterability

In order to have a better notion of how filterability changed along the time, a correlation between filterability and MLSS was made. The correlation factors are presented in Figure 7-3.

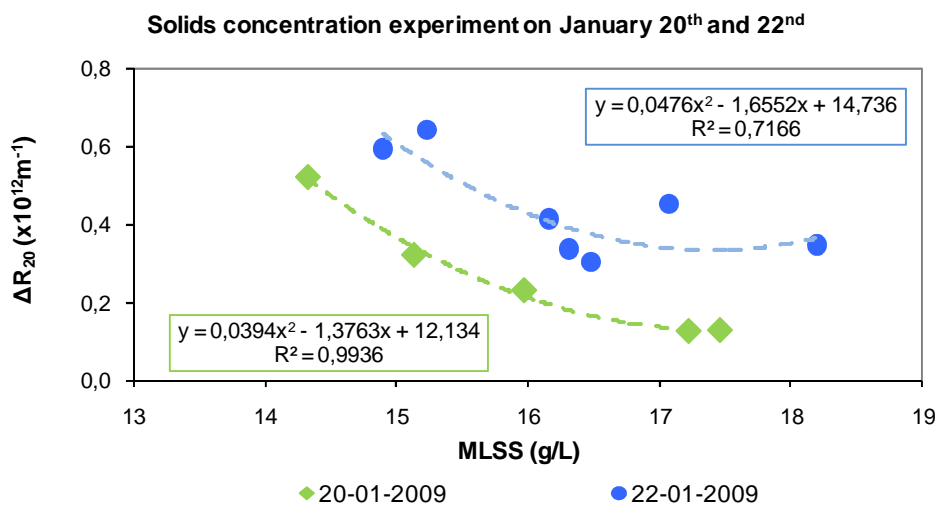


Figure 7-3 – Correlation between ΔR_{20} and MLSS in January 20th and 22nd

Correlations were found in both experiments: on day 20th, the relationship between filterability and MLSS was highly significant ($R^2=0.99$); on day 22nd, a strong correlation was also found but at a lower level ($R^2=0.73$).

In spite of the correlations found, it was previously demonstrated in the *Blanks Characterization* experiment that no correlation between filterability and MLSS was observed for five different MBRs (see Section 5.6.2). On the other hand, it has been

reported that higher MLSS concentrations showed an improvement in filterability (Madaeni *et.al.*, 1999; Le-Clech *et.al.*, 2003). The effect of increasing HRT has probably other impacts on the sludge quality beyond the increase of solids content. Meng *et.al.*, (2007a) reported that, when HRT decreased, the filamentous bacteria grew easily followed by a significant increase in the EPS concentration and sludge viscosity. Chae *et.al.*, stated that a reduction from 10 to 4 h promoted a decline in sludge settleability, caused by the increase of EPS and average particle size. As a consequence, the total resistance filtration increased. Therefore, other mechanisms might have been involved in changing the characteristics of the sludge, most likely EPS.

When comparing days 20th and 22nd, although both showed the same behavior, the results from the experiment on the 22nd were more irregular. This is probably due to the different techniques used to change the normal operation HRT. The temperature was not an influencing parameter since both experiments were performed under similar temperatures.

7.2 Particle counting in the range size of 2-100 μm

7.2.1 Results and Discussion

It was observed that 99% of the cumulative particle number was found in the range 2-87 μm . Therefore, and as it happened with the previous experiments, further analysis will only be considered in this interval.

The PSD was the same as observed in the blanks from Heenvliet for the blanks characterization experiment (see Sub-chapter 5.3).

The cumulative particle number shows different patterns for each day, see Figure 7-4.

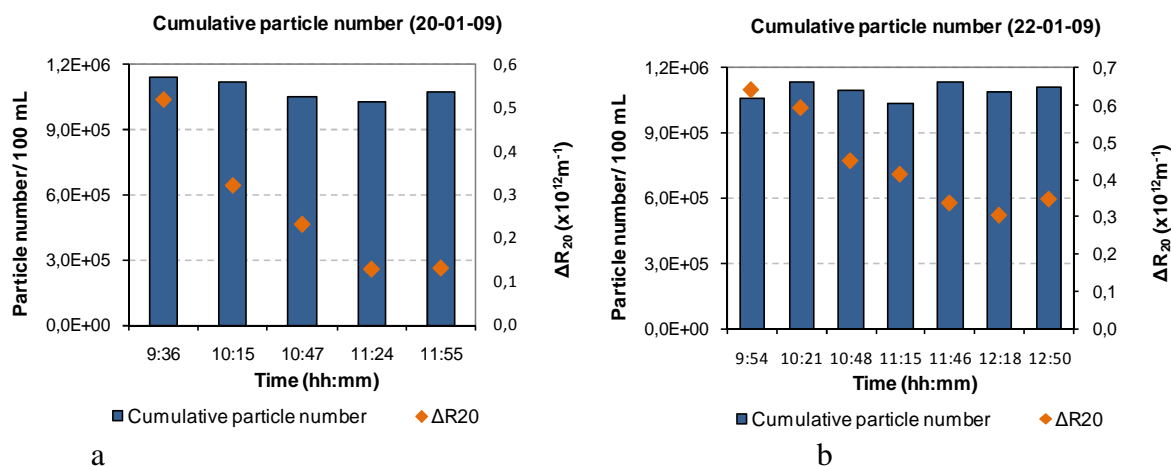


Figure 7-4 – Cumulative particle number and ΔR_{20} on January 20th (a) and 22nd (b)

On day 20th there was a slight decrease of the cumulative particle number as filterability improved. A correlation factor of 0.90 was found for this relationship. In spite of this high correlation, it has to be stated that the variations of the cumulative particle number were very subtle. For day 22nd no correlation was found since the cumulative particle number varied up and down while filterability improved.

Since the cumulative particle number did not suffer considerable changes along time, it is more likely and prudent to say that no correlation between cumulative particle number in the range 2-87 μm and filterability was found. Also, no relationship between filterability and maximum particle number was found. In relation to the mean particle size for maximum number, it varied between 18 μm , 25 μm and 26 μm , the same values observed for other blanks from Heenvliet. No relationship with filterability was found either.

In the particle volume analysis no correlations between filterability and particle volume parameters were found.

7.3 Viscosity

7.3.1 Results and discussion

The viscosity measurements comprehended sludge with MLSS between 14.3 g/L and 18.2 g/L. It was observed that at 150s^{-1} some samples showed a modification in their structure since apparent viscosity started to increase. For that reason the interval of shear rates concerned is from 5s^{-1} till 100s^{-1} .

All samples showed non-Newtonian and shear thinning behavior. In general, the apparent viscosity was higher for samples with higher solids content. When the opposite was observed it was due to slight differences in the solids content.

Figures 7-5 and 7-6 show how apparent viscosity decreased along the shear rate for both days.

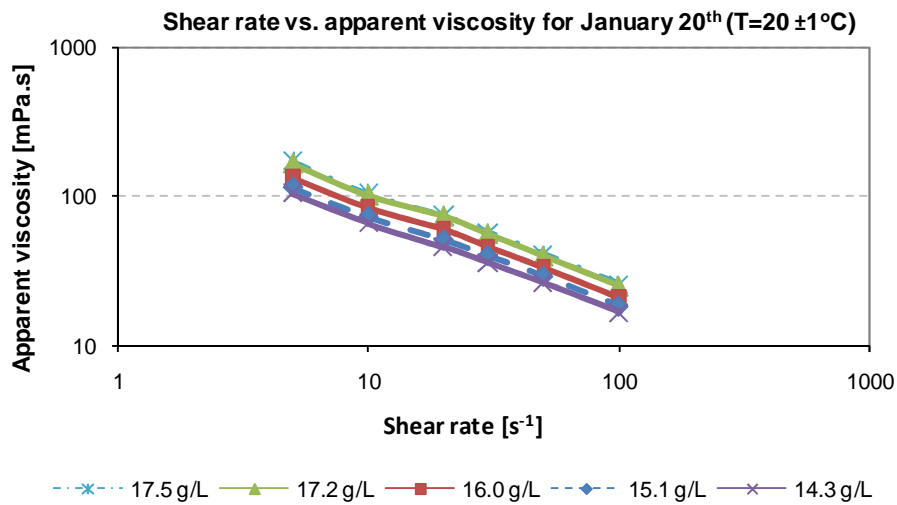


Figure 7-5 – Shear rate vs. apparent viscosity for day 20th

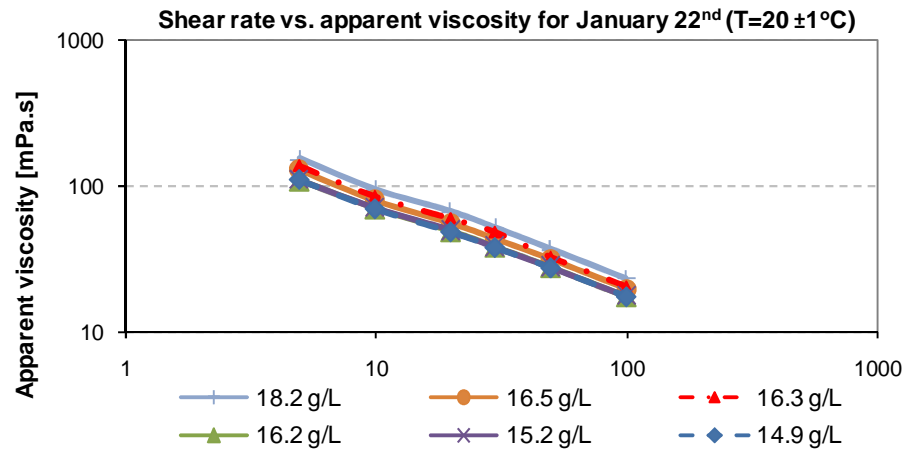


Figure 7-6 – Shear rate vs. apparent viscosity for day 22nd

The correlation factors between MLSS and apparent viscosity were found with high significance for both days, although in different levels.

On day 20th, a correlation factor of 1.00 was found at all shear rates, elucidating the major impact of solids content in apparent viscosity.

For day 22nd the correlations factors were not so high, varying between 0.78 and 0.83, which still demonstrates a major influence of MLSS in the apparent viscosity. This might be a consequence of the behavior observed before in the MLSS concentrations (see Figures 7-1 and 7-2).

In Figures 7-7 and 7-8 the filterability is plotted together with the apparent viscosity measured at a shear rate of 100 s⁻¹ for days 20th and 22nd.

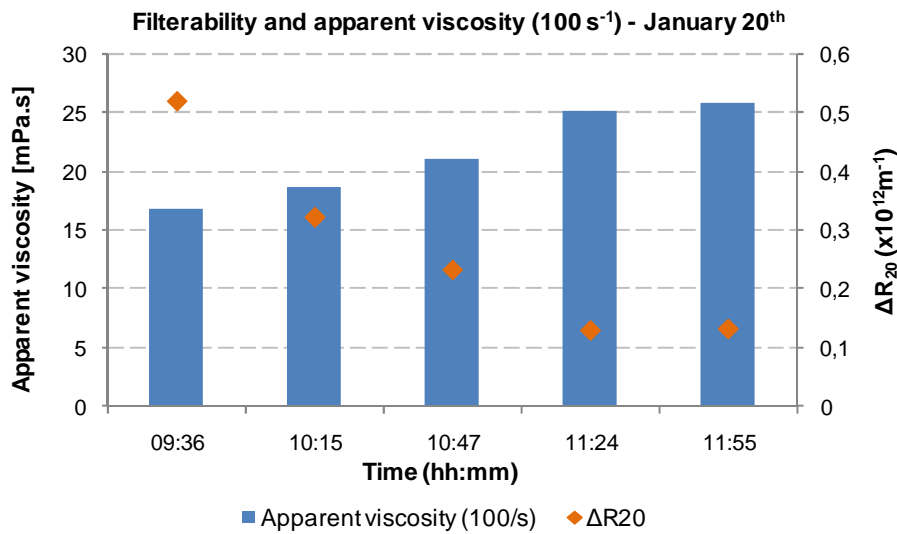


Figure 7-7 – Filterability and apparent viscosity ($100 s^{-1}$) – January 20th

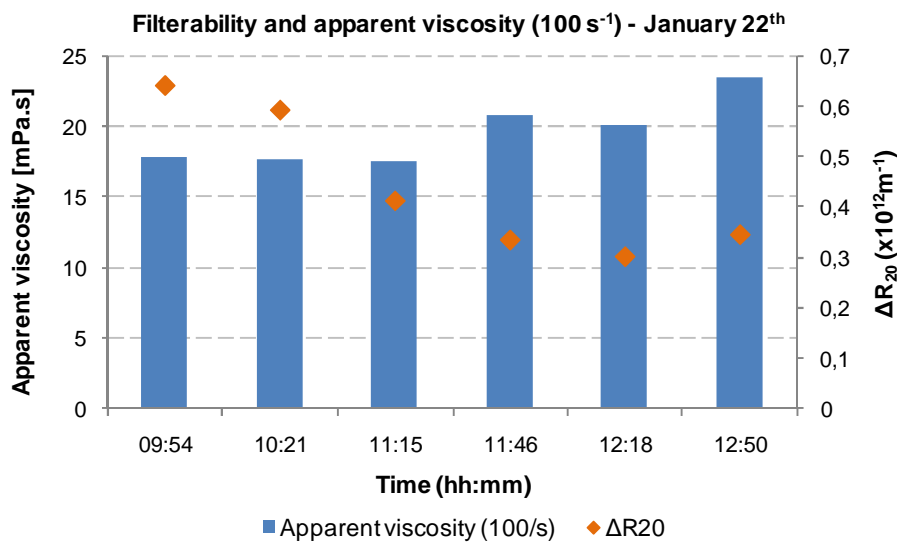


Figure 7-8 – Filterability and apparent viscosity ($100 s^{-1}$) – January 22nd

From Figure 7-7 it is clear that filterability increased as apparent viscosity increased. This is a natural consequence of the increase registered for MLSS concentrations. A correlation factor of 0.99 was found between filterability and apparent viscosity at $100 s^{-1}$.

When looking at Figure 7-8, the apparent viscosity also increased while filterability improved, though not in a linear way. This is confirmed by the correlation factor of 0.59 between filterability and apparent viscosity.

These results are contradictory to what has been reported in literature. The increase in apparent viscosity is expected to contribute to membrane fouling since higher shear rates are required to maintain a turbulent regime, which is fundamental to a sustainable membrane filtration. For that reason, the results show that apparent viscosity was not a main factor contributing to the increase of the additional resistance in the membrane, while other factors have prevailed to improve considerably the filterability of the sludge.

7.4 Conclusions

The solids concentration experiment was carried out in Heenvliet WWTP on January 20th and 22nd. The goal for this experience was to change in a “natural” way the MLSS of the sludge in the MT. By increasing the HRT it was possible to achieve higher MLSS concentrations.

The filterability improved considerably in both days, especially since it was a short-term experience (3 hours for each day). On both days an increase of approximately 3 g/L occurred from the initial blank MLSS.

The particle counting in range 2-100 μ m did not reveal any relationship between filterability and particle number/volume.

In relation to viscosity, as expected, an increase was observed during the experiment. High correlation factors were found between apparent viscosity and MLSS. The relationship between filterability and apparent viscosity was very significant for day 20th ($R^2=0.99$) while for day 22nd a poor correlation was found ($R^2=0.59$). Since apparent viscosity has a negative impact on membrane filtration, this suggests that apparent viscosity does not have a major impact on membrane filtration and other mechanisms have prevailed in improving the sludge quality.

Through this experiment it was possible to confirm that manipulating operating conditions in the MBR has an effect on membrane filterability. In particular, it was observed that an improvement in membrane filtration occurred when HRT was changed from 17 hours to 30.8-40.8 hours at the same time that MLSS varied from 14.3 till 18.2 g/L, approximately.

However, it has to be noted that this is only true for a short-term experience (~3hours), for which considerations for a continuous MBR operation cannot be established.

8 GENERAL CONCLUSIONS AND RECOMMENDATIONS FOR FURTHER RESEARCH

8.1 General conclusions

This thesis is a result of research conducted between September 2008 and February 2009. During this period, five full-scale MBRs located between The Netherlands and Germany were visited to collect sludge and study the characteristics/components of activated sludge and its impact on membrane filterability.

Three different experiments were done aiming at different objectives:

- the *Blanks Characterization* experiment, for a characterization of the sludge in full-scale MBRs
- the *Dilutions* experiment, to study the impact of different MLSS in filterability, through two dilutions, D10p and D20p, composed of activated sludge and permeate collected in the WWTP
- the *Solids Concentration* experiment, to see the impact of different MLSS by changing the operating conditions in Heenvliet full-scale MBR

In addition to the filterability test, five key parameters for the sludge analysis were chosen: mixed liquor suspended solids (MLSS), particles in range 2-100 μm , particles in range 0.4-5.0 μm , soluble microbial products (SMP), and viscosity. A relationship between filterability and each of these parameters was tried in order to explain the results observed.

In the *Blanks Characterization* and *Dilutions* experiments no direct correlation between filterability and MLSS was found. Also, the viscosity did not show a major role in membrane filterability.

The particle counting in range 2-100 μm did not show a clear relationship with membrane filterability.

From the analysis of sludge from a full-scale MBR, a three-way relationship was observed between filterability, SMP and temperature. Seasonal variations, the temperature differences, had an impact on membrane filterability, since at lower temperatures a worst filterability was registered. A high relationship between filterability and SMP was found in which filterability was better at lower SMP concentrations. Also, a relationship between SMP and temperature was found with high significance. One possible explanation for this triple relationship is that temperature seems to influence the release of SMP into the activated sludge, and SMP concentrations seem to be a major factor in influencing membrane filterability through the build up of a gel layer near the membrane surface. In a long-term operation it is most likely that SMP will highly contribute to membrane fouling.

A strong correlation between SMP and particle counting parameters in range 0.4-1.0 μm was also found. Although SMP particles are considered to be smaller than in the observed range, particle counting in range 0.4-1.0 μm seems to be a good indicative of the SMP levels in the activated sludge.

This is also supported by the results from the *Dilutions* experiment. When considering D10p and D20p separately, it was observed that in each dilution type the filterability could be attributed to the SMP concentrations. A relationship between particles in range 0.4-1.0 μm and SMP was also observed, though at a lower level. Although the dilutions D10p and D20p are artificial sludge, it is a good outcome to see that the same results observed with “real” sludge are reflected in this type of “artificial” sludge.

The *Solids Concentration* experiment showed that an improvement in membrane filtration occurred when the hydraulic retention time (HRT) was changed from 17 hours to 30.8-40.8 hours while at the same time MLSS varied approximately from 14.3 till 18.2 g/L. In spite of the fact that for this experiment a better filterability is observed for higher MLSS, it cannot be assured that MLSS played a role in filterability, especially when no correlation was found in the Blanks Characterization and Dilutions experiments. Through the Solids Concentration experiment it was possible to confirm that the manipulation of the operating conditions in the MBR has an effect on membrane filterability. Although, it must be noted that this is only true for a short-term experience (~3hours), and therefore considerations for a continuous MBR operation cannot be established.

8.2 Recommendations for further research

As said before in literature review, Extracellular polymeric substances (EPS) are largely appointed as one of the most crucial contributors for membrane fouling. It would be interesting to see the evolution of EPS and/or SMP along the biotreatment process in an MBR system. Thus, the SMP should be periodically measured in the different processes of the biological treatment such as anaerobic, anoxic, aerobic, membrane tank, and final effluent. Then different biotreatment sequences should be tested to see if the concentrations of SMP in the different processes changed. At the same time, filterability is being continuously measured to study the impact of the different processes applied.

The same type of study should be developed by changing the operating conditions in the MBR. For example, the effects of different HRTs should be studied as well as their impact on the SMP concentrations and consequently on membrane filterability. Also, the solids retention time (SRT) should be manipulated to see both the impact on the membrane filtration performance and the SMP levels.

In addition, the particle counting in range 0.4-1.0 μm could turn out to be a useful tool to predict membrane fouling in MBR operation. The implementation of such measuring method on an online MBR operation would be appealing.

9 REFERENCES

Åhl, R., Leiknes, T., Ødegaard, H. (2006) Tracking particle size distributions in a moving bedbiofilm membrane reactor for treatment of municipal wastewater, *Water Science & Technology*, Vol. 53, pp. 33–42

Al-Halbouni, D., Traber, J., Lyko, S., Wintgens, T., Melin, T.,Tacke, D., Janot, A., Dott, W., Hollender, J.(2008) Correlation of EPS content in activated sludge at different sludge retention times with membrane fouling phenomena, *Water Research*, Vol. 423, pp. 1475-1488

Al-Halbouni, D., Dott, W., Hollender, J.(2009) Occurrence and composition of extracellular lipids and polysaccharides in a full-scale membrane bioreactor, *Water Research*, Vol. 43, pp. 97-106

Bae, T. and Tak, T. (2005) Interpretation of fouling characteristics of ultrafiltration membranes during the filtration of membrane bioreactor mixed liquor, *Journal of Membrane Science*, Vol. 264, pp. 151-160

Benschop, M. (2008) Influence of temperature on filtration in membrane bioreactors, *Msc Thesis*, Delft University of Technology, Delft, The Netherlands

Berg van den G. and Smolders, C. (1990) Flux decline in ultrafiltration processes, *Desalination*, Vol. 77, pp. 101-133

Bouhabila, E., Aïm, R., Buisson, H. (2001) Fouling characterization in membrane bioreactors, *Separation and Purification Technology*, Vol. 22-23, pp. 123-132

Chae, S.-R., Ahn, Y.-T., Kang, S.-T., Shin, H.-S. (2006) Mitigated membrane fouling in a vertical submerged membrane bioreactor, *Journal of Membrane Science*, Vol. 280, pp. 572–581.

Cheryan, M. (1998) *Ultrafiltration and Microfiltration Handbook*, Technomic Publishing Co., Inc., Lancaster, PA

Cho, B., Fane, A. (2003) Fouling phenomena in a MBR: transmembrane pressure transients and the role of EPS (extracellular polymeric substances), *Water Science and Technology*, Vol. 3, pp. 261-266

Cicek, N., Macomber, J., Davel, J., Suidan, M., Audic, J., Genestet, P. (2000) Effect of solids retention time on the performance and biological characteristics of a membrane bioreactor, *Water Science and Technology*, Vol. 43, pp. 43-50

Davies, J., Le, M., Heath, C. (1998) Intensified activated sludge process with submerged membrane microfiltration, *Water Science and Technology*, Vol. 38, pp. 421-428

Defrance, L. and Jaffrin, Y. (1999) Comparison between filtrations at fixed transmembrane pressure and fixed permeate flux: application to a membrane bioreactor used for wastewater, *Journal of Membrane Science*, Vol. 152, pp. 203-210

Defrance, L., Jaffrin, Y. Gupta, B., Paullier, P., Geaugey, V. (2000) Contribution of various constituents of activated sludge to membrane bioreactor fouling, *Bioresource Technology*, Vol.73, pp. 105-112

Dubois, M., Gilles, K.A., Hamilton, J.K., Rebers, P.A., Smith, F. (1956) Colorimetric method for determination of sugars and related substances, *Analytical Chemistry*, Vol. 28, pp 350-356

Evenblij, H. and Van der Graaf, J. (2004) Occurrence of EPS in activated sludge from a membrane bioreactor treating municipal wastewater, *Water Science and Technology*, Vol. 50, pp. 293-300

Evenblij, H., Geilvoet, S.P., Van der Graaf, J.H.J.M., Van der Roest, H.F. (2005). Filtration characterization for assessing MBR performance: three cases compared, *Desalination*, Vol. 178, pp 115-124

Evenblij, H. (2006), Filtration Characteristics in Membrane Bioreactors. *PhD thesis*, Delft University of Technology, The Netherlands.

Flemming, H.C. and Wingender, J. (2001) Relevance of microbial extracellular polymeric substances (epss) – part I: Structural and ecological aspects, *Water Science Technology*, Vol. 43, pp. 1-8

Frølund, B., Palmgren, R., Keiding, P.H., Nielsen, K. (1996) Extraction of extracellular polymers from activated sludge using a cation exchange resin, *Water Science & Technology*, Vol. 30, pp. 1749-1758.

Geilvoet, S., Moreau, A., Lousada-Ferreira, M., van Nieuwenhuijzen, A., van der Graaf, J. (2007) Filtration characterisation, SMP analyses and particle size distribution in the submicron range of MBR activated sludge. IWA International *Conference on Particle Separation*, Toulouse, France

Geilvoet, S., Moreau, A., Lousada-Ferreira, M., van Nieuwenhuijzen, A., van der Graaf, J. (2007a) Filtration characterization and sludge quality monitoring at a full-scale MBR during its first year of operation. 4th IWA *Conference on Membranes for Water and Wastewater Treatment*; Harrogate, UK

Geilvoet S. P. (2009) The Delft Filtration Characterization method, Assessing membrane bioreactors activated sludge filtration. *PhD thesis (in preparation)*, Delft University of Technology, The Netherlands.

Harada, H., Momonoi, K., Yamazaki, S., Takizawa, S. (1994) Application of anaerobic-UF membrane reactor for treatment of a waste-water containing high-strength particulate organics, *Water Science & Technology*, Vol. 30, pp. 307–319.

Hasar, H., Kinaci, C., Ünlü, A., Toğrul, Ipek, U. (2004) Rheological properties of activated sludge in a sMBR, *Biochemical Engineering Journal*, Vol. 20, pp. 1-6

Itonaga, T., Kimura, K., Watanabe, Y. (2004) Influence of suspension viscosity and colloidal particles on permeability of membrane used in membrane bioreactor (MBR), *Water Science Technology*, Vol. 50, pp. 301–309.

Ivanovic, I., Leiknes, T. (2008) Impact of aeration rates on particle colloidal fraction in the biofilm membrane bioreactor (BF-MBR), *Desalination*, Vol. 231, pp. 182–190

Jiang, T., Kennedy, M., Guinzbourg, B., Vanrolleghem, P., Schippers, J. (2005) Optimising the operation of a MBR pilot plant by quantitative analysis of the membrane fouling mechanism, *Water Science Technology*, Vol. 51, pp. 19-25

Judd, Simon (2006) *The MBR book: Principles and Applications of Membrane Bioreactors in Water and Wastewater Treatment* (1st Edition). Elsevier, Oxford

Koros, J., Ma, Y., Shimidzu, T. (1996) Terminology for membrane and membrane processes; IUPAC recommendations 1996, *Pure & Applied Chemistry*, Vol. 68, pp. 1479-1489

Laera, G., Giordano, C., Pollice, A., Saturno, D., Mininni, (2007) Membrane bioreactor sludge rheology at different solid retention times, *Water Research*, Vol. 41, pp. 4197-4203

Lapidou, C.S. and B.E. Rittmann (2002) A unified theory for extracellular polymeric substances, soluble microbial products, and active and inert biomass, *Water Research*, Vol. 36 pp. 2711-2720

Le-Clech, P., Jefferson, B., Judd, S. (2003) Impact of aeration, solids concentration and membrane characteristics on the hydraulic performance of a membrane bioreactor, *Journal of Membrane Science*, Vol. 218, pp. 117-129

Le-Clech, P., Fane, A., Leslie, G., Childress, A. (2005) The operator's perspective, *Filtration Separation*, Vol. 42, pp. 20-23

Le-Clech, P., Chen, V., Fane, A. (2006) Fouling in membrane bioreactors used in wastewater treatment (review), *Journal of Membrane Science*, Vol. 284, pp. 17-53

Lee, W., Kang, S., Shin, H. (2003) Sludge characteristics and their contribution for microfiltration in submerged membrane bioreactors, *Journal of Membrane Science*, Vol. 216, pp. 217-227

Lesjean, B., Rosenberger, S., Laabs, C., Jekel, M., Gnirss, R., Amy, G. (2005) Correlation between membrane fouling and soluble/colloidal organic substances in membrane bioreactors for municipal wastewater treatment, *Water Science & Technology*, Vol.51 pp. 1–8

Lesjean, B. and Huisjes, E. (2008) Survey of the European MBR market: trends and perspectives, *Desalination*, Vol. 231, pp. 71-81

Liu, R., Huang, X., Wang, C., Chen, L., Qian, Y. (2000) Study on hydraulic characteristics in a submerged membrane bioreactor process, *Process Biochemistry*, Vol. 36, pp. 249-254

Lojkine, H., Field, R., Howell, J. (1992) Crossflow microfiltration of cell suspensions: a review of models with emphasis on particle size effects, *Trans. Inst. Chem. Eng*, Vol. 70, pp149-164

Lousada-Ferreira, M., Geilvoet, S., Moreau, A., Atasoy, E., Krzeminski, A., van Nieuwenhuijzen, J., van de Graaf (2008) *MLSS: Still a poorly understood parameter?*, in: *International Conference on Membranes in drinking water production and wastewater treatment*, Toulouse, France.

Lowry, O.H., Rosebrough, N.J., Farr, A.L., Randall, R.J. (1951) Protein measurement with the Folin phenol reagent, *Journal of Biological Chemistry*, Vol. 193, pp. 265-275

Lyko, S., Wintgens, T., Al-Halbouni, D., Baumgarten, S., Tacke, D., Drensla, K., Janot, A., Dott, W., Pinnekamp, J., Melin, T. (2008) Long-term monitoring of a full-scale municipal membrane bioreactor - Characterisation of foulants and operational performance, *Journal Membrane of Science*, Vol. 317, pp. 78-87

Meng, F., Shi, B., Yang, F., Zhang, H. (2007a) New insights into membrane fouling in submerged membrane bioreactor based on rheology and hydrodynamics concepts, *Journal of Membrane Science*, Vol. 302, pp. 87-94

- Meng, F., Shi, B., Yang, F., Zhang, H. (2007b) Effect of hydraulic retention time on membrane fouling and biomass characteristics in submerged membrane bioreactors, *Bioprocess and biosystems engineering*, Vol. 30, pp. 359-367
- Metcalf & Eddy (2003) *Wastewater engineering: treatment and reuse* (4th international edition). McGraw-Hill, New York
- Mulder, M. (1996) *Basic principles of membrane technology*, Kluwer Academic Publishers, Dordrecht
- Nagaoka, H., Ueda, S., Miya, A. (1996) Influence of bacterial extracellular polymers on the membrane separation activated sludge process, *Water Science and Technology*, Vol. 34, pp. 165-172
- Nagaoka, H. and Akoh, H. (2008) Decomposition of EPS on the membrane surface and its influence on the fouling mechanism in MBRs, *Desalination*, Vol. 231, pp. 150-155
- Nataraj, S., Schomäcker, R., Kraume, M., Mishra, I., Drews, A. (2008) Analyses of polysaccharide fouling mechanisms during crossflow membrane filtration, *Journal of Membrane Science*, Vol. 308, pp. 152-161
- Poele, S. te (2005) Foulants in Ultrafiltration of wwtp effluent, *PhD Thesis*, Delft University of Technology, Delft, The Netherlands
- Rojas, M., Kaam, R., Schetrite, S., Albasi, C. (2005) Role and variations of supernatant compounds in submerged membrane bioreactor fouling, *Desalination*, Vol. 179, pp. 95-107
- Rosenberger, S. and Kraume, M. (2002) Filterability of activated sludge in membrane bioreactors, *Desalination*, Vol. 151, pp. 195-200
- Rosenberger, S., Kubin, K., Kraume, M. (2002) Rheology of activated sludge in Membrane Bioreactors, *Engineering in Life Sciences*, Vol. 2, pp. 269-275

Rosenberger, S., Laabs, C., Lesjean, B., Gnirss, R., Amy, G., Jekel, M., Schrotter, J. (2006) Impact of colloidal and soluble organic material on membrane performance in membrane bioreactors for municipal wastewater treatment, *Water Research*, Vol. 40, pp. 710-720

Stephenson, T., Judd, S., Jefferson, B., Brindle, K. (2000) *Membrane Bioreactors for Wastewater Treatment*, IWA Publishing, London

Seyssiecq, I., Ferrasse, J.-H., Roche, N. (2003) State-of-art: rheological characterisation of wastewater treatment sludge, *Biochemical Engineering Journal*, Vol. 16, pp. 41-56

Seyssiecq, I., Marrot, B., Djerroud, D., Roche, N. (2008) In situ triphasic rheological characterisation of activated sludge, in an aerated bioreactor, *Biochemical Engineering Journal*, Vol. 142, pp. 40-47

Wisniewski, C. and Grasmick, A. (1998) Particle size distribution in a membrane bioreactor and consequences for membrane fouling, *Colloids and Surfaces A: Physicochemical and Engineering Aspects*, Vol. 138, pp. 403-411

Wu, Z., Wang, Z., Zhou, Z., Yu, g., Gu, G. (2007) Sludge rheological and physiological characteristics in a pilot-scale submerged membrane bioreactor, *Desalination*, Vol. 212, pp. 152-164

Yamamoto, K., Hiasa, M., Mahmood, T., Matsuo, T. (1999) Direct solid-liquid separation using hollow fiber membrane in an activated-sludge aeration tank, *Water Science & Technology*, Vol. 21, pp. 43-54

APPENDICES

Appendix I – MBR market in Europe

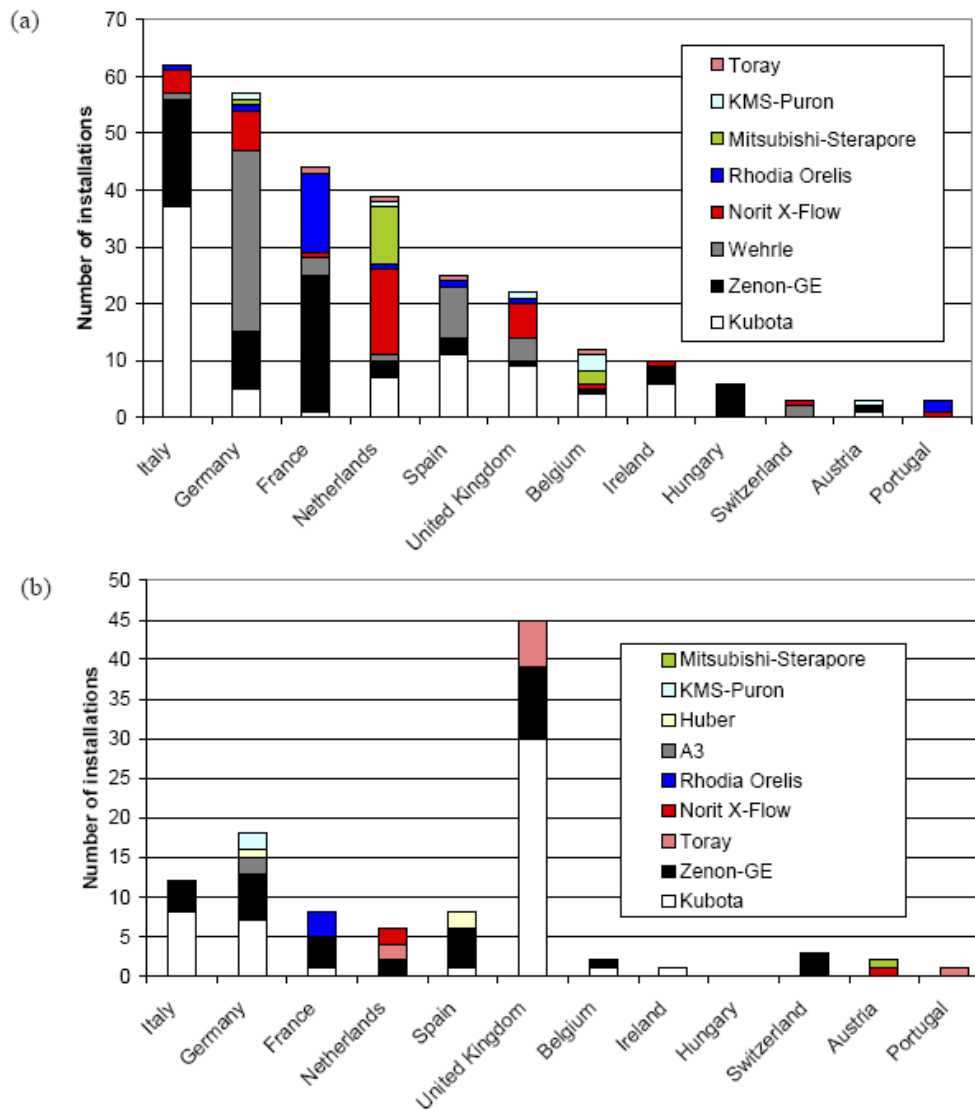


Figure 1 - Geographical distribution of MBR references in Europe: (a) 285 industrial units, (b) 105 municipal plants

Lesjean, B. and Huisjes, E. (2008) Survey of the European MBR market: trends and perspectives, *Desalination*, Vol. 231, pp. 71-81

Appendix II – Product details ultrafiltration membrane

Compact membrane	
Duty	UF
Membrane type	F 5385
Membrane material	Polyvinilidene fluoride (PVDF)
Internal diameter [mm]	8.0
Clean water flux in module at 25°C [$\text{lm}^{-2}\text{h}^{-1}$ at 100 kPa]	> 750
Pore size [μm]	0.03
Max. pressure [kPa]	500
Max. temperature [°C]	70
pH feed	2-10

Appendix III – Product details particle counter in range 2-100 μm

Remote Sensor (Model PCX)

Met One's laser-diode-based particle counting sensors are specifically designed for drinking water applications. Water is directed into the sensor and funneled through an optical flow cell measuring 750 x 750 microns. Each particle that passes through the sensor generates a signal corresponding to its size. Each sensor comes with a calibration curve showing the signal response versus size of each sensor. Met One uses NIST-traceable spheres of known size to calibrate each sensor. This information is stored in the memory of the sensor, and is used to separate the particle counts into the proper size category.

General Specifications

Sensor

Smallest Particles Counted: down to 2 microns

Largest Particles Counted: up to 750 microns

Distance from Display to Sensor: 4,000' maximum (Farthest Sensor)

Power: 115 VAC (+/-10%); Optional 220 VAC (+/-10%); 50/60 Hz

Enclosure: NEMA 4X-Rated

Indicators: Power, Particle/Alarm, Calibration Status

Flow Rate: 100mL/Minute, Nominal

Max. Pressure: 100 psig, not more than 1 minute duration.

Fluid Connections

Inlet: Quick Disconnect. Connects to 1/4-Inch O.D Tubing

Outlet: Quick Disconnect. Connects to 1/4-Inch O.D. Tubing

Accessories/Options

Flow Control: Both "active" and "passive"/manual control devices available

Wiring/Cabling

Computer/WaterWare Data Acquisition system

Water Quality Software (WQS) for monitoring filter performance, generating reports

NEMA-Enclosed Power Supply (**required when Analog I/O Card is ordered**)

Analog Input/Output Card to accept input signals from external devices/to provide an analog output level proportional to concentration of particles

Appendix IV – Product details particle counter in range 0.4-5.0 μm

PERFORMANCE CHARACTERISTICS

MicroCount 100, 100S (0.1 μm Option)

Sensitivity	0.1-5.0 μm @ 100 mL/min
Concentration Limit (10% optical coincidence)	100, 000 particles/mL
Flow Rate	100 mL/min (Typical); 200 mL/min (Maximum)
View Volume (% of flow sampled)	3% @ 150 mW
Light Source	150 mW (Typical) Near IR (837 nm) Laser Diode
Collection Optics	90° Light Scatter (0.1 μm to 0.4 μm) Near Forward Scatter (0.4 μm to 5.0 μm)
Maximum Operating Pressure	MicroCount 100 (uses quartz cell): 150 psi (1034 kPa) MicroCount 100S (uses sapphire cell): 75 psi (517 kPa)

POWER REQUIREMENTS (ALL SENSORS)

System Supplied	+5 Volts dc $\pm 1\%$ +15 Volts dc $\pm 1\%$ -15 Volts dc $\pm 1\%$
-----------------	---

PHYSICAL CHARACTERISTICS (ALL SENSORS)

Dimensions	15.2 cm (L) x 20.3 cm (W) x 10.7 cm (H) 6.0" x 8.0" x 4.2"
Weight	2.5 Kg (5.5 lbs)

ENVIRONMENT CHARACTERISTICS (ALL SENSORS)

Operating	7° - 45° C (44.6° - 113° F) 30-95% Relative Humidity (non-condensing)
Non-operating	-40° - 71° C (-40° - 159.8° F) 0-98% Relative Humidity (non-condensing)
Sample	7° - 45° C (44° - 113° F)

INPUT/OUTPUT

Electronic

Counter & Signals	Standard DB-15 Connector
-------------------	--------------------------

Mechanical

Wetted Parts	Kel-F, Quartz, Sapphire (on 100S and 200S Sensors)
Seals	Kal-Rez
Purge Capability	0.125 in (3.2 mm) Hose barb Dry filtered nitrogen @ 15 psi (103 kPa) maximum

Sample In/Out Connections

Liquid Sensors	0.25 in (6.36 mm) Flare-Tek fittings Teflon tubing
----------------	---

Appendix V – Product details Anton Paar rheometer

	Torque range	0.5 μNm^* to 150 mNm
	*) with enhanced compensation option	
	Torque resolution	0.01 μNm
	Angular resolution	< 1 μrad
	Speed range	10^{-5} to 1000 min^{-1} / 3000 min^{-1} ** (meas.)
	**) with reduced torque, on request	
	Frequency range	10^{-4} to 1000 min^{-1} / 3000 min^{-1} ** (preset)
	Frequency range	10^{-4} to 100 Hz
	Temperature range	-80 to 600 °C
	(depending on the thermostating unit)	
	Shear stress range ***:	10^{-3} to 10^5 Pa
	Shear rate range ***:	10^{-6} to 10^5 s^{-1}
	Viscosity range ***:	$0.5 \cdot 10^{-3}$ to $8.5 \cdot 10^8$ Pas
	***) depending on the measuring system	
	air bearing, automatic gap setting, automatic gap control for temperature sweeps, Physica Quick Coupling.	
Measuring geometries	Concentric cylinder-measuring systems according to DIN 53 019/ISO 3219 Cone/plate and plate/plate measuring systems according to DIN 53 018 High-Shear measuring systems Special measuring systems	
Thermostating- and measuring devices	TEK 130P (C/P, P/P, -30 ... 130 °C, Peltier heating) TEK 180 (C/P, P/P, -20 ... 180 °C) TEK 300 (C/P, P/P, -20 ... 300 °C) TEK 600 (C/P, P/P, -80 ... 600 °C)	TEZ 180 (C, -20 ... 180 °C) TEZ 400 (C, AT ... 400 °C) TEZ HS 90 (C, -20 ... 90 °C, High-Shear-Tests) TEZ 150E (C -20 ... 150 °C, Electro-rheology) FEV + TEK 600 (measurement of solid torsion bars, -80 ... 600 °C)
	Geometries: C/P ... cone/plate, P/P ... plate/plate, C ... zylinder AT ... ambient temperature	
Test types	Shear rate tests (CSR) Shear step tests Shear stress tests (CSS) Creep tests Normal force tests Electro-rheological tests	Oscillatory tests: (with t - or γ -preset) - amplitude sweep - frequency sweep - temperature funktion - time sweep - temperature-frequency-test
	Combine all test types within one test. Superimposed flow (oscillation with superimposed rotation). Multiwave (Superposition of several oscillations with different frequencies).	
Measured/evaluated variables	Dynamic Viscosity η Complex Viscosity η^* , η' , η'' Complex shear modulus G^* Storage modulus G' Loss modulus G'' Complex compliance J^* , J' , J'' Shear stress τ Deformation γ Loss factor $\tan(\delta)$ Normal force F_N	Kinematic viscosity Temperature Torque Speed Shear rate Frequency Angular frequency Time Loss angle Displacement
		ν T M D, $\dot{\gamma}$ f ω t δ φ

Appendix VI – Standard Methods for MLSS

2540 D. Total Suspended Solids Dried at 103–105°C

1. General Discussion

a. Principle: A well-mixed sample is filtered through a weighed standard glass-fiber filter and the residue retained on the filter is dried to a constant weight at 103 to 105°C. The increase in weight of the filter represents the total suspended solids. If the suspended material clogs the filter and prolongs filtration, it may be necessary to increase the diameter of the filter or decrease the sample volume. To obtain an estimate of total suspended solids, calculate the difference between total dissolved solids and total solids.

b. Interferences: See Section 2540A.2 and Section 2540B.1. Exclude large floating particles or submerged agglomerates of nonhomogeneous materials from the sample if it is determined that their inclusion is not representative. Because excessive residue on the filter may form a water-entrapping crust, limit the sample size to that yielding no more than 200 mg residue. For samples high in dissolved solids thoroughly wash the filter to ensure removal of dissolved material. Prolonged filtration times resulting from filter clogging may produce high results owing to increased colloidal materials captured on the clogged filter.

2. Apparatus

Apparatus listed in Section 2540B.2 and Section 2540C.2 is required, except for evaporating dishes, steam bath, and 180°C drying oven. In addition:

Aluminum weighing dishes.

3. Procedure

a. Preparation of glass-fiber filter disk: If pre-prepared glass fiber filter disks are used, eliminate this step. Insert disk with wrinkled side up in filtration apparatus. Apply vacuum and wash disk with three successive 20-mL portions of reagent-grade water. Continue suction to remove all traces of water, turn vacuum off, and discard washings. Remove filter from filtration apparatus and transfer to an inert aluminum weighing dish. If a Gooch crucible is used, remove crucible and filter combination. Dry in an oven at 103 to 105°C

for 1 h. If volatile solids are to be measured, ignite at 550°C for 15 min in a muffle furnace. Cool in desiccator to balance temperature and weigh. Repeat cycle of drying or igniting, cooling, desiccating, and weighing until a constant weight is obtained or until weight change is less than 4% of the previous weighing or 0.5 mg, whichever is less. Store in desiccator until needed.

b. Selection of filter and sample sizes: Choose sample volume to yield between 2.5 and 200 mg dried residue. If volume filtered fails to meet minimum yield, increase sample volume up to 1 L. If complete filtration takes more than 10 min, increase filter diameter or decrease sample volume.

c. Sample analysis: Assemble filtering apparatus and filter and begin suction. Wet filter with a small volume of reagent-grade water to seat it. Stir sample with a magnetic stirrer at a speed to shear larger particles, if practical, to obtain a more uniform (preferably homogeneous) particle size. Centrifugal force may separate particles by size and density, resulting in poor precision when point of sample withdrawal is varied. While stirring, pipet a measured volume onto the seated glass-fiber filter. For homogeneous samples, pipet from the approximate midpoint of container but not in vortex. Choose a point both middepth and midway between wall and vortex. Wash filter with three successive 10-mL volumes of reagent-grade water, allowing complete drainage between washings, and continue suction for about 3 min after filtration is complete. Samples with high dissolved solids may require additional washings. Carefully remove filter from filtration apparatus and transfer to an aluminum weighing dish as a support. Alternatively, remove the crucible and filter combination from the crucible adapter if a Gooch crucible is used. Dry for at least 1 h at 103 to 105°C in an oven, cool in a desiccator to balance temperature, and weigh. Repeat the cycle of drying, cooling, desiccating, and weighing until a constant weight is obtained or until the weight change is less than 4% of the previous weight or 0.5 mg, whichever is less. Analyze at least 10% of all samples in duplicate. Duplicate determinations should agree within 5% of their average weight. If volatile solids are to be determined, treat the residue according to 2540E.

4. Calculation

$$\text{mg total suspended solids/L} = \frac{(A - B) \times 1000}{\text{sample volume, mL}}$$

where:

A = weight of filter + dried residue, mg, and

B = weight of filter, mg.

5. Precision

The standard deviation was 5.2 mg/L (coefficient of variation 33%) at 15 mg/L, 24 mg/L (10%) at 242 mg/L, and 13 mg/L (0.76%) at 1707 mg/L in studies by two analysts of four sets of 10 determinations each. Single-laboratory duplicate analyses of 50 samples of water and wastewater were made with a standard deviation of differences of 2.8 mg/L.

Clesceri, L., Greenberg, A., Eaton, A. (1998) *Standard Methods for the Examination of Water and Wastewater – 20th Edition*, American Public Health Association

Appendix VII – Blanks Characterization experiments results

- **Filtration characteristics - ΔR_{20} , MLSS and Temperature**

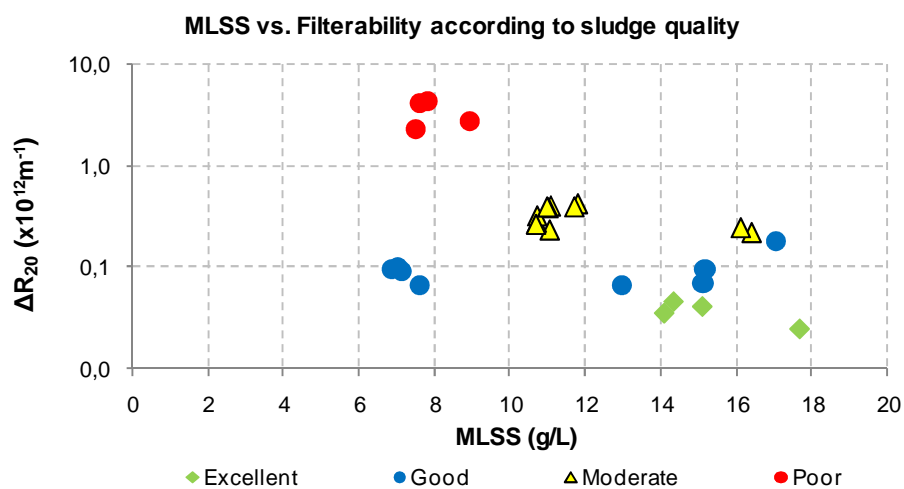


Figure 1 – MLSS vs. ΔR_{20} for all blanks

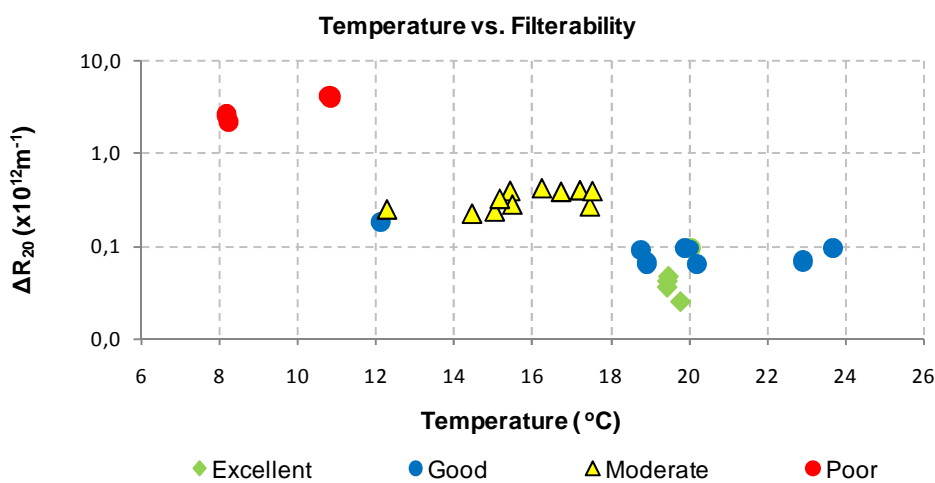


Figure 2 – Temperature vs. ΔR_{20} for all blanks

- Particle counting in range 2-100 μm

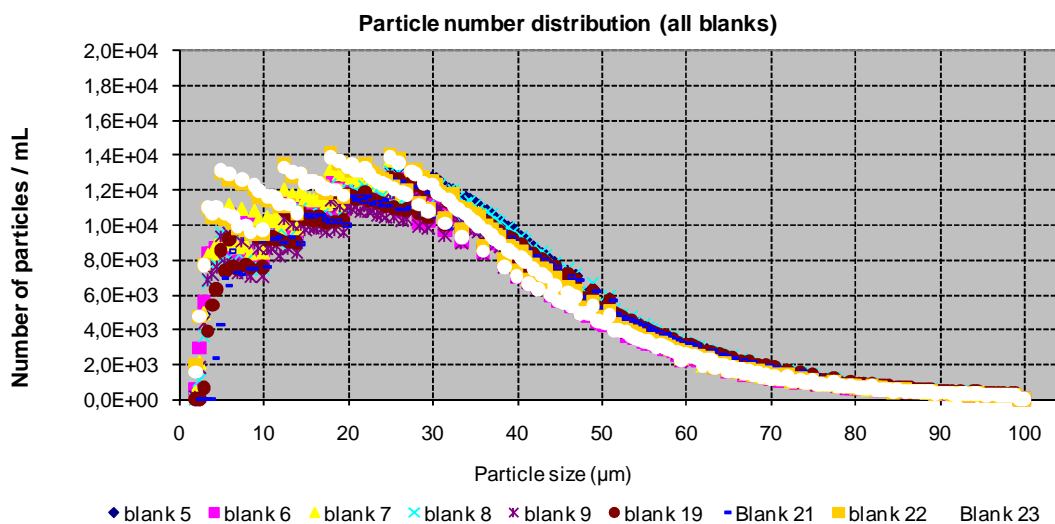


Figure 3 – Particle number distribution in the range 2-100 μm

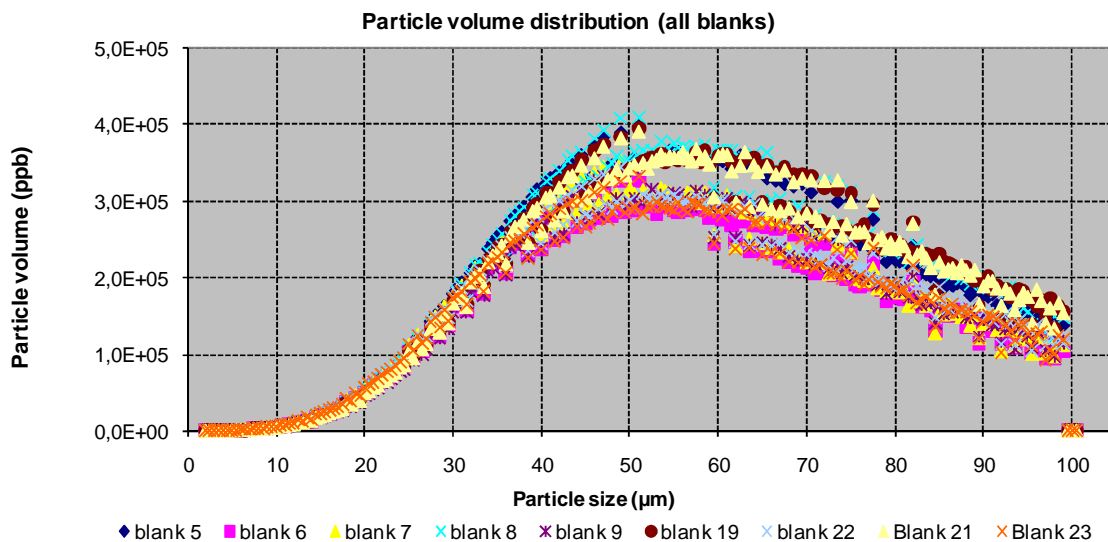


Figure 4 – Particle volume distribution in the range 2-100 μm

- Particle counting in range 0.4-1.0 μm

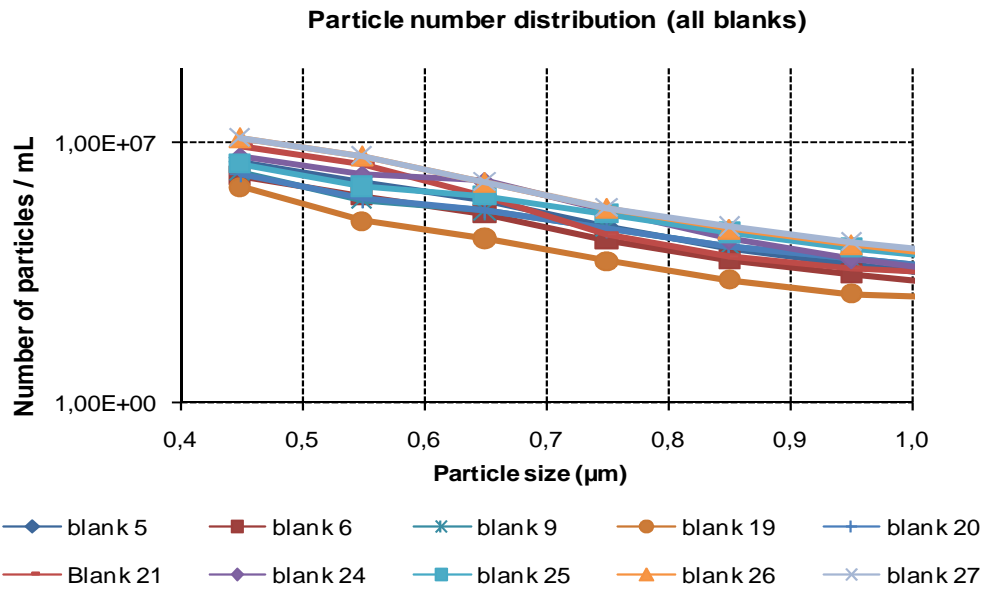


Figure 5 – Particle number distribution in the range 0.4-5.0 μm

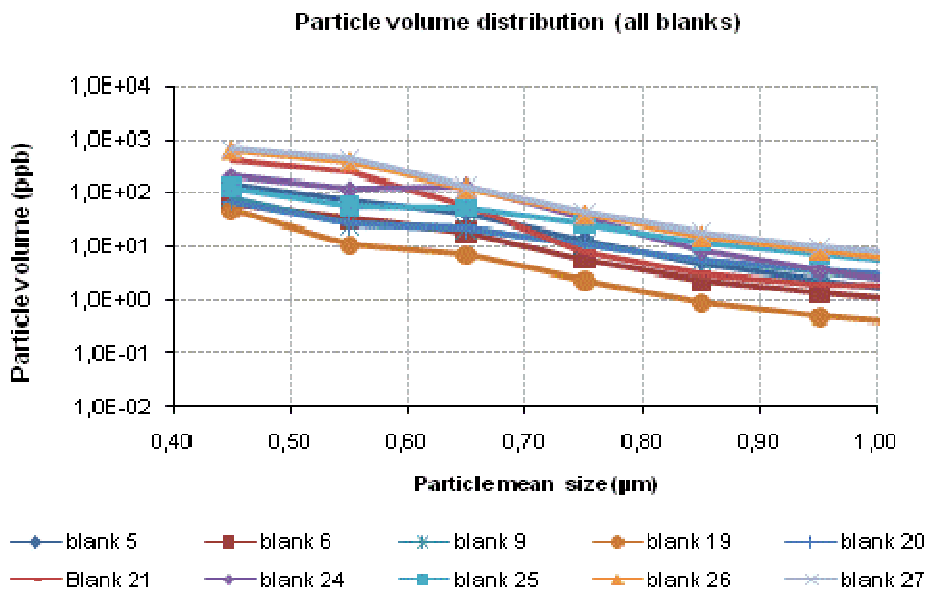


Figure 6 – Particle volume distribution in the range 0.4-5.0 μm

• Soluble Microbial Products

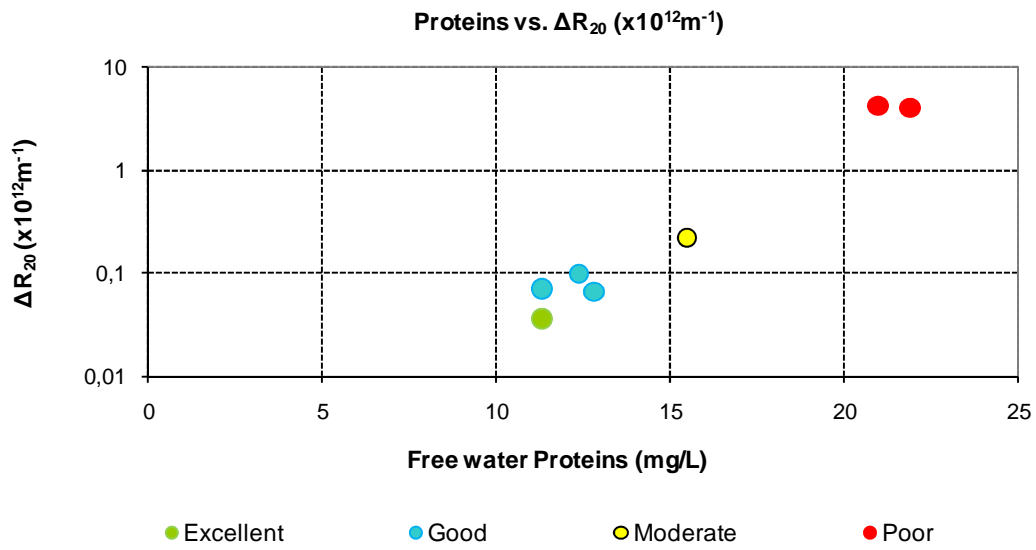


Figure 7 – Proteins vs. filterability

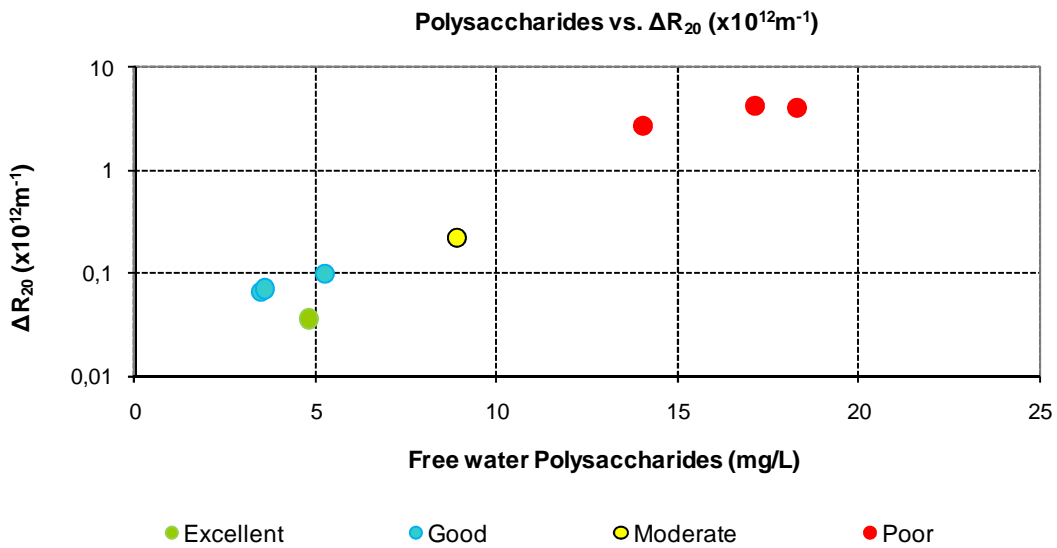


Figure 8 – Polysaccharides vs. filterability

• Viscosity

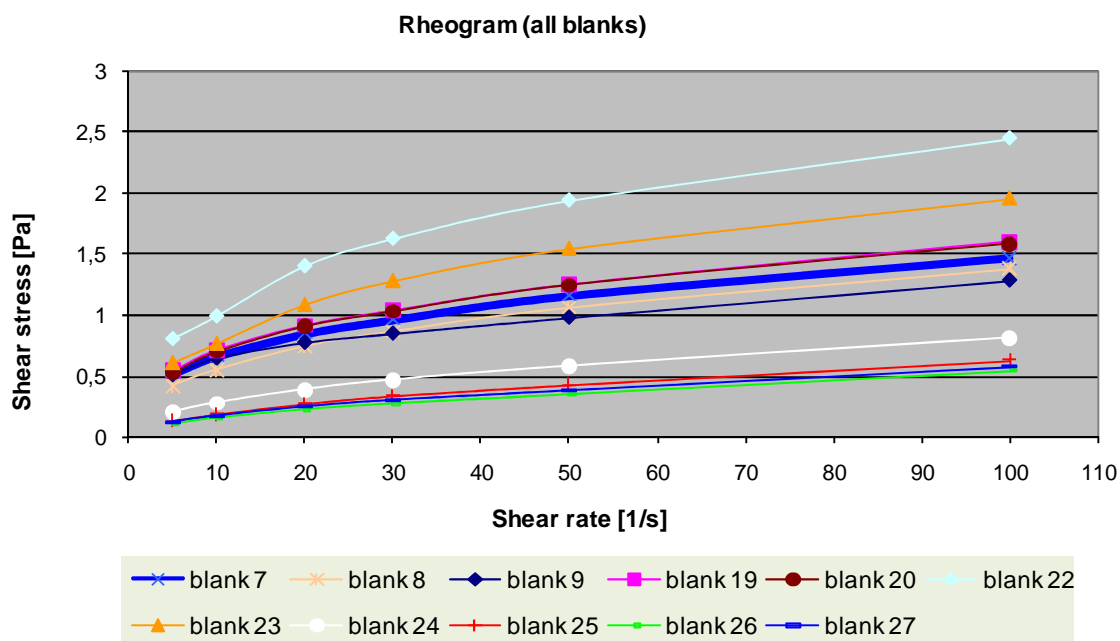


Figure 9 – Rheogram for all blanks

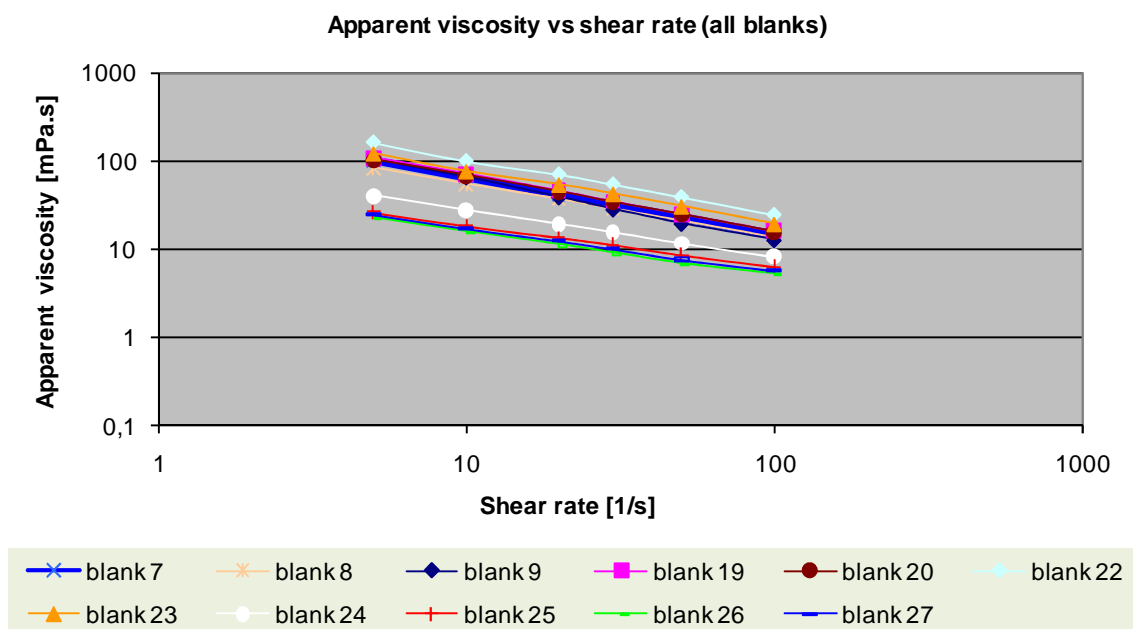


Figure 10 – Apparent viscosity and shear rate

Table 1 – Apparent viscosity obtained from the rheometer measurements

Shear Rate [s ⁻¹]	Viscosity [mPa-s]										
	blank 7	blank 8	blank 9	blank 19	blank 20	blank 22	blank 23	blank 24	blank 25	blank 26	blank 27
5	161.2	121.2	83.37	108.9	104.4	104.1	102.2	40.24	22.54	24.88	26
10	99.17	76.3	54.73	71.39	69.53	66.16	64.76	27.52	15.88	17.24	18.28
20	70.12	54.17	37.04	45.69	45.23	42.16	38.76	19.2	11.38	12.4	13.47
30	54.19	42.6	28.8	34.5	34.24	31.91	28.3	15.42	9.18	10.06	11.15
50	38.79	30.86	21.18	24.9	24.88	23.06	19.58	11.51	7.006	7.6	8.495
100	24.47	19.55	13.78	15.96	15.84	14.61	12.82	8.078	5.371	5.697	6.242
150	18.84	15.28	11.09	12.71	12.5	11.53	10.51	6.87	4.739	5.01	5.435

Table 2 – Apparent viscosity obtained with Rosenverger’s formula

Shear Rate [s ⁻¹]	Viscosity [mPa-s]										
	blank 7	blank 8	blank 9	blank 19	blank 20	blank 22	blank 23	blank 24	blank 25	blank 26	blank 27
5	145.72	170.16	121.93	171.77	170.42	225.59	198.29	58.94	43.81	46.74	44.86
10	97.13	112.23	82.27	113.21	112.38	145.97	129.43	41.83	31.75	33.72	32.46
20	64.74	74.02	55.51	74.62	74.11	94.45	84.48	29.69	23.01	24.33	23.49
30	51.06	58.02	44.10	58.47	58.09	73.22	65.82	24.29	19.06	20.10	19.44
50	37.87	42.69	33.00	43.01	42.74	53.13	48.07	18.87	15.04	15.80	15.31
100	25.24	28.16	22.26	28.35	28.19	34.38	31.37	13.39	10.90	11.40	11.08
150	19.91	22.07	17.69	22.21	22.09	26.65	24.45	10.96	9.03	9.42	9.17

Table 3 – Apparent viscosity obtained with Laera’s formula

Shear Rate [s ⁻¹]	Viscosity [mPa-s]										
	blank 7	blank 8	blank 9	blank 19	blank 20	blank 22	blank 23	blank 24	blank 25	blank 26	blank 27
5	85.74	91.84	79.03	92.22	91.90	103.53	98.09	54.81	46.35	48.13	47.00
10	45.01	48.18	41.52	48.37	48.21	54.25	51.42	28.95	24.55	25.48	24.89
20	24.65	26.35	22.77	26.45	26.36	29.61	28.09	16.01	13.65	14.15	13.83
30	17.86	19.07	16.52	19.14	19.08	21.40	20.31	11.70	10.02	10.37	10.15
50	12.43	13.25	11.52	13.30	13.26	14.82	14.09	8.26	7.11	7.35	7.20
100	8.35	8.88	7.77	8.91	8.89	9.90	9.42	5.67	4.93	5.09	4.99
150	6.99	7.43	6.52	7.45	7.43	8.25	7.87	4.81	4.21	4.33	4.25

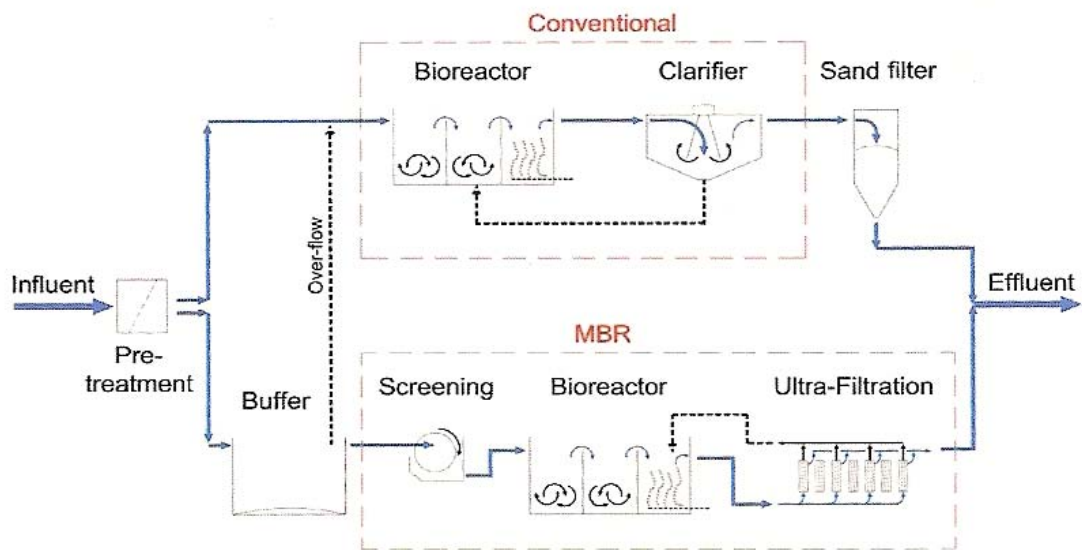


Figure 3 – Ootmarsum WWTP schematic diagram

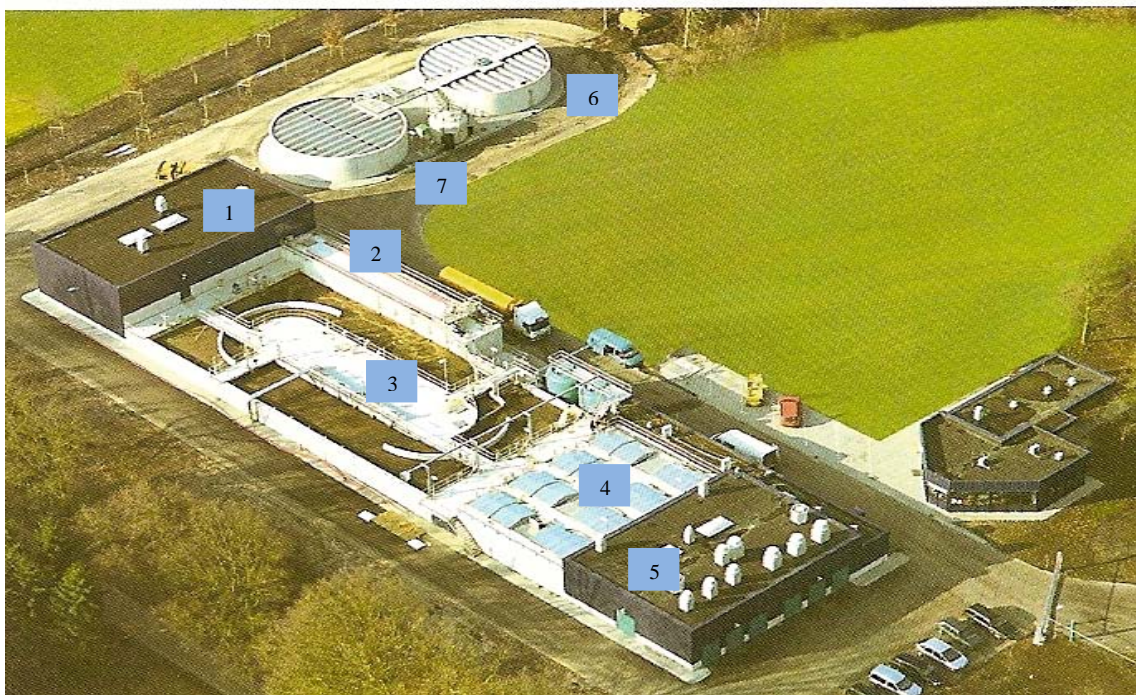


Figure 4 – Varsseveld WWTP: 1- Sewage water collection; 2- sand and oil trap; 3- oxidation ditch; 4- Membrane tanks; 5- Machines room; 6- Sludge thickener; 7 – Sludge storage

Brandão, D. (2008) Particle size distribution in the range of 2-100 μm and filterability on MBR systems, Msc Thesis, Universidade Nova de Lisboa, Lisboa, Portugal

Appendix IX – Dilutions experiment results

- Filtration characteristics - ΔR_{20} and MLSS

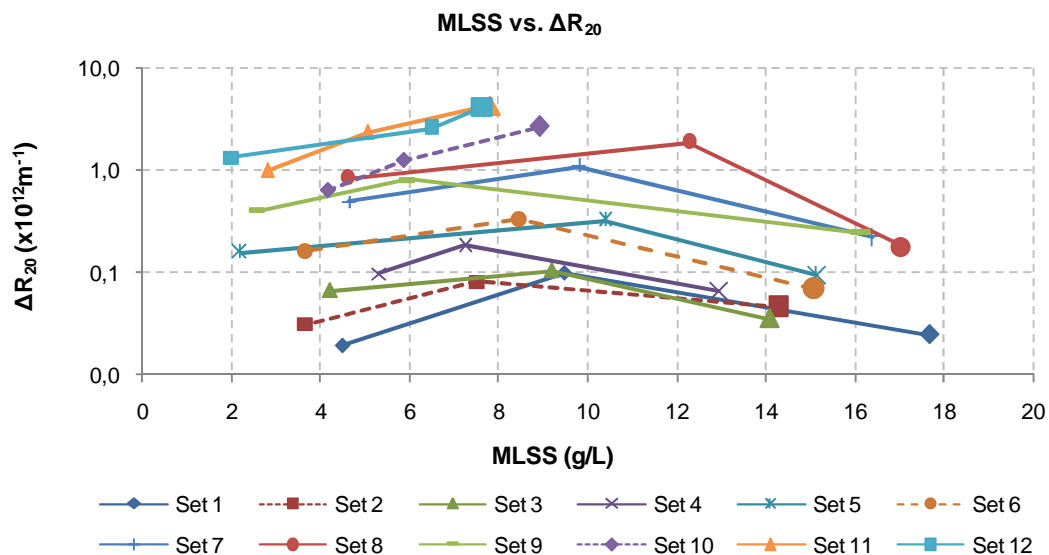
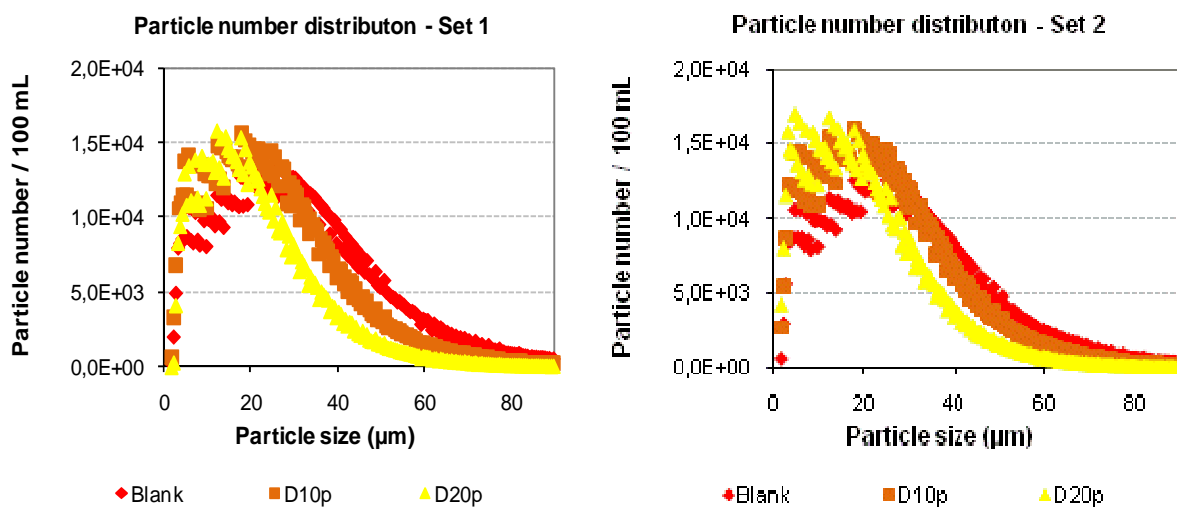
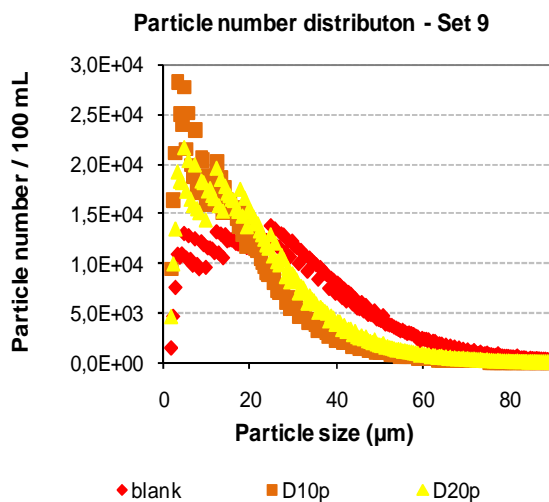
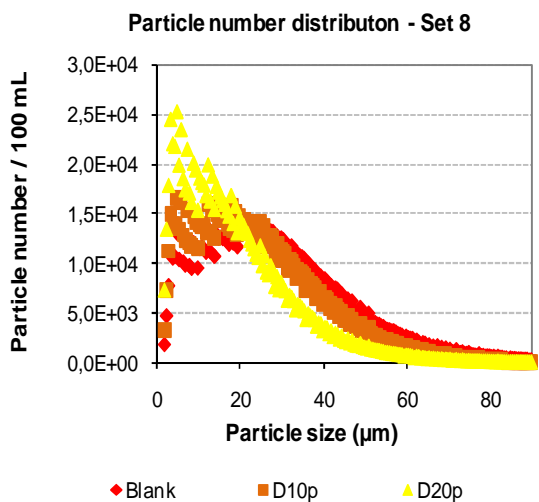
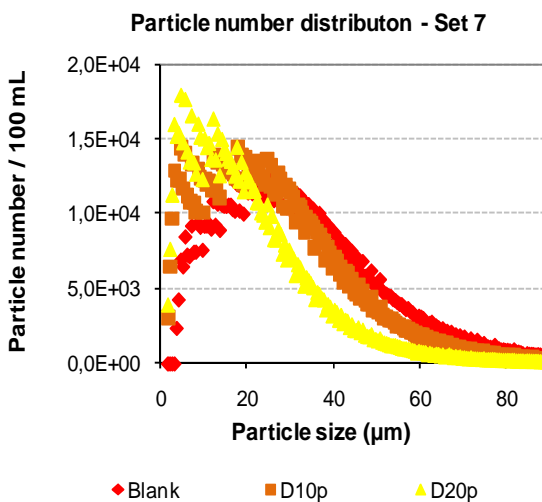
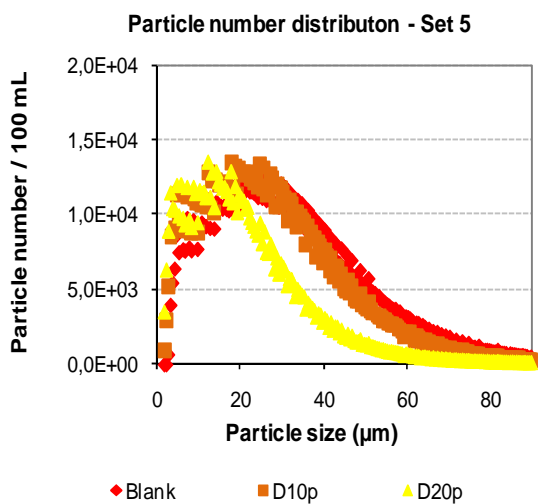
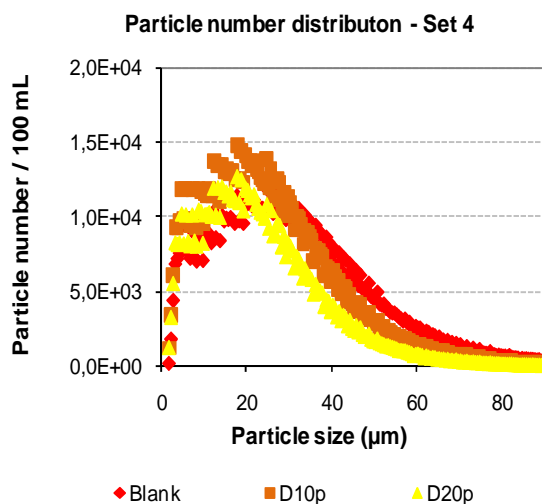
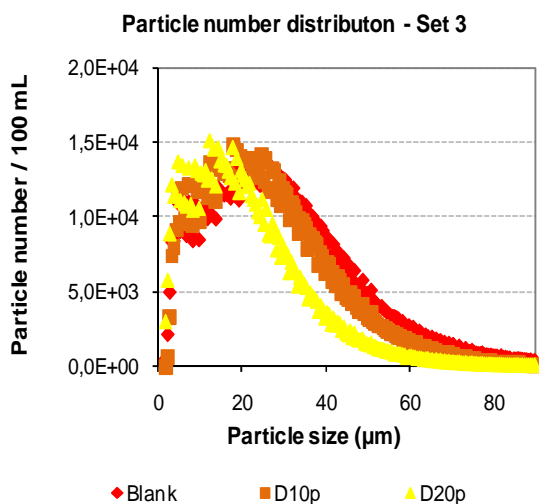


Figure 1 – MLSS vs. ΔR_{20} for all sets

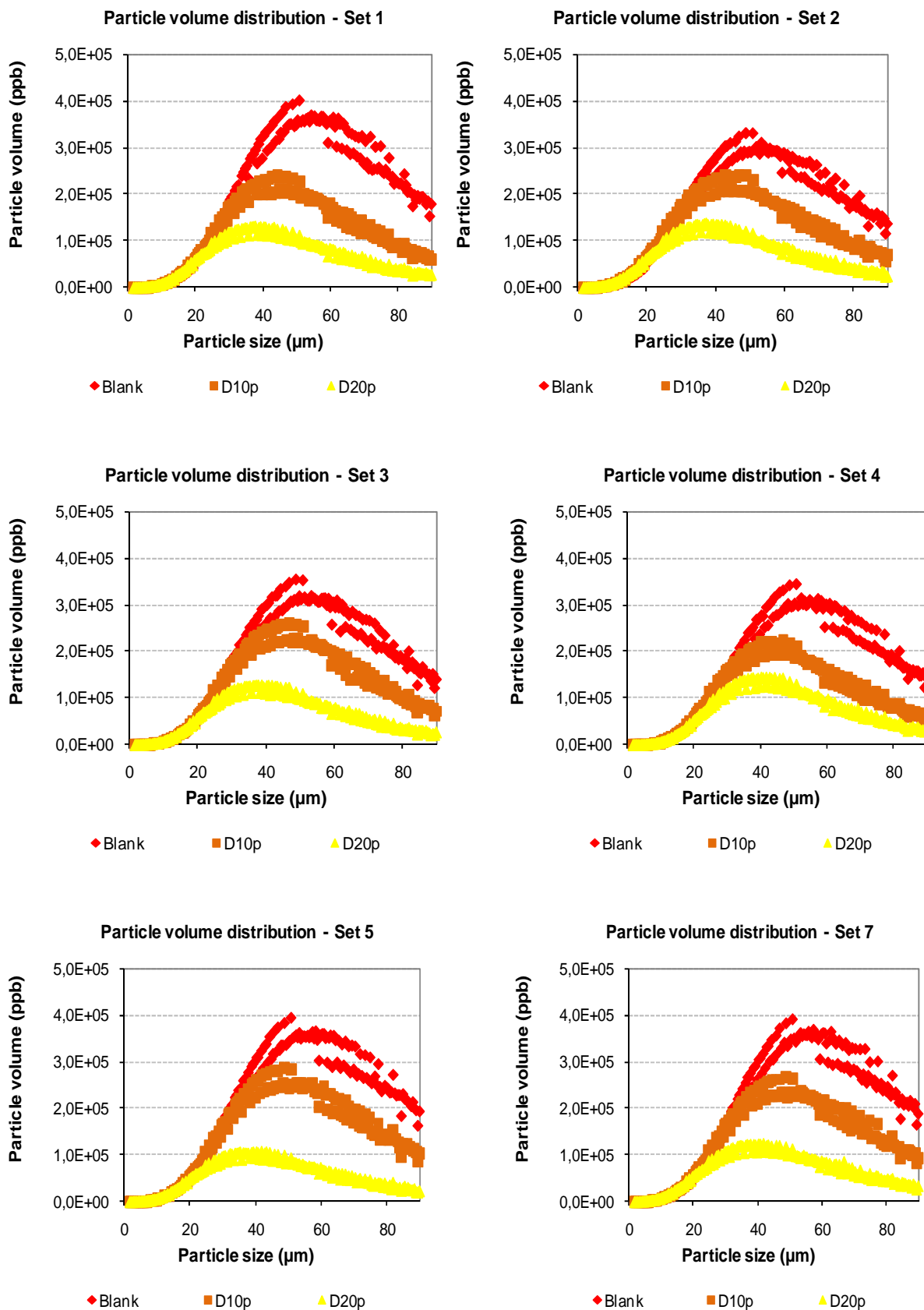
- Particle counting in range 2-100 μm

Particle number distribution by set

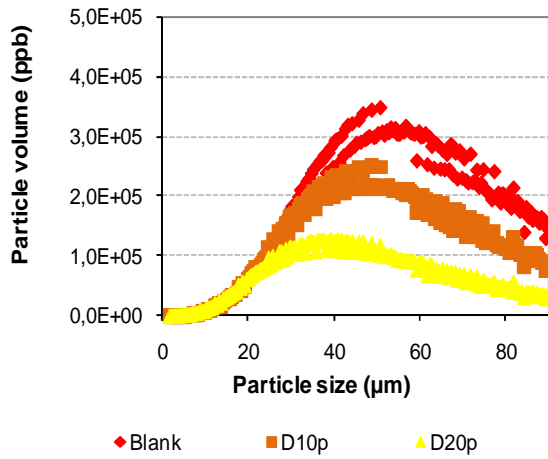




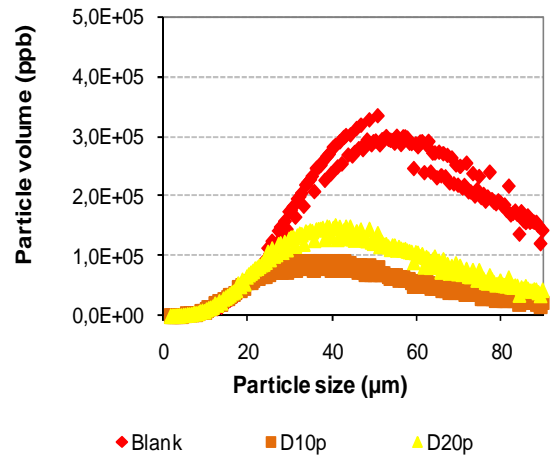
Particle volume distribution by set



Particle volume distribution - Set 8

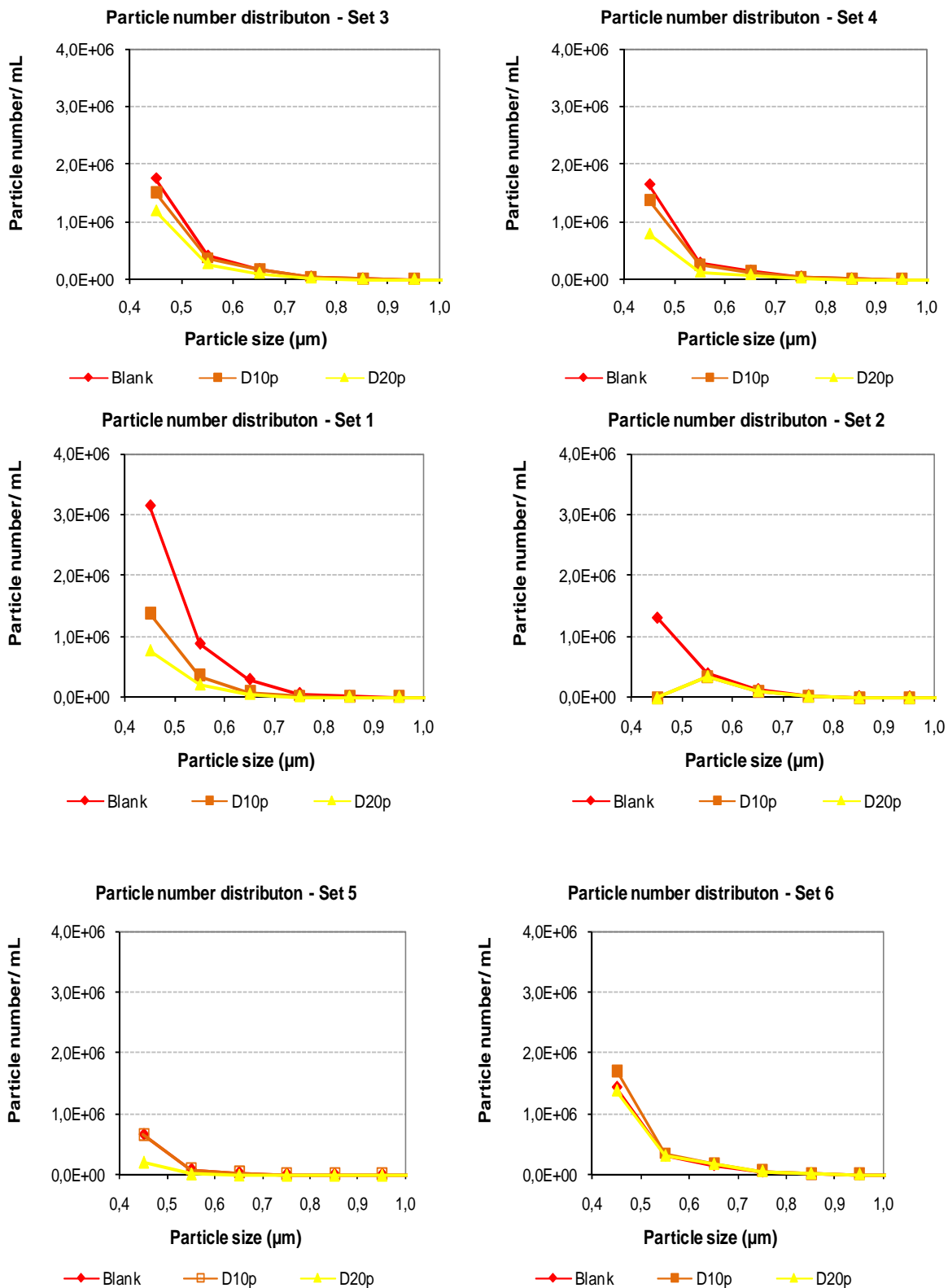


Particle volume distribution - Set 9

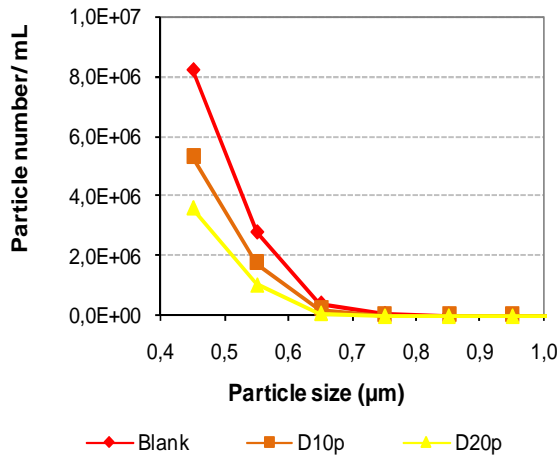


• Particle counting in range 0.4-1.0 μm

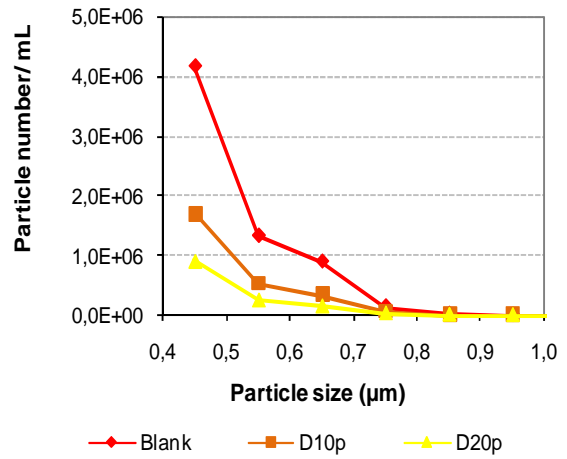
Particle number distribution by set



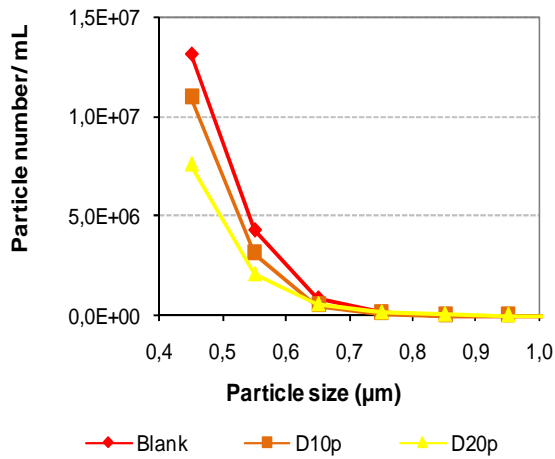
Particle number distributon - Set 7



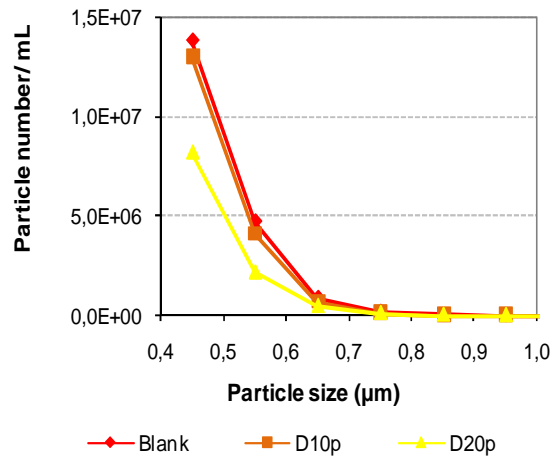
Particle number distributon - Set 10



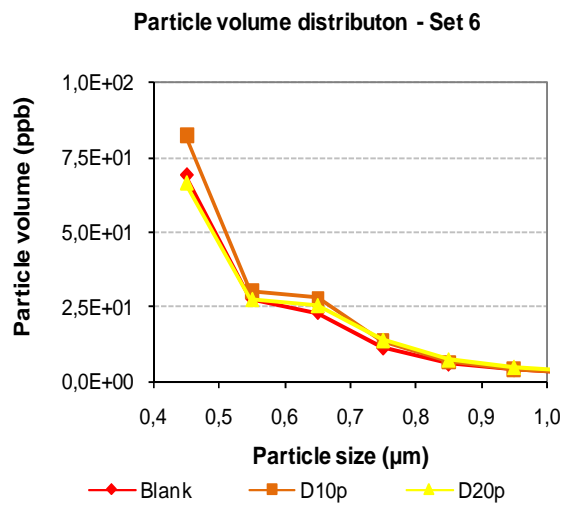
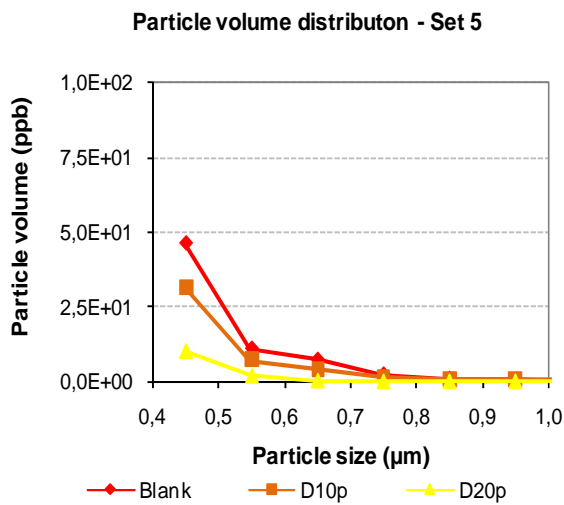
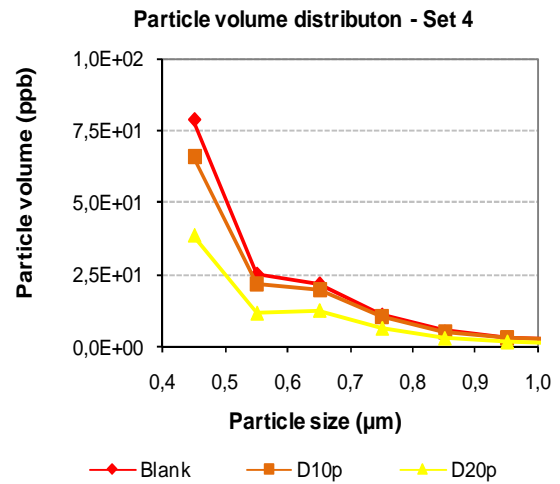
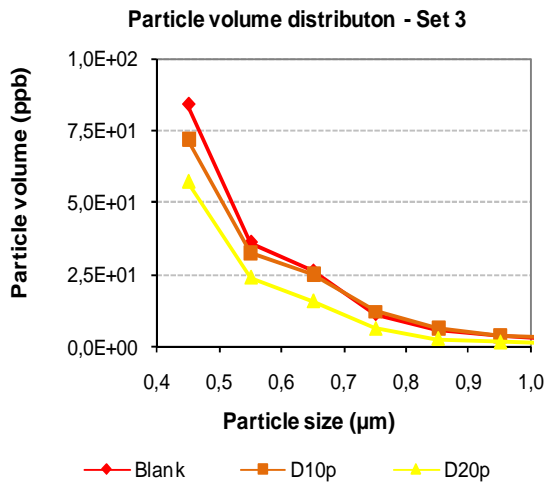
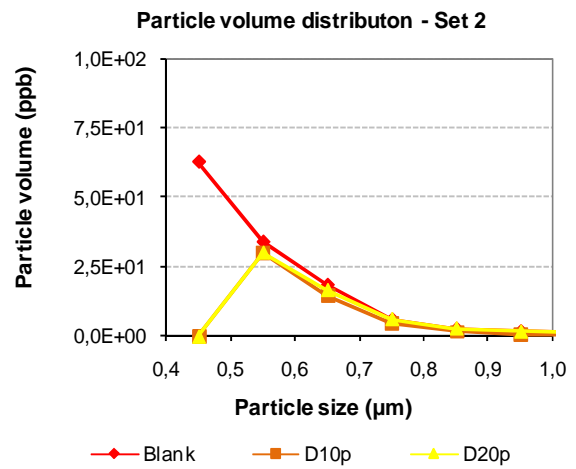
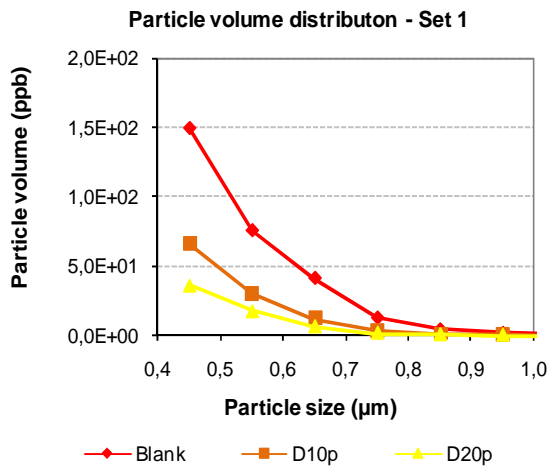
Particle number distributon - Set 11



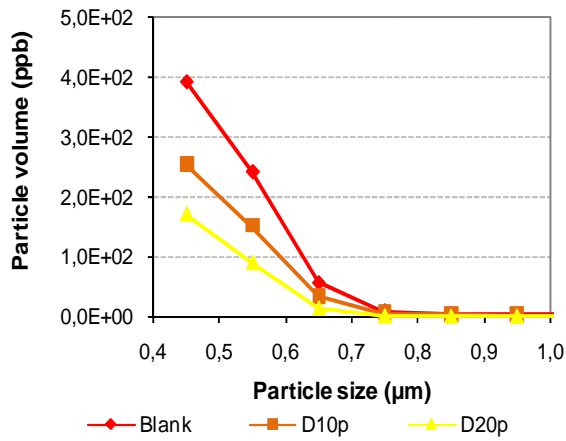
Particle number distributon - Set 12



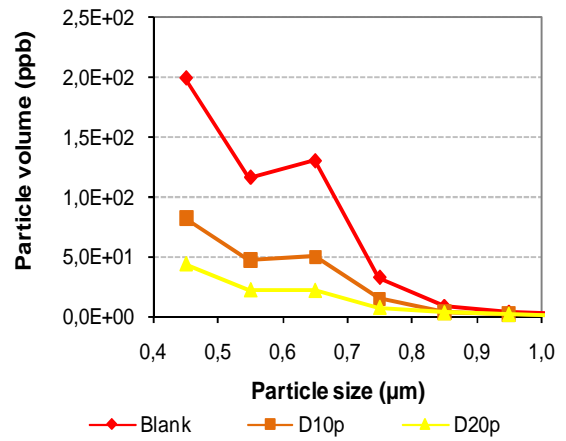
Particle volume distribution by set



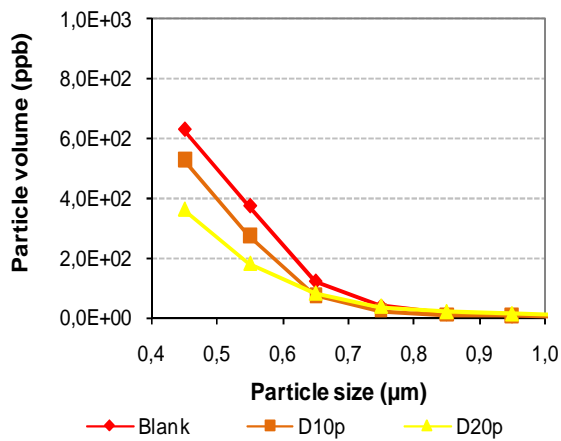
Particle volume distributon - Set 7



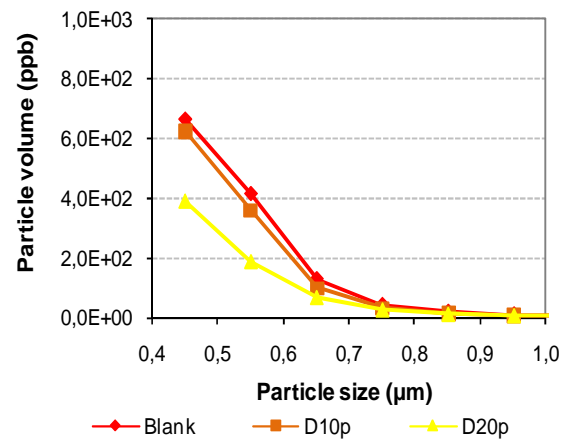
Particle volume distributon - Set 10



Particle volume distributon - Set 11



Particle volume distributon - Set 12



• Soluble Microbial Products

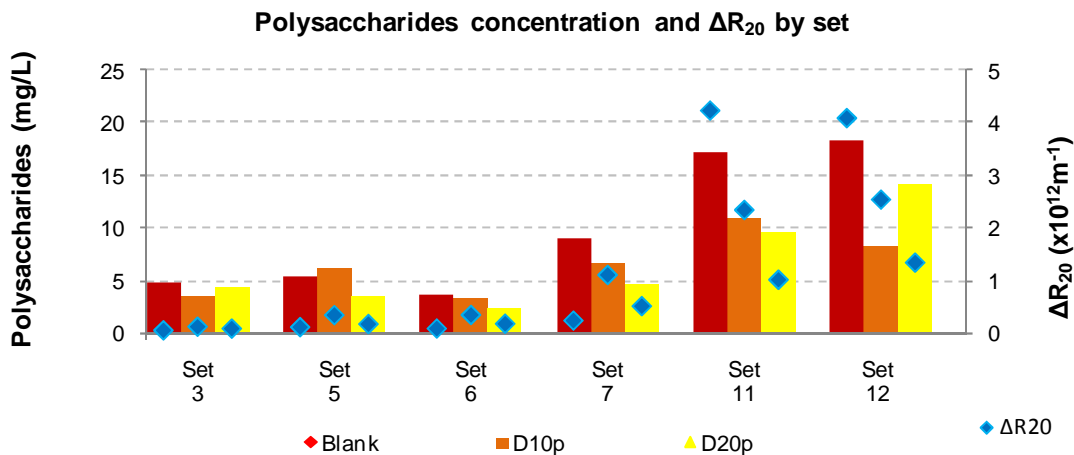


Figure 1 – Polysaccharides concentration and ΔR_{20} along the sets

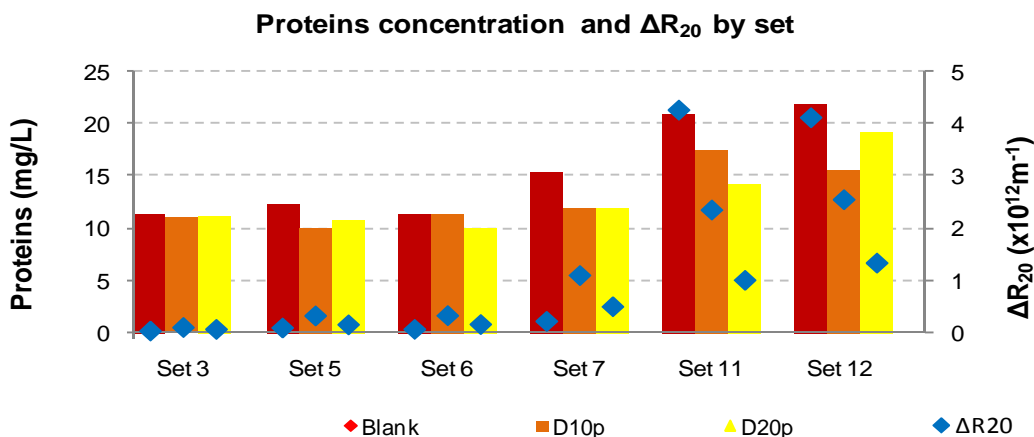


Figure 2 – Proteins concentration and ΔR_{20} along the sets

• Viscosity

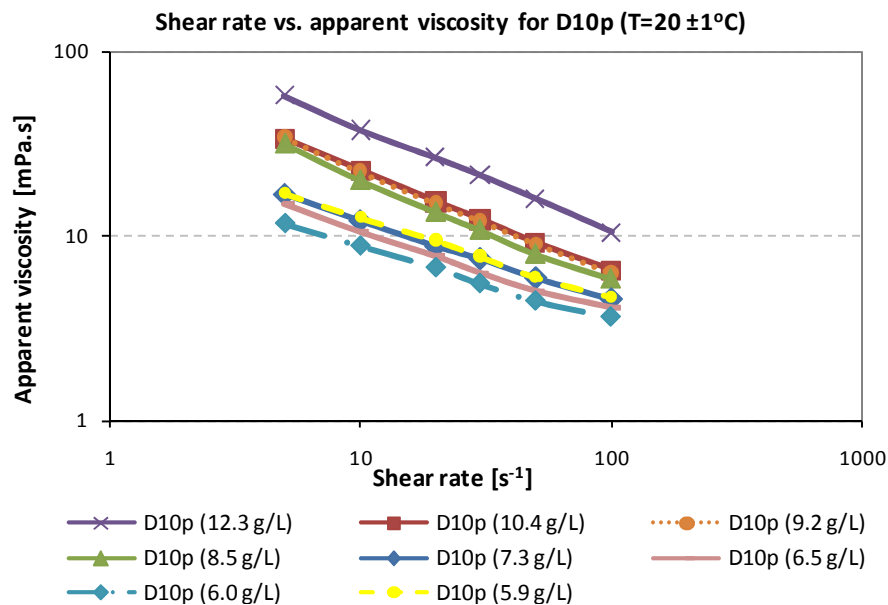


Figure 1 – Shear rate vs. Apparent viscosity for D10p

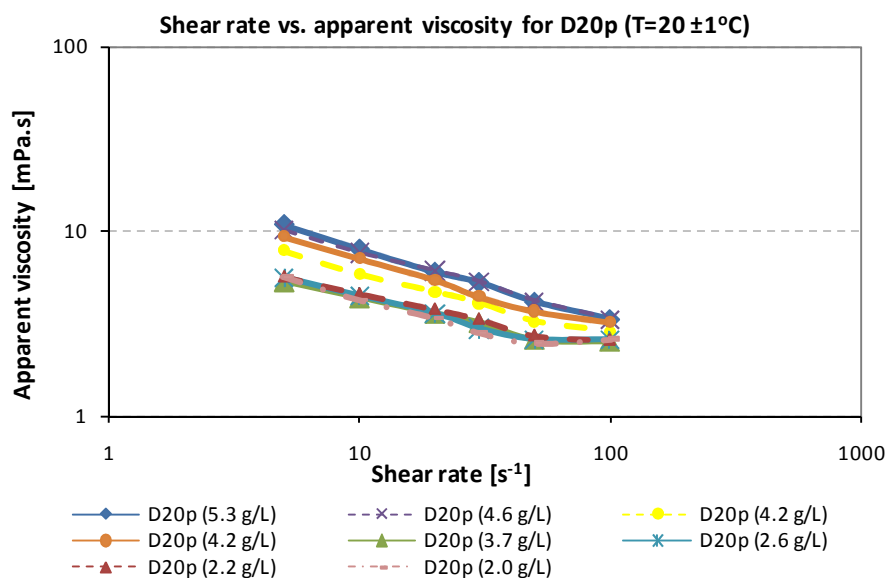


Figure 2 – Shear rate vs. Apparent viscosity for D20p

Appendix X – Solids Concentration experiment results

- Filtration characteristics - ΔR_{20} and MLSS

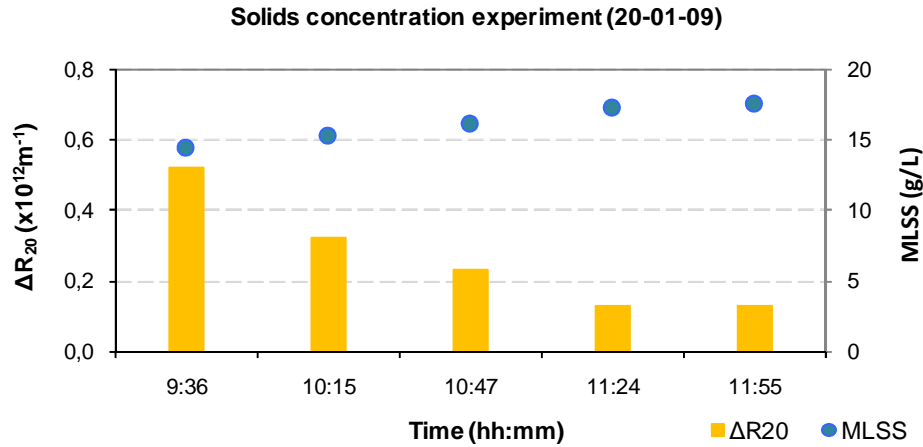


Figure 1 – MLSS and ΔR_{20} along time in 20-01-09

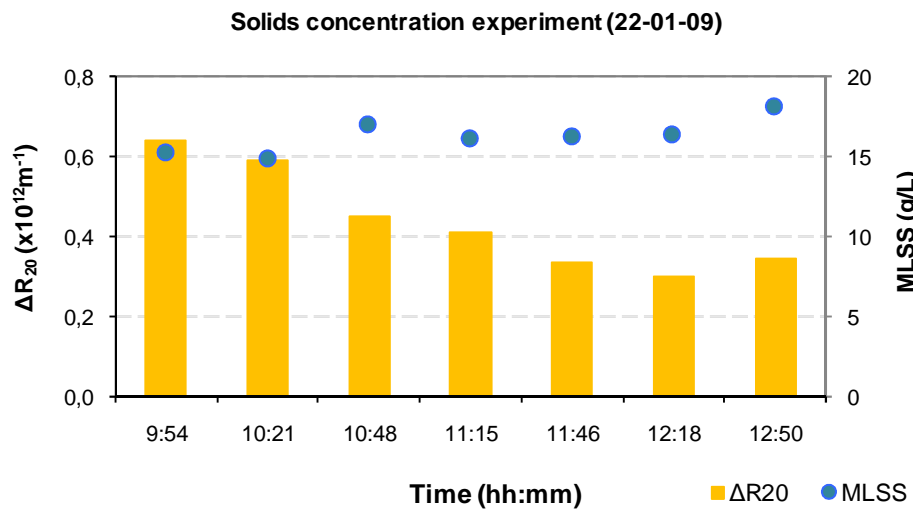


Figure 2 – MLSS and ΔR_{20} along time in 22-01-09

- Particle counting in range 2-100 μm

Particle number distribution

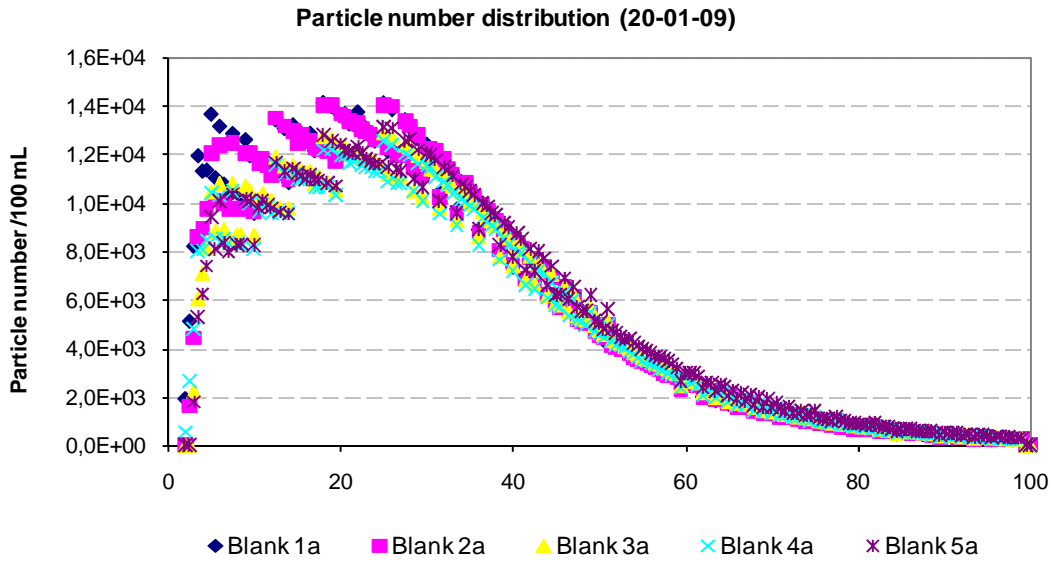


Figure 1 – Particle number distribution in 20-01-09

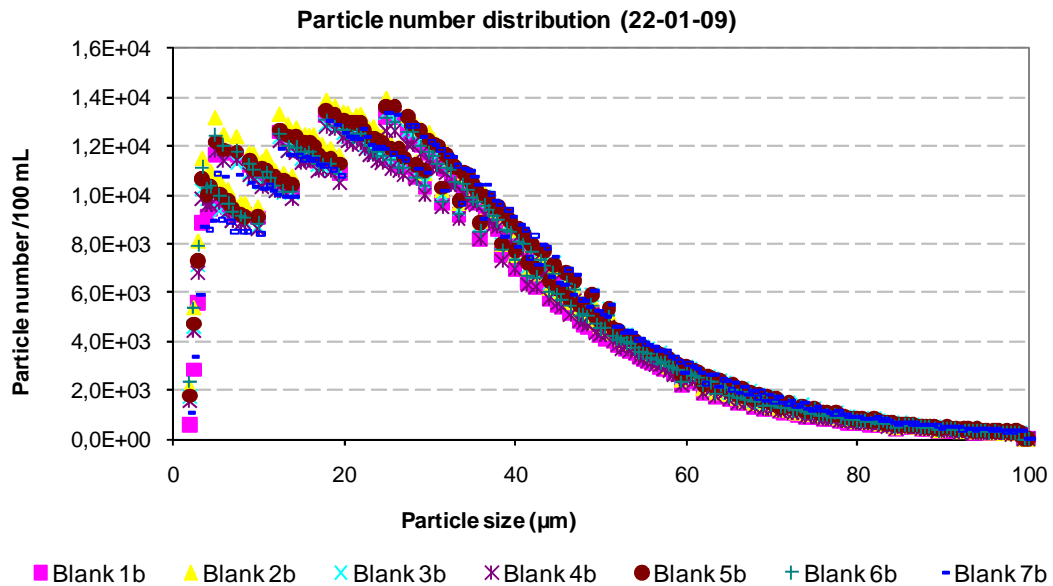


Figure 2 – Particle number distribution in 22-01-09

Particle volume distribution

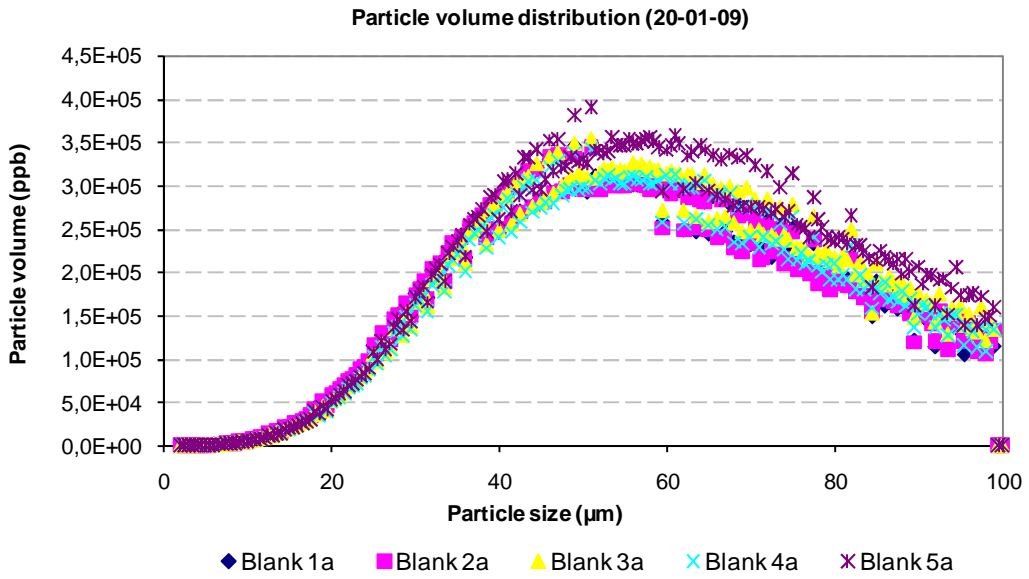


Figure 3 – Particle volume distribution in 20-01-09

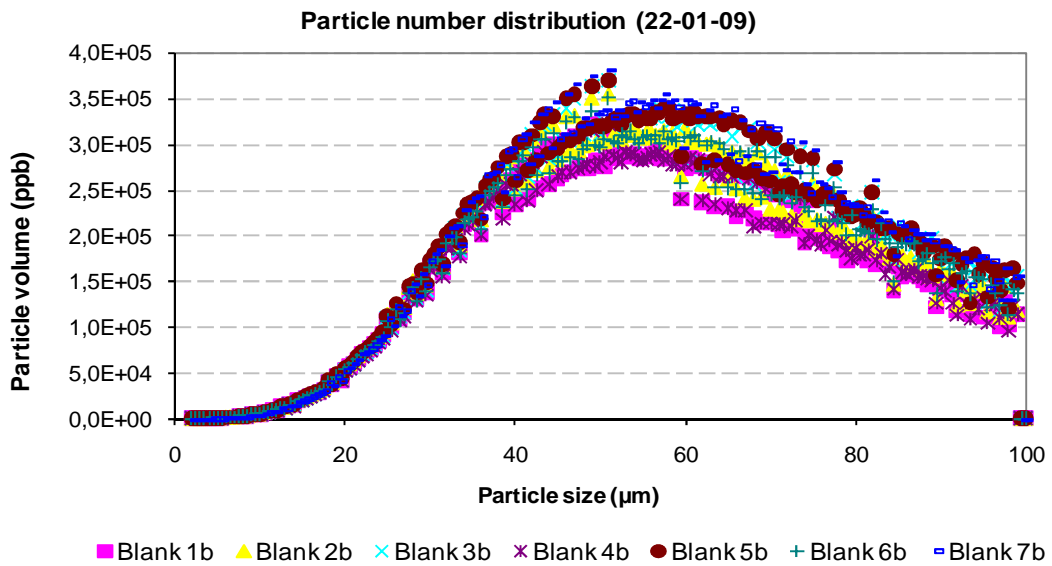


Figure 4 – Particle volume distribution in 22-01-09

Viscosity

Apparent viscosity vs shear rate (20-01-09)

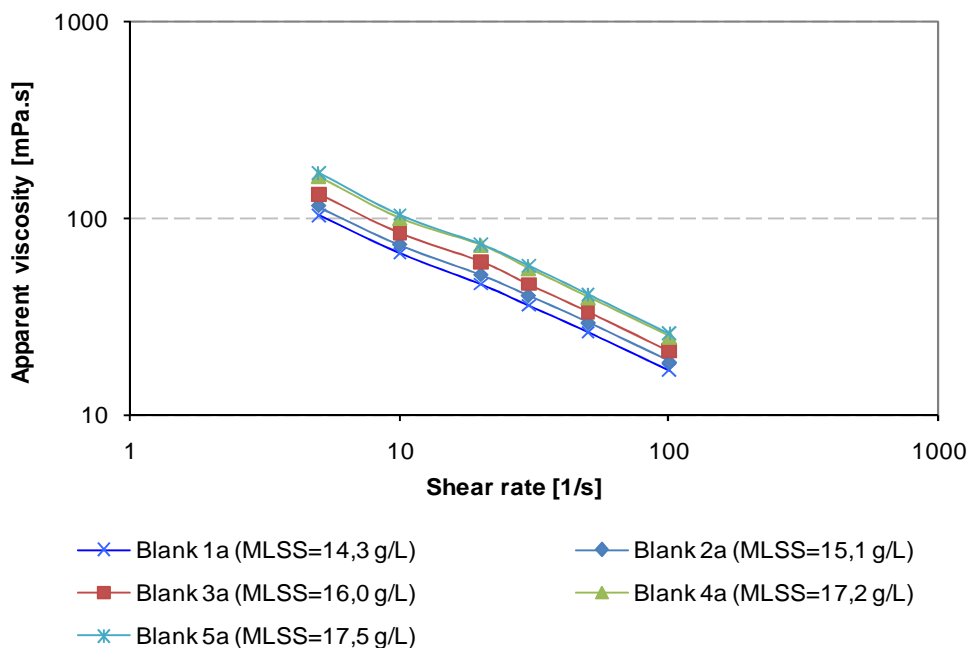


Figure 1 – Shear rate vs. apparent viscosity in 20-01-09

Apparent viscosity vs shear rate (22-01-09)

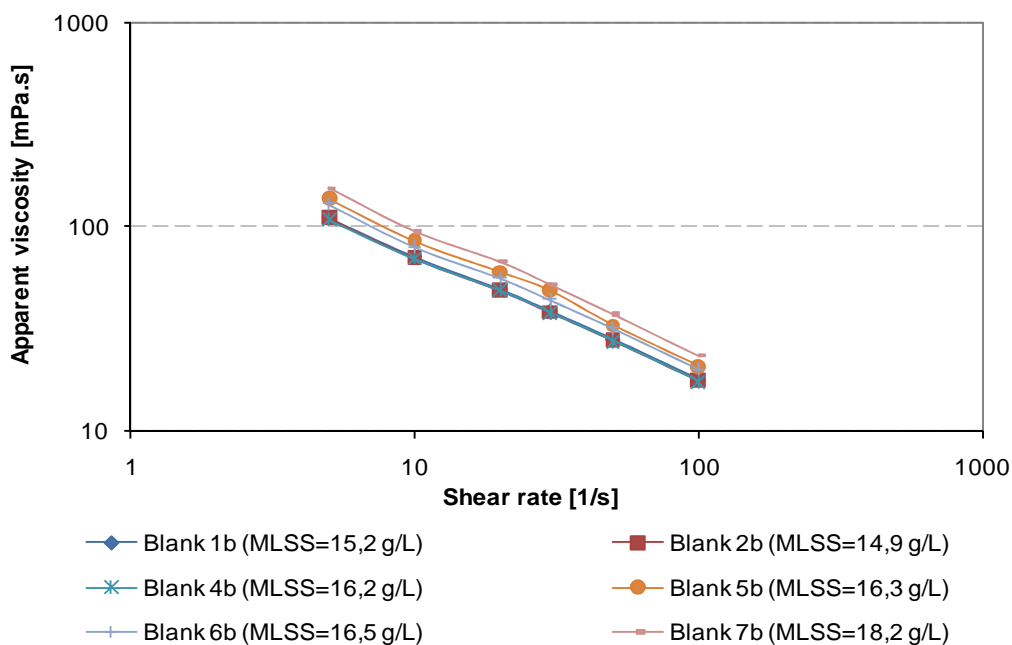


Figure 2 – Shear rate vs. apparent viscosity in 22-01-09